AN ABSTRACT OF THE THESIS OF

Fumio Arisaka for the degree of Doctor of Philosophy

in Biochemistry and Biophysics presented on May 5, 1977

Title: Allosteric Properties and the Association Equilibria of Hemocyanin from Callianassa californiensis

Abstract approved: Redacted for Privacy

K. E. Van Holde

Monomer-tetramer association equilibrium and the oxygen binding of the hemocyanin from Callianassa californiensis were measured at a number of pH values and magnesium ion concentrations. Magnesium binding of the hemocyanin was also measured at several pH values. A thermodynamic model, which satisfied the constraints from the experimental results, was developed and the parameters in the model were determined from the experimental data.

For the measurement of association equilibrium, weight average sedimentation coefficients were first measured by velocity sedimentation at a number of pH values and Mg^{2+} concentrations. It turned out that at pH values above 7.65 the reequilibration process was so slow that the boundaries of both components were clearly separated and the plateau region between the two boundaries was virtually horizontal.

The ratio of the components from the velocity sedimentation was thus confirmed to be the equilibrium value under the conditions. At pH 8.0 the apparent equilibrium constant was determined for both oxy and deoxy state. The association profile with respect to the magnesium ion concentration shifted significantly to the right upon deoxygenation, indicating stronger association for the oxygenated form.

Oxygen binding studies revealed that the role of Mg^{2+} and H^{+} can be interpreted as allosteric effectors in the framework of the "extended non-exclusive" Monod-Wyman-Changeux theory. It was also shown that the hemocyanin could show a high cooperativity of oxygen binding (as judged from the Hill coefficient, n_H), even when no significant amount of tetramer is present, e.g. at pH 8.2 with 10 mM $MgCl_2$. This supported the suggestion by Miller and Van Holde (1974) that the monomer, which consists of six polypeptide chains is the allosteric unit.

Altogether, about 42 strong magnesium binding sites were found per monomer (17S) from the Mg^{2+} binding study. Competition between one Mg^{2+} and two H^{+} was suggested. No significant difference in Mg^{2+} binding between oxy and deoxy states was found, which implied that the number of the oxygen-linked Mg^{2+} binding sites was small compared to the total number of the Mg^{2+} binding sites.

The data analysis based on the model which is developed herein further revealed that: (i) among the 42 magnesium binding sites about four were oxygen linked and about three were involved in the association process; and (ii) the ratio of the allosteric conformational equilibrium constants in monomer and tetramer has the relatively small value of 1.7. The latter observation implies that the shift of the association equilibrium upon oxygenation will not affect the oxygen binding curve significantly. This observation justifies the analysis of the oxygen binding curve, where the effect of the shift in association equilibrium is neglected.

A possible relationship between the thermodynamic model and the structural one based on the recent x-ray diffraction study by Kuiper et al. (1975) will also be discussed.

Allosteric Properties and the Association Equilibria of Hemocyanin from *Callianassa californiensis*

by

Fumio Arisaka

A THESIS

submitted to

Oregon State University

in partial fulfillment of
the requirements for the
degree of

Doctor of Philosophy

Completion May 5, 1977

Commencement June 1977

APPROVED:

Redacted for Privacy

Professor of Biochemistry and Biophysics
in charge of major

Redacted for Privacy

Chairman of Department of Biochemistry
and Biophysics

Redacted for Privacy

Dean of Graduate School

Date thesis is presented May 5, 1977

Typed by Deanna L. Cramer for Fumio Arisaka

ACKNOWLEDGEMENTS

I wish to express my sincere appreciation to Professor K.E. Van Holde, my thesis advisor, for his guidance, understanding and encouragement.

I also thank Drs. Sonia Anderson, Robert Becker, Donald R. Buhler and Irvin Isenberg for use of their instrument and valuable discussions.

I would like to acknowledge appreciation to Neal Eldred and Karen Miller for the cooperation and discussions during the course of this study.

Thanks also goes to Ms. Mary Rasmusson for the introduction to the atomic absorption, Dr. Steven Spiker and James Mardian for their instruction in the light scattering experiment.

Among the many others who were helpful in this work special thanks are extended to the people in our laboratory, especially: Mary Helen Carroll, Jeffrey Corden, Dr. Tim Kovacic, Dr. Dennis Lohr, Georgia Riedel, Kelly Tatchell and Dr. Wolfgang Weischet.

The financial support from the Japan Society for the Promotion of Science (1974-1975) and Yoshida Foundation (1975-1976) is greatly acknowledged.

To my fiance, Hiroko,

my mother and late father

TABLE OF CONTENTS

LIST OF TABLES

LIST OF FIGURES

List of Figures -- continued

List of Figures -- continued

ALLOSTERIC PROPERTIES AND THE ASSOCIATION EQUILIBRIA OF HEMOCYANIN FROM *CALLIANASSA CALIFORNIENSIS*

INTRODUCTION

This thesis deals with the functional properties of the hemocyanin from the ghost shrimp, *Callianassa californiensis*. Attempts will be made to correlate those properties, such as the effect of divalent cations and pH on the binding of oxygen, with the association equilibrium of the hemocyanin molecule.

In the Theory section, a thermodynamic model, which satisfies the constraints from the experimental results, will be developed. Since the detailed molecular structure of the hemocyanin is not available at the present stage, the model is soley thermodynamic rather than structual. At the end of the discussion section, however, I will discuss a possible relationship between the thermodynamic model and a structural one, based on the recent x-ray diffraction study of an arthropod hemocyanin (Kuiper *et al.*, 1975). The results of the Theory section will be used to analyze the experimental data in the Results and Discussion sections.

Hemocyanins are high molecular weight copper containing respiratory proteins found in many species of arthropods and molloscs. They serve for oxygen transport and/or

storage in these animals. The literature on hemocyanins until 1971 has been reviewed by Van Holde and van Bruggen (1971). The stoichiometry of one oxygen molecule to two copper atoms has been well established. The minimal functional unit, which has two copper atoms, has a molecular weight of about 75,000 daltons for arthropods and 50,000 daltons for molluscs. The possession of carbohydrate (one-eight percent) appears to be common in both arthropods and molluscs (Hall and Wood, 1976; Kuiper, 1976), but its function has been unknown.

Although amino acid compositions are similar for both arthropods and molluscs (Table IV), the molecular architecture of the hemocyanins from the two phyla are quite different.

Arthropod hemocyanins are observed to have molecular weights in the hemolymph ranging from 4.5×10^5 to 3.3×10^6 daltons (sedimentation coefficients 17S-60S). The stable molecular species among those depend on the species of the animals. Apparently a 17S structure is the universal building block for the arthropod hemocyanin molecules. Although the 17S structure can be dissociated into six polypeptide chains (5S; MW 75,000 daltons) under extreme conditions, the 17S component is referred to as the structural monomer since from it all structures observed <u>in vivo</u> are assembled. The 5S subunit has two copper atoms which bind one oxygen molecule. Recently a pseudo-hexagonal structure

of the monomer (17S) molecule has been elucidated by an x-ray diffraction analysis and electron microscopic studies of an arthropod hemocyanin, Panulirus interruptus (Fig. 31; Kuiper et al., 1975).

On the other hand, molluscan hemocyanins show molecular weights ranging from approximately 3.8×10^6 to 13×10^6 daltons (60S-130S). A detailed hollow-cylindrical structure has been shown by three dimensional image reconstruction (Mellema and Klug, 1972). The hollow-cylindrical structure of the gastropod hemocyanin is conventionally referred to as a whole molecule which corresponds to a 100S component. Depending on pH and ionic conditions, it dissociates into 1/2, 1/10 and 1/20 molecules (Siezen and van Driel, 1974), which correspond to 60S, 20S and 11S components respectively. It has been concluded that the 1/20 molecule which has a molecular weight of 360,000 daltons consists of a single polypeptide chain (Brouwer et al., 1976). Each polypeptide chain has about seven "domains," each of which has a capacity to bind oxygen. Proteolytic digestion of the polypeptide chain gives individual "domains" of molecular weight of about 50,000 daltons, which retain oxygen binding capacity. Thus, the quaternary structures of anthropod and molluscan hemocynin are fundamentally different.

Callianassa californiensis belongs to the crustaceans (arthropod). Under the physiological conditions

Callianassa hemocyanin exists in the hemolymph of the organism in two forms, designated C and I (Roxby, et al., 1974). Hemocyanin C is present in the hemolymph as particles with a sedimentation coefficient of about 39S. When the isolated material is dialyzed into buffer (pH 7.6) containing no divalent cations, it dissociates completely into 17S particles. This component is competent to completely reassociate to the 39S form upon dialysis into buffers containing 0.05 M or more Mg^{2+} or Ca^{2+}. Hemocyanin I is present in the hemolymph as 17S particles. It is incompetent to associate to the 39S form under any conditions tested, including high levels of divalent cations. The 17S and 39S forms of hemocyanin C are in dynamic equilibrium in the presence of divalent cations. The molecular weight of 4.3×10^5 and 17×10^5 daltons have been found for the 17S particle and 39S particle respectively, which implies the latter is a tetramer of the former. The monomers (17S) of hemocyanin C are each made up of six polypeptide chains with molecular weights of about 74,000. Those six subunits show two or three bands in SDS gel electrophoresis (Neal Eldred, unpublished results) and electrophoretically heterogeneous (Miller et al., 1977). Subunits of Hemocyanin I show a similar electrophoretic pattern, but there is some difference in the abundance of each component (Eldred, unpublished results).

Hemocyanin C from Callianassa californiensis is one of the rare cases, where truely reversible dynamic equilibrium between two distinct states of aggregation appear to be present. Although, as we shall see, most of the experimental results can be interpreted in terms of the dynamic equilibrium between monomer and tetramer in the exact thermodynamic sense, the full implication of the microheterogeneity of the hemocyanin should be kept in mind. Many of the properties described in this thesis may represent average quantities for a microheterogeneous population. A preparative separation method of purified polypeptide chains, which has been successfully used for Limulus hemocyanin (Sullivan et al., 1974), has not been successful for other hemocyanins including Callianassa hemocyanin.

The oxidation state of copper atoms and the mode of oxygen binding have been another current topic of hemocyanins. The Cu(I) state in the deoxy-hemocyanin has been confirmed by both spectroscopic and chemical methods. The oxidation state of copper in the oxy-hemocyanin, however, has been controversial because of a number of contradictory observations (Van Holde and van Bruggen, 1971). Among those observations, the absorption spectra are similar to those of many Cu(II) complexes and very like those of a number of Cu(II) proteins, but no ESR spectrum has generally been observed. Recently Freedman et al. (1976) have suggested an attractive model on the mode of oxygen binding

to hemocyanins based on a resonance Raman spectroscopy. Among several possibilities, their argument favored μ-dioxygen bridging with nonplanar, C_2 symmetry. Their MO scheme of Cu-O_2-Cu has illustrated that (a) the oxygen is bound as peroxide, O_2^{2-}, (b) the copper will be present as Cu(II) and (c) the complex is diamagnetic, assuming that the separation between the highest levels ϕ_A and ϕ_S, which are from copper d bands is large enough to have ϕ_A doubly occupied and ϕ_S empty at room temperature. The MO diagram for the C_2 configuration thus accounts for the magnetic properties, oxidation states, and O_2 vibrational frequency in the hemocyanin. They assigned $4b \rightarrow \phi_S(O_2^{2-} \rightarrow Cu(II))$ at ~570 nm and $5a \rightarrow \phi_S(O_2^{2-} \rightarrow Cu(II))$ at ~490 nm for Cancer and Busycon hemocyanins, where 4b and 5a come from doubly degenerated oxygen 1 πg orbital. They also concluded that the ~340 nm transition involved charge transfer between N (imidazole) and Cu(II). In terms of the MO scheme, oxygenation and the concomitant formation of Cu(II)-hemocyanin are considered to create a vacant ϕ_S orbital which, in turn, becomes a suitable terminal orbital for charge transfer from N (imidazole). As far as the structure of active site is concerned, there seems to be no significant difference between arthropods and molluscs, judging from their results for both Cancer (arthropod) and Busycon (mollusc). The slight difference in absorption

spectra between these two phyla, as Freedman et al. suggest, may be due to slight geometric alterations in the O_2 binding sites.

The structure around the copper atoms has not been clear except that the involvement of histidine residues has been strongly suggested and the involvement of cysteine residues is unlikely (Van Holde and van Bruggen, 1971).

In this thesis attention will be focused exclusively on the functional properties of hemocyanin C from Callianassa californiensis. As mentioned earlier, the hemocyanin is in dynamic equilibrium between monomer and tetramer in the presence of divalent cations. More recent sedimentation equilibrium studies by Blair and Van Holde (1976) have further revealed that the association proceeds in two steps: (1) a monomer-dimer association which is sensitive to Mg^{2+} concentration and insensitive to temperature, and (2) a dimer-tetramer association which is highly temperature dependent but insensitive to Mg^{2+}. It has also been known that (1) both $Mg^{2+}(Ca^{2+})$ and H^{+} affect the oxygen binding affinity of the hemocyanin, the former enhancing the affinity but the latter decreasing it, and (2) the binding of oxygen affects the association equilibrium significantly (Miller and Van Holde, 1974). Those observations have suggested that it is necessary to extend the allosteric theory to include the association equilibrium

for the full analysis of the problem. The following Theory section is devoted to an effort along that line.

THEORY

The purpose of this section is to present or derive some thermodynamic equations which will be used to analyze the experimental data. For the purposes of this discussion, hemocyanin from Callianassa californiensis is characterized as a system which consists of a macromolecule and three ligands, i.e. a substrate (oxygen molecule) and two species of effectors, hydrogen ions and divalent cations (Mg^{2+} or Ca^{2+}). Under normal conditions in the presence of Mg^{2+}, the hemocyanin is in equilibrium between a monomer which consists of six polypeptide chains and a tetramer which consists of totally twenty four polypeptide chains:

$$4\ M \rightleftharpoons Te$$

According to Schellman (J.A. Schellman, 1975), the chemical potential of a macromolecule, P, which binds one species of ligand, L, can be given as below:

$$\mu = \mu_0^0 + RT\ \ln C_p - RT\ \ln \sum \qquad (1)$$

$$\sum = 1 + K_1 a_L + \text{------} + K_n a_L^n \qquad (2)$$

where C_p is the total molar concentration of the macromolecule, $\sum$ is the binding polynomial, K_i is the ith

phenomenological association constant defined as $K_i \equiv (PL_i)/((P_o)a_L^i)$, where (P_0) is the concentration of the macromolecule without ligand, a_L is the activity of free ligand. It is assumed that the protein concentration is low enough so that it behaves ideally. From eq. (1), we see that the chemical potential of the macromolecule is the sum of the chemical potential that would be obtained in the absence of binding plus the free energy of binding given by $-RT \ln \sum$. (The quantity $J\Pi = RT \ln \sum$ is the binding potential defined and developed by Wyman, 1965.) The binding polynomial is easily extended to the system which has three species of ligands. In that case the binding polynomial may be written as:

$$\sum = 1 + K_{100}a_A + \text{------} + K_{ijk}a_A^i a_B^j a_C^k + \text{------} + K_{lmn}a_A^l a_B^m a_C^n \tag{3}$$

$$= \sum_{i,j,k=0}^{l,m,n} K_{ijk}a_A^i a_B^j a_C^k$$

$$K_{ijk} \equiv \frac{(P_{ijk})}{(P_0)(a_A)^i(a_B)^j(a_C)^k},$$

where l, m, and n are the numbers of binding sites of ligands, A, B, and C respectively; P_{ijk} is a macromolecule to which are bound i molecules of ligand A, j molecules of ligand B and k molecules of ligand C, respectively.

Now the chemical potentials of monomer and tetramer in the present case may be written as:

$$\mu_M = \mu_M^0 + RT \ln(M) - RT \ln \sum_M \tag{4}$$

$$\mu_{Te} = \mu_{Te}^0 + RT \ln(Te) - RT \ln \sum_{Te} \tag{5}$$

The condition of equilibrium is $\mu_{Te} = 4\mu_M$, from which eq. (4) and (5) give:

$$RT \ln \frac{(Te)}{(M)^4} = -\mu_{Te}^0 + 4\mu_M^0 + RT \ln \frac{(\sum_{Te})}{(\sum_M)^4}$$

$$\frac{(Te)}{(M)^4} = K = \exp\{-\beta(\mu_{Te}^0 - 4\mu_M^0 - RT \ln \frac{(\sum_{Te})}{(\sum_M)^4})\} \tag{6}$$

$$= K_0 \frac{\sum_{Te}}{(\sum_M)^4}, \quad \beta = \frac{1}{RT}$$

where K_0 is the association constant to tetramer in the absence of ligands. The problem is then reduced to finding the expressions of $\sum_M$ and $\sum_{Te}$. In order to do so, we have to make a model of this system. The model has been chosen to have features that are dictated by qualitative properties we have observed for the Callianassa system.

I assume that (i) the monomer, which contains six oxygen binding sites, is the allosteric unit, e.g. the

binding of oxygen is not linked between monomer units in tetramer (for justification of this assumption, see Miller and Van Holde, 1974 and also the results of the oxygen binding study in this thesis; (ii) there are three kinds of magnesium binding sites, one of which is linked to oxygen binding (h sites), the second is not, but involved in the association to tetramer (p sites), and the rest which does not have either role (r sites); (iii) one hydrogen ion and one magnesium ion compete for any kind of binding site (see the results of the association equilibrium, the magnesium binding study and the oxygen binding study in this thesis). Although the extended model which takes the hybrid state into consideration (Buc, Johannes and Hess, 1973) fits better the oxygen binding data for hemocyanin (Miller and Van Holde, 1974), I take (iv) the simpler non-exclusive Monod-Wyman-Changeux model in the first place for simplicity (Rubin and Changeux, 1966). I will consider the more general theory, which include hybrid states, in the last part of this section. In making these assumptions, we are considering the equilibrium scheme depicted in Fig. 1, where equilibrium constants K_1 and L'_{Te} are defined in a clockwise direction in the reaction scheme, but L'_M and K_2 are defined anticlockwise. Since the free energy change must be zero for the whole cycle, these equilibrium constants must obey the relationship $L'^{-4}_M K_1 L'^{4}_{Te} K^{-1} = 1$, and one of the constants is redundant.

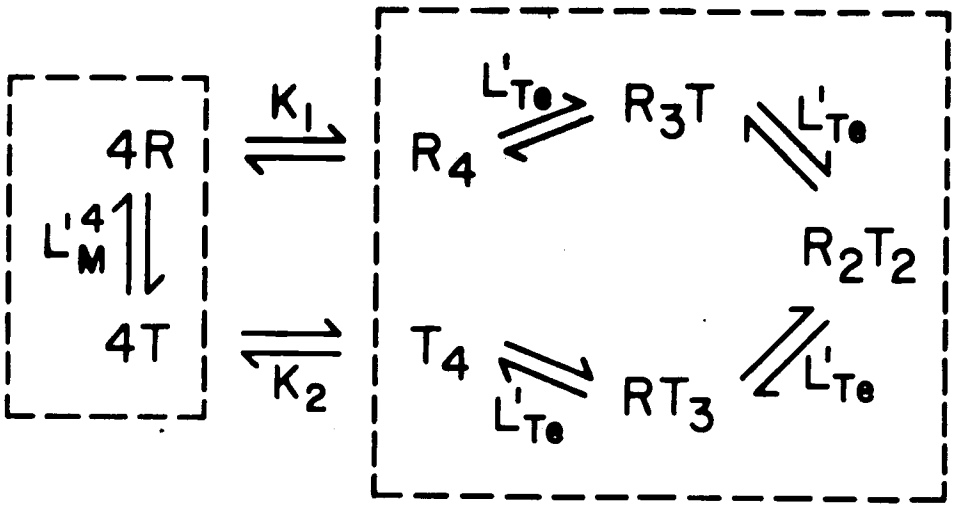

Figure 1

The scheme in Fig. 1 implicitly includes equilibria like $R + 3T \rightleftharpoons RT_3$, for example, which has the association constant $L'^{-3}_M K_1 L'^3_{Te}$ (or $L'_M K_2 L'_{Te}$). The allosteric equilibrium constants L'_M and L'_{Te} are functions of all three ligands, but K_1 and K_2 are functions of only two ligands, Mg^{2+} (or Ca^{2+}) and H^+. This means that I am assuming that any influence of oxygen on the association equilibrium is indirect, arising only from the different association constants (K_1, K_2) of the R and T states. Since we assumed that the Mg^{2+} binding sites linked to association are <u>not</u> linked to oxygen binding, the binding polynomial is factorable into two parts, one being a function of all three ligands and the other being a function of two ligands only, i.e.:

$$\sum_M = f_M(a_A, a_B, a_C) \cdot g_M(a_B, a_C)$$

$$\sum_{Te} = f_{Te}(a_A, a_B, a_C) \cdot g_{Te}(a_B, a_C) \qquad (7)$$

(For factorability of the binding polynomial, see Wyman, 1967.)

Heck has pointed out that we can define the binding potential as that function whose partial derivative with respect to the chemical potential of a component yields the amount of that component in chemical combination with the macromolecule (Heck, 1971):

$$\frac{\partial \Pi}{\partial \mu} = \bar{\nu} \tag{8}$$

Since $\Pi = RT \ln \sum$ and $\mu = \mu_0 + RT \ln a_L$, eq. (8) becomes:

$$\frac{\partial \ln \sum}{\partial \ln a_L} = \bar{\nu} \tag{8a}$$

That is to say, we can define the binding polynomial as that function, the derivative of whose logarithm with respect to the logarithm of the activity of a ligand yields the amount of that ligand in chemical combination with the macromolecule. Eq. (8a) is also directly derived from the general expression of the binding polynomial (2) or (3). We can now use eq. (8a) to determine the expression of $\sum$, if we know $\bar{\nu}$ as a function of L.

In case of oxygen binding, from the assumption of the non-exclusive MWC model, we have:

$$\bar{\nu} = n\bar{Y} = \frac{n\alpha(1+\alpha)^{n-1} + nL'c\alpha(1+c\alpha)^{n-1}}{(1+\alpha)^n + L'(1+c\alpha)^n} \tag{9}$$

$$L' = \left\{ \frac{d\beta + (1+\gamma)^2}{\beta + (1+e\gamma)^2} \right\}^h L^0, \qquad (10)$$

where α is the reduced concentration of the substrate ($k_R a_A$), in this case reduced oxygen partial pressure (Miller and Van Holde, 1974), β and γ are the reduced activities of the effectors ($\beta = k'_R a_B$, $\gamma = k''_T a_C$), c is the ratio of the binding constant of oxygen for T state and R state (k_T/k_R), n and h are the numbers of the substrate (oxygen) and effectors per allosteric unit respectively. In order to obtain eq. (10), it is assumed that the two effectors compete each other for the same binding sites as mentioned above. Comparing the equations (8a) and (9), we see:

$$\sum = (1+L')^{-1}\{(1+\alpha)^n + L'(1+c\alpha)^n\} \qquad (11)$$

Eq. (11) is verified by taking the logarithm and partially differentiating with respect to ln α. Note that $1/(1+L')$ and $L'/(1+L')$ are the fractions of R state and T state respectively. We may write for our system, n being six:

$$f_M = (1+L'_M)^{-1}\{(1+\alpha)^6 + L'_M(1+c\alpha)^6\}$$

$$f_{Te} = (1+L'_{Te})^{-4}\{(1+\alpha)^6 + L'_{Te}(1+c\alpha)^6\}^4 \qquad (12)$$

f_M and f_{Te} are defined in eq. (7) (see Fig. 1 for L'_M and

L'_{Te}). The power 4 for f_{Te} comes from the fact that there are four monomer units which are not linked to each other. It is assumed that c and k_R will not change in monomer and tetramer.

If there are (p + r) binding sites on a macromolecule for B, each of which consists of a pair of groups, each group capable of binding one mole of ligand C (in this case hydrogen ion), or each pair of groups capable of binding one mole of ligand B, then the average number of bound ligand B is given as below, neglecting the electrostatic interaction:

$$\bar{\nu}_B = \frac{(p+r)k_B a_B}{k_B a_B + (1+k_C a_C)^2} \tag{13}$$

(see, e.g., C. Tanford, 1961). From this, we may write:

$$\sum = \{k_B a_B + (1+k_C a_C)^2\}^{p+r}$$

For g_M and g_{Te}, I simply assume that the affinity of p binding sites on the monomer for ligand B is negligible, but the affinity for ligand C is very strong. On the other hand, I assume that 4p binding sites on the tetramer have strong affinity for ligand B, but not for ligand C. Putting $k_B = 0$ and $k_C = 0$ for the binding polynomial of p (for monomer) and 4p (for tetramer) binding sites, we obtain:

$$g_M = (1+k_C a_C)^{2p}\{k_B a_B + (1+k_C a_C)^2\}^r$$

$$g_{Te} = (1+k_B a_B)^{4p}\{k_B a_B + (1+k_C a_C)^2\}^{4r} \qquad (14)$$

The power 4p and 4q in g_{Te} come from the fact that the tetramer has totally 4p + 4q independent binding sites. From (7), (12) and (14), we obtain:

$$\sum_M = (1+L'_M)^{-1}\{(1+\alpha)^6 + L'_M(1+c\alpha)^6\}(1+k_C a_C)^{2p}\{k_B a_B + (1+k_C a_C)^2\}^r$$

$$\sum_{Te} = (1+L'_{Te})^{-4}\{(1+\alpha)^6 + L'_{Te}(1+c\alpha)^6\}^4(1+k_B a_B)^{4p}\{k_B a_B + (1+k_C a_C)^2\}^{4r}$$

$$L'_M = \left\{\frac{d\beta + (1+\gamma)^2}{\beta + (1+e\gamma)^2}\right\}^h L^0_M \,, \quad L'_{Te} = \left\{\frac{d\beta + (1+\gamma)^2}{\beta + (1+e\gamma)^2}\right\}^h L^0_{Te} \qquad (15)$$

where $\beta = k'_R a_B$, $\gamma = k''_T a_C$; it is assumed that the difference between L'_M and L'_{Te} solely comes from the difference between L^0_M and L^0_{Te}. Equation (15) naturally satisfy the relations:

$$(\bar{\nu}_A)_M = 6(\bar{Y}_A)_M = \frac{\partial \ln \Sigma_M}{\partial \ln \alpha} = \frac{6\{\alpha(1+\alpha)^5 + L'_M c\alpha(1+c\alpha)^5\}}{(1+\alpha)^6 + L'_M(1+c\alpha)^6}$$

$$(\bar{\nu}_A)_{Te} = 24(\bar{Y}_A)_{Te} = \frac{\partial \ln \Sigma_{Te}}{\partial \ln \alpha} = \frac{24\{\alpha(1+\alpha)^5 + L'_{Te}c\alpha(1+c\alpha)^5\}}{(1+\alpha)^6 + L'_{Te}(1+c\alpha)^6}$$

Putting eq. (15) into eq. (6), we obtain:

$$K = K_0\{\frac{(1+L'_M)}{(1+L'_{Te})} \cdot \frac{(1+\alpha)^6 + L'_{Te}(1+c\alpha)^6}{(1+\alpha)^6 + L'_M(1+c\alpha)^6}\}^4 \frac{(1+k_Ba_B)^{4p}}{(1+k_Ca_C)^{8p}} \qquad (16)$$

This is the principal result of this section. It expresses the association constant between monomer and tetramer as a function of the concentrations of all three ligands. To obtain a simpler picture of the effect of oxygen binding on the association, let us take the limit $\alpha \to 0$ and $\alpha \to \infty$ of eq. (16):

$$K_{\alpha\to 0} = K_0 \frac{(1+k_Ba_B)^{4p}}{(1+k_Ca_C)^{8p}} \qquad (17\text{-}1)$$

$$K_{\alpha\to\infty} = K_0 \{\frac{(1+L'_M)}{(1+L'_{Te})} \cdot \frac{(1+c^6L'_{Te})}{(1+c^6L'_M)}\}^4 \frac{(1+k_Ba_B)^{4p}}{(1+k_Ca_C)^{8p}} \qquad (17\text{-}2)$$

Eq. (17-1) and (17-2) correspond to the association equilibria of the fully deoxygenated and fully oxygenated state of the hemocyanin respectively (see the results of association equilibrium studies in the Results section). The fraction of R state, $\bar{R}$, in the present case has the range:

$$\frac{1}{1 + L'_M} \leq \bar{R} \leq \frac{1}{1 + L'_{Te}c^6}$$

If L'_M is large enough and $L'_{Te}c^6$ is small enough so that R has the range between 0 and 1 in the limit of $\alpha \to 0$ and $\alpha \to \infty$, $K_{\alpha\to 0} = K_2$ and $K_{\alpha\to\infty} = K_1$. The quantities K_1, K_2, L'_M and L'_{Te} are defined in Fig. 1. Since $10^3 \leq L'_M$ or $L'_{Te} \leq 10^{12}$ under the normal conditions and $c^6 \simeq 10^{-12}$ for the hemocyanin, these conditions are satisfied, with the exception that $L'_{Te} \sim 10^{12}$ (see the discussion of oxygen binding study, in the Discussion section).

If we take the partial derivative of ln K with respect to the logarithm of the concentrations of the three ligands, we obtain the following results:

$$(1)\quad \frac{\partial \ln K}{\partial \ln a_A} = \frac{\partial \ln K}{\partial \ln \alpha} = 4\{\frac{\alpha(1+\alpha)^5 + L'_{Te}c\alpha(1+c\alpha)^5}{(1+\alpha)^6 + L'_{Te}(1+c\alpha)^6} - \frac{\alpha(1+\alpha)^5 + L'_M c\alpha(1+c\alpha)^5}{(1+\alpha)^6 + L'_M(1+c\alpha)^6}\} = \Delta\bar{A} \qquad (18\text{-}1)$$

$$\Delta\bar{A} = 4\ \{(\bar{Y}_A)_{Te} - (\bar{Y}_A)_M\}$$

From this, we see that if the left hand side of eq. (18-1) can be measured in some way, $(\bar{Y}_A)_{Te} - (\bar{Y}_A)_M$ namely the difference in 0_2 saturation between tetramer and monomer will be known. It is unfortunately not practical to

determine K as a function of partial pressure of oxygen at the present stage; such experiments would require precise control of oxygenation under conditions where the association equilibrium could be studied.

$$(2) \qquad \frac{\partial \ln K}{\partial \ln a_B} = \frac{4p\ k_B a_B}{1 + k_B a_B} + \delta_B = \Delta\bar{B} + \delta_B \qquad (18\text{-}2)$$

$$\Delta\bar{B} = \frac{4p\ k_B a_B}{1 + k_B a_B}$$

$$= (\bar{B})_{Te} - (\bar{B})_M$$

$$\delta_B = \frac{4\beta h(L'_M - L'_{Te})\{(1+\gamma)^2 - d(1+e\gamma)^2\}\{(1+\alpha)^6 - (1+c\alpha)^6\}\{L'_{Te}L'_M(1+c\alpha)^6 - (1+\alpha)^6\}}{(1+L'_{Te})(1+L'_M)xx'f_M f_{Te}}$$

$$x = d\beta + (1+\gamma)^2,\ x' = \beta + (1+e\gamma)^2$$

$$f_M = (1+\alpha)^6 + L'_M(1+c\alpha)^6,\ f_{Te} = (1+\alpha)^6 + L'_{Te}(1+c\alpha)^6$$

Apparently $\delta_B \to 0$, in the limit of $a_B \to 0$. Although the expression of δ_B is not simple, we see that in the limit of $\alpha = 0$, $\delta_B = 0$. In the limit of $\alpha \to \infty$, δ_B has the form:

$$\delta_B = \frac{4\beta h(L'_M - L'_{Te})\{(1+\gamma)^2 - d(1+e\gamma)^2\}(1-c^6)(L'_{Te}L'_M c^6 - 1)}{(1+L'_{Te})(1+L'_M)(1+L'_{Te}c^6)(1+L'_M c^6)xx'}$$

where $L'_M > L'_{Te}$, $d,e < 1$. The sign of δ_B, therefore, depends on the magnitude of the term $L'_{Te}L'_M c^6 - 1$. If $L'_{Te}L'_M c^6 < 1$, $\delta_B < 0$, and if

$L'_{Te}L'_{M}c^6 > 1$, $\delta_B > 0$. At pH 8.0, where $L'_{Te} \sim 10^6$, $c^6(L'_{M}L'_{Te} + 1) > 1$ (see the results of oxygen binding study) and $\delta_B \gtrsim 0$. Since $\delta_B = 0$ in the absence of the substrate, we could estimate the magnitude of δ_B comparing the slope of the plot ln K vs. ln a_c between oxygenated state and de-oxygenated state. I will come back to this problem in the results section.

(3)
$$\frac{\partial \ln K}{\partial \ln a_c} = \frac{-8P\ k_c a_c}{1 + k_c a_c} + \delta_C \qquad (18\text{-}3)$$

$$= \Delta\bar{C} + \delta_C$$

$$\Delta\bar{C} = \frac{-8P\ k_c a_c}{1 + k_c a_c} = (\bar{C})_{Te} - (\bar{C})_{M}$$

$$\delta_C = \frac{-8\gamma h(L'_M - L'_{Te})\,[(1+\gamma)x' - e(1+e\gamma)x]\{(1+\alpha)^6 - (1+c\alpha)^6\}\{L'_{Te}L'_M(1+c\alpha)^6 - (1+\alpha)^6\}}{(1+L'_{Te})(1+L'_M)xx'f_M f_{Te}}$$

On the same basis as in (2), δ_C can be either positive or negative.

δ_B and δ_C arise from the partial derivatives of the term below in eq. (16) with respect to a_B or a_C:

$$\left\{ \frac{1+L'_M}{1+L'_{Te}} \quad \frac{(1+\alpha)^6 + L'_{Te}(1+c\alpha)^6}{(1+\alpha)^6 + L'_M(1+c\alpha)^6} \right\}^4$$

where L'_M and L'_{Te} are functions of a_B and a_C whose forms are given in eq. (15). That is to say, δ_B and δ_C are considered to be some contribution from the Mg^{2+} and H^+ which do not bind tetramer or monomer preferentially, but prefer to bind R state or T state, thereby affecting the association equilibrium constant indirectly.

I now turn to a more general model, in which hybrid hexamers containing hybrid mixtures of R and T states are taken into consideration. As mentioned previously, the extended MWC model which takes the symmetrical hybrid state $H(r_3t_3)$ into account (Buc, Johannes and Hess, 1973) fits better for the hemocyanin (Miller and Van Holde, 1974), where r and t denote the R state and T state of the subunit respectively (in this paper, R, T and H designate the states of monomer which consists of six subunits). The hybrid state was introduced in order to account for the fact that the maximum Hill coefficient, n_H, is smaller than expected from the concerted model. Only symmetrical species were incorporated to the model, based on the fact that the curve $n_H = f(\alpha_{1/2})$ is reasonably symmetrical (Johannes and Hess, 1973). A diagram corresponding to Fig. 1 is depicted in Fig. 2. According to Buc, Johannes and Hess (1973), L', H' and q are defined as below:

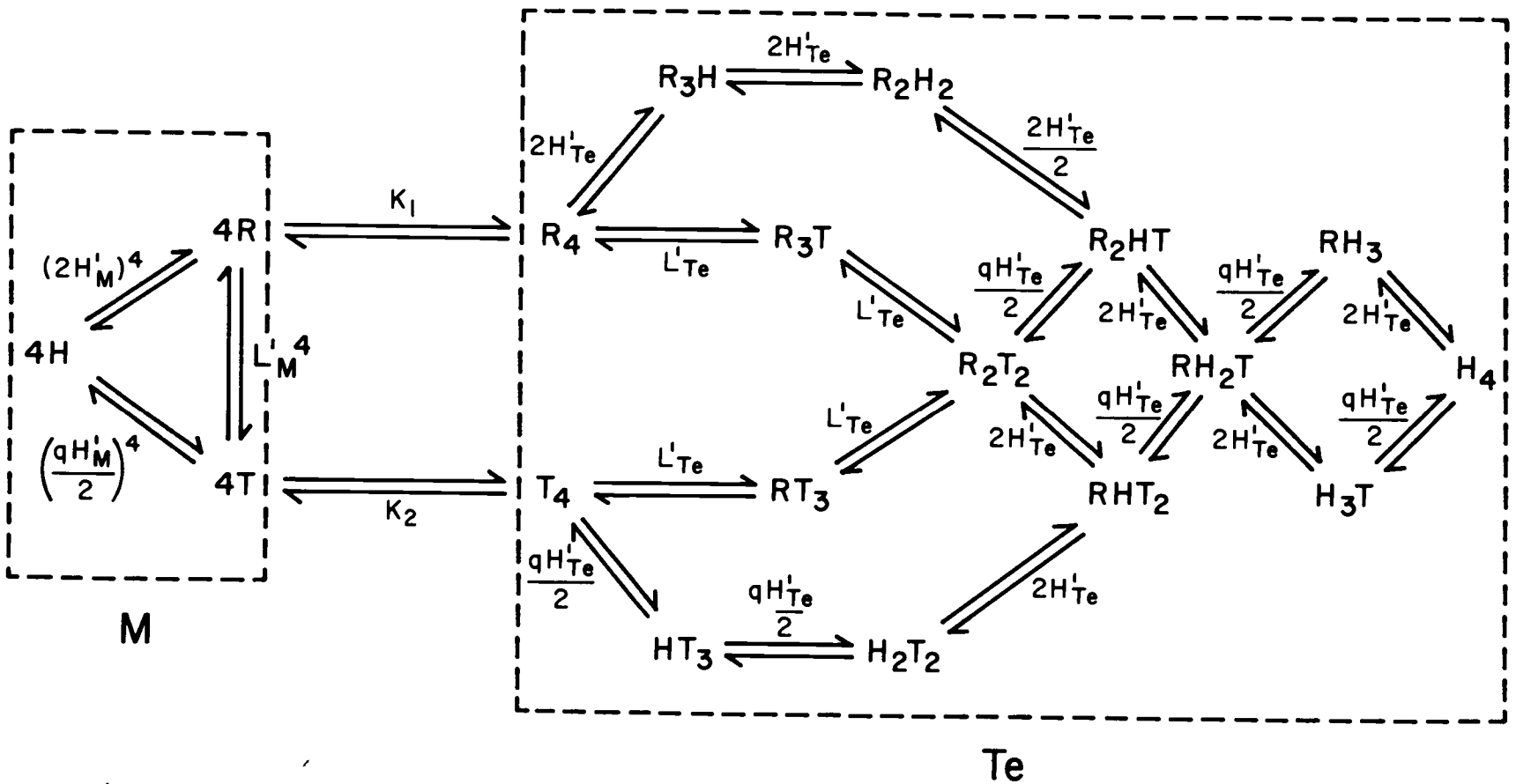

Figure 2. A conformational equilibrium coupled with monomer-tetramer association in the framework of the extended model

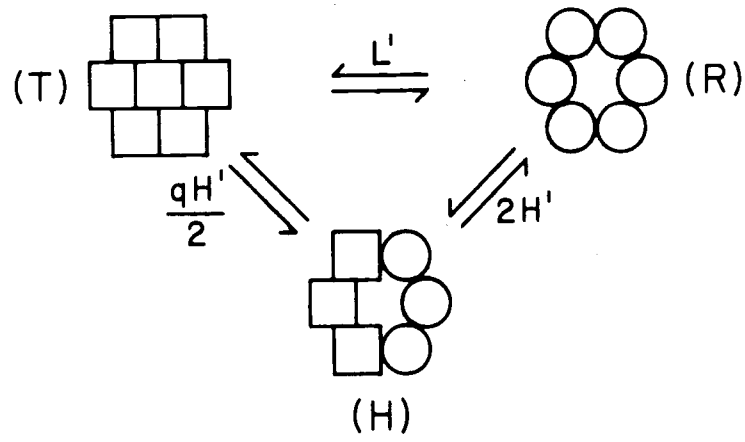

with $\frac{[T]}{[R]} \equiv L'$, $\frac{[H]}{[R]} \equiv 2H'$, $\frac{[T]}{[H]} \equiv qH'/2$. $H' = \sqrt{L'/q}$.

As assumed before based on the experimental results (Miller and Van Holde, 1974; also the results of the oxygenbinding study in the present paper), it is also assumed here that the binding of ligands are not linked between monomer units in tetramer. Upon association to tetramer, the conformational equilibrium constants change from L'_M and H'_M to L'_{Te} and H'_{Te}. The binding polynomyal of this system corresponding to f_M and f_{Te} in eq. (7) is derived with the aid of a diagram in Fig. 3, which is an extension of Fig. 10 of Johannes and Hess (1973):

$$f = (1+\alpha)^6 + L'(1+c\alpha)^6 + 2\sqrt{L'/q}\,(1+\alpha)^3(1+c\alpha)^3 \qquad (19)$$

It immediately follows that,

$$\frac{\partial \ln f}{\partial \ln \alpha} = \bar{\nu}_A = 6\bar{Y}_A$$

$$= \frac{6\alpha(1+\alpha)^5+6L'c\alpha(1+c\alpha)^5+6\sqrt{L'/q}\{\alpha(1+\alpha)^2(1+c\alpha)^3+c\alpha(1+\alpha)^3(1+c\alpha)^2\}}{(1+\alpha)^6+L'(1+c\alpha)^6+2\sqrt{L'/q}(1+\alpha)^3(1+c\alpha)^3}$$

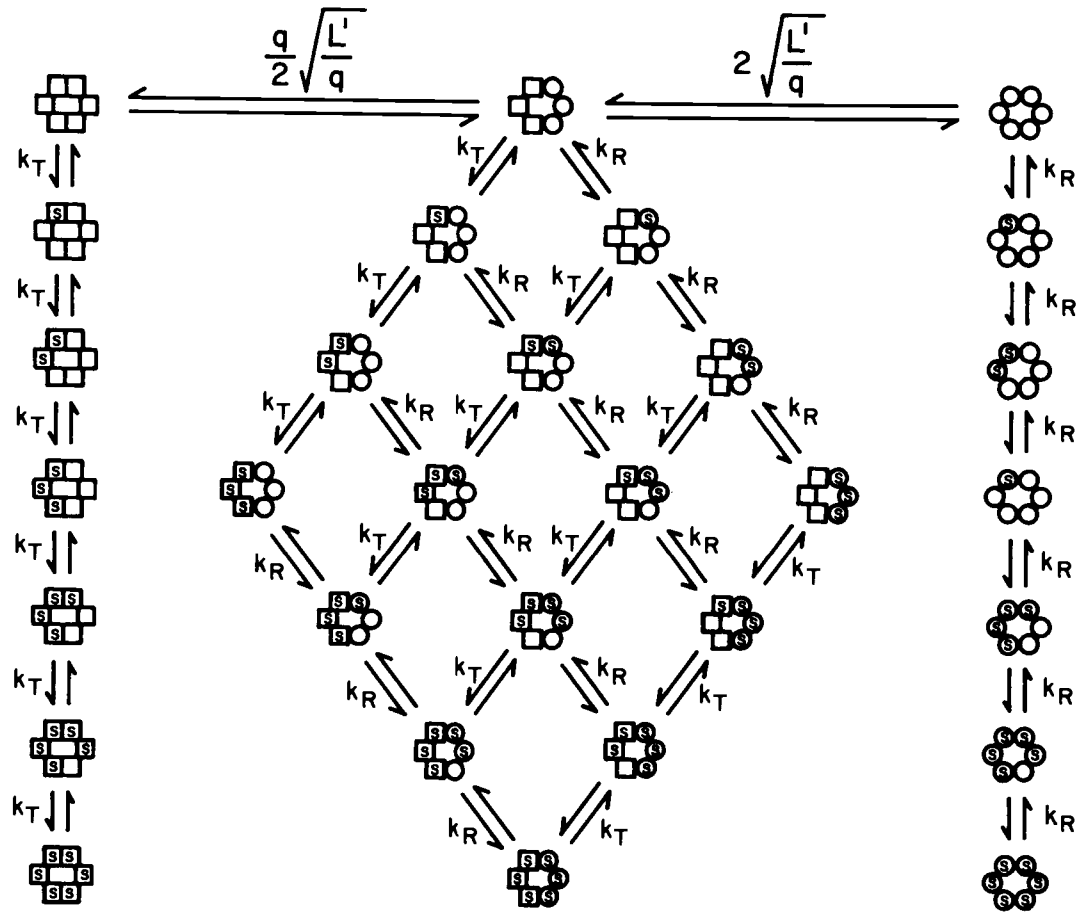

Figure 3. Binding scheme for a hexamer, using the extended model, and including a hybrid state.

Thus we obtain:

$$f_M = (1+L'_M + 2\sqrt{L'_M/q})^{-1}\{(1+\alpha)^6 + L'_M(1+c\alpha)^6 + 2\sqrt{L'_M/q}\ (1+\alpha)^3(1+c\alpha)^3\} \tag{20-1}$$

$$f_{Te} = (1+L'_{Te} + 2\sqrt{L'_{Te}/q})^{-4}\{(1+\alpha)^6 + L'_{Te}(1+c\alpha)^6 + 2\sqrt{L'_{Te}/q}\ (1+\alpha)^3(1+c\alpha)^3\}^4 , \tag{20-2}$$

where q is assumed to be the same in both monomer and tetramer for the sake of simplicity. Substituting eq. (20-1), (20-2) and (14) into eq. (7) and combining with eq. (16), we obtain eq. (21) instead of eq. (16):

$$K = K_0 \left\{\frac{(1+L'_M+2\sqrt{L'_M/q})}{(1+L'_{Te}+2\sqrt{L'_{Te}/q})}\right. \cdot \left.\frac{(1+\alpha)^6+L'_{Te}(1+c\alpha)^6+2\sqrt{L'_{Te}/q}(1+\alpha)^3(1+c\alpha)^3}{(1+\alpha)^6+L'_M(1+c\alpha)^6+2\sqrt{L'_M/q}(1+\alpha)^3(1+c\alpha)^3}\right\}^4 \cdot \frac{(1+k_Ba_B)^{4P}}{(1+k_Ca_C)^{8P}} \tag{21}$$

Consequently, we obtain a series of equations below:

Corresponding to eq. (17-1) and (17-2),

$$K_{\alpha\to 0} = K_0 \frac{(1+k_Ba_B)^{4P}}{(1+k_Ca_C)^{8P}} \tag{22-1}$$

$$K_{\alpha\to\infty} = K'\left\{\frac{1+L'_M+2\sqrt{L'_M/q}}{1+L'_{Te}+2\sqrt{L'_{Te}/q}} \cdot \frac{1+c^6L'_{Te}+2c^3\sqrt{L'_{Te}/q}}{1+c^6L'_M+2c^3\sqrt{L'_M/q}}\right\}^4 (1+k_Ba_B)^{4P}$$

$$\simeq K'\left\{\frac{1+L'_M+2\sqrt{L'_M/q}}{1+L'_{Te}+2\sqrt{L'_{Te}/q}}\right\}^4 (1+k_Ba_B)^{4P} ,$$

Following the same argument for eq. (17-1) and (17-2), $K_{\alpha\to 0} = K_2$ and $K_{\alpha\to\infty} = K_1$ except where L'_{Te} and L'_M is close to 10^{12}. Corresponding to eq. (18-1) through (18-3),

$$(1)' \quad \frac{\partial \ln K}{\partial \ln a_A} = \frac{\partial \ln K}{\partial \ln \alpha} = 4X$$

$$\left[\frac{\alpha(1+\alpha)^5+c\alpha L'_{Te}(1+c\alpha)^5+\sqrt{L'_{Te}/q}\{\alpha(1+\alpha)^2(1+c\alpha)^3+c\alpha(1+\alpha)^3(1+c\alpha)^2\}}{(1+\alpha)^6+L'_{Te}(1+c\alpha)^6+2\sqrt{L'_{Te}/q}(1+\alpha)^3(1+c\alpha)^3}\right. \tag{23-1}$$

$$\left. - \frac{\alpha(1+\alpha)^5+c\alpha L'_M(1+c\alpha)^5+\sqrt{L'_M/q}\{\alpha(1+\alpha)^2(1+c\alpha)^3+c\alpha(1+\alpha)^3(1+c\alpha)^2\}}{(1+\alpha)^6+L'_M(1+c\alpha)^6+2\sqrt{L'_M/q}(1+\alpha)^3(1+c\alpha)^3}\right]$$

$$= \Delta\bar{A} , \qquad \Delta\bar{A} = 4\{(\bar{Y}_A)_{Te} - (\bar{Y}_A)_M\}$$

$$(2)' \quad \frac{\partial \ln K}{\partial \ln a_B} = \frac{4P\, k_Ba_B}{1+k_Ba_B} + \delta'_B \tag{23-2}$$

$$= \Delta\bar{B} + \delta'_B , \quad \Delta\bar{B} = (\bar{B})_{Te} - (\bar{B})_M$$

$$\delta'_B = 0 \text{ when } \alpha\ (=k_A a_A) = 0 \text{ or } a_B = 0$$

$$(3)' \quad \frac{\partial \ln K}{\partial \ln a_C} = \frac{-8P\ k_C a_C}{1 + k_C a_C} + \delta'_C \qquad (23\text{-}3)$$

$$= \Delta\bar{C} + \delta'_C\ ,\ \Delta\bar{C} = (\bar{C})_{Te} - (\bar{C})_M$$

$$\delta'_C = 0 \text{ when } \alpha = 0 \text{ or } a_C = 0$$

These equations express, as before, the way in which the association constant depends upon the activities of the three kinds of ligand molecules.

MATERIALS AND METHODS

Isolation and Purification of Hemocyanin

Callianassa californiensis, the ghost shrimp, were collected at Yaquina Bay, Oregon and bled by puncturing the ventral abdominal sinus with a capillary tube. The hemolymph was first centrifuged at 6,000 r.p.m. for 30 min to remove the clotting materials and other debris, and filtered with a millipore filter with a pore size of 0.8 μm. The filtrate was then purified by gel filtration on a Bio-Gel A5m column as described by Roxby et al. (1974). The column was eluted with 0.1 ionic strength Tris buffer (pH 7.65) containing 0.05 M $MgCl_2$ and 0.01 M $CaCl_2$. Elution profiles show two clearly separated peaks, corresponding to components with sedimentation coefficients of approximately 39 and 17S, respectively. The 39S material shows reversible dissocation into 17S particles upon removal of divalent cations and reassociates to 39S form when Mg^{2+} is dialyzed back in. The 17S component from the column, however, is incompetent to associate to the 39S form under any conditions tested. In this research I worked exclusively with the "competent" 39S material.

Preparation of Solutions

Solutions were prepared using 0.1 ionic strength Tris buffer, as described by Long (1961). For pH's lower than 7.0, cacodylic acid-sodium cacodylate buffer was employed. Doubly distilled water was used. The hemocyanin concentrations were routinely determined with a Cary 15 spectrophotometer, using the $E^{1\%}_{1cm}$ value of 14.0 for the associated 39S form and 13.3 for the dissociated 17S form at 280 nm, as given by Roxby et al. (1974). In the case of Mg^{2+} binding studies, the final concentrations of the sample were determined by measuring copper content by using atomic absorption spectroscopy as described below.

Preparation of Apohemocyanin

Apohemocyanin was prepared according to the procedure of Cohen and Van Holde (1964). A sample of about 100 mg was dialyzed against 0.1 I Tris, pH 7.65 without divalent cations. The dialysis bag was then placed in one l of 0.1 I Tris, pH 7.65 and bubbled with N_2. Four hours later, 0.490 g of NaCN was added and N_2 bubbling continued for 20 hrs. The dialysis bag was then transferred to 0.1 I Tris, pH 7.65 to dialyse out excess NaCN with several changes of buffer. The absorption of 337 nm of the hemocyanin disappeared completely and no Cu was detected by atomic absorption spectroscopy. (The limit of detection was about 0.05

ppm, this would indicate that no more than 0.1 percent of the copper remained.)

Sedimentation Velocity

Sedimentation velocities were measured with the Spinco Model E analytical ultracentrifuge. The ultraviolet optical scanner was used exclusively. During the time when these experiments were being done, the linearity of the scanner with respect to absorbance was checked (R. T. Kovacic, 1976). A wave length between 280 nm and 300 nm was used, depending on the protein concentration. Protein concentration was usually about 1 mg/ml. When a single component or well resolved multiple components were present, each sedimentation coefficient was determined from the motion of the point of half maximum absorbance and the weight average sedimentation coefficient, $\bar{s}_w$, was then calculated, if multiple components were present, $\bar{s}_w$ is defined as below:

$$\bar{s}_w \equiv \frac{\sum_i s_i C_i}{\sum_i C_i} = \frac{\sum_i s_i A_i}{\sum_i A_i}, \tag{24}$$

where C_i is the weight concentration of the component i, s_i is the sedimentation coefficient of the component i at the

concentration C_i and A_i is the absorption of i component from the scanner. In these experiments the number of the components is two; e.g., a 17S form and a 39S form. Under the normal conditions, i.e. at pH values higher than 7.3, the reaction of the association to 39S and the dissociation into 17S is so slow that the boundaries are well resolved throughout a run. In such cases the ratio of the two components was determined by the ratio of the height of each component from the scans. When it was necessary, the effect of radial dilution was taken into consideration in order to obtain the correct relative amount of the two forms. It can be shown that:

$$\left(\frac{C_1}{C_2}\right)(t) = \left(\frac{C_1}{C_2}\right)_{t=t_0} e^{-2(S_1-S_2)\omega^2(t-t_0)} , \qquad (25)$$

where $(C_1/C_2)(t)$ is the ratio of the concentration of component 1 (39S) and component 2 (17S) at time t, S_1 and S_2 are the sedimentation coefficients of those components, ω is the angular velocity and t is the time. The effective zero time can be obtained if ln r is plotted with respect to t and extrapolated to ln r_0, r_0 being the position of the meniscus. From (25),

$$\ln\left(\frac{C_1}{C_2}\right) = \ln\left(\frac{C_1}{C_2}\right)_0 - K(t - t_0) \qquad (26)$$

$$K = 2(S_1 - S_2)\omega^2$$

If $\ln(C_1/C_2)$ is plotted against $(t - t_0)$ and extrapolated to $t = t_0$, the correct ratio of the two components are obtained. It turned out that the error of $\bar{s}_w$ values, if we neglect the radial dilution, was between zero and five percent and there are no significant qualitative differences. Therefore, except in cases where the numerical values of a thermodynamic quantity were calculated, the effect of radial dilution was neglected.

At pH value of 7.3 or lower, on the other hand, boundaries appeared to be diffuse and were not well resolved. Under these conditions, the association-dissocation reactions were sufficiently rapid that re-equilibration occurred during the experiment. In such cases the second moment of the concentration gradient was calculated from the scans, using a Hewlett-Packard 9821A calculator connected with a Hewlett-Packard 9864A digitizer. The second moment of the concentration gradient r_m is defined as below:

$$r_m^2 \equiv \{\int_0^{r_p} r^2 \frac{dC}{dr} \cdot \alpha r\} / \{\int_0^{r_p} \frac{dC}{dr} \cdot dr\}$$

which, upon integration by parts yields the form:

$$r_m^2 = r_p^2 - \frac{2}{A_p} \int_0^{r_p} r \, A dr$$

where r_p is any radial position in the plateau region, r_a is an arbitrary position in the solution column cleared of the sedimenting material, A is the absorbance at the radial position r, and A_p is the absorbance at r_p. The program, written by Neal Eldred, calculates the second moment of the boundaries of each scan and then calculates the weight average sedimentation coefficient (see Miller et al., 1977). For a single component the conventional half maximum absorbance method coincides well with the result obtained by this method. Sedimentation experiments were performed at 20°C except for some experiments connected with oxygen binding studies, where samples were run at 25°C.

In experiments in which deoxygenated hemocyanin was used, the cell was loaded under a nitrogen atmosphere in a glove bag. Hemocyanin is almost fully oxygenated when in contact with air under normal conditions. At low pH or low concentration of Mg^{2+}, however, it is not fully saturated. Therefore, in all experiments specified as "oxygenated" the cells were loaded under an oxygen atmosphere in a glove bag.

Light Scattering

The light scattering was measured on a computer controlled polarization spectrometer constructed in Professor I. Isenberg's laboratory (Ayres et al., 1974). The measurements were made at 90° by setting the excitation

and emission monochrometers at 435 nm and the incident and emission polarizers in a vertical position. The fluctuations in intensity I_E were corrected by measuring I_E/L, where L is the lamp intensity which was measured simultaneously. A volume of 0.35 ml of twice concentrated hemocyanin solution in Tris pH 8.0, 0.1 I was mixed with the same volume of Tris buffer pH 8.0, 0.1 I with 0.1 M $MgCl_2$ in a cell which has the path length of 5 mm. The time course of the change in scattered intensity was automatically recorded. For each measurement 1500 samples of signals were averaged in two minutes.

Oxygen Binding Studies

Measurement of oxygenation of the hemocyanin was based on the 337 nm absorbance band as described by Miller and Van Holde (1974). Hemocyanin (4.5 ml of 3.0 mg/ml) was placed in a glass tonometer of 108 ml with sidearms of 0.17, 1.18 or 5.69 ml depending on the oxygen affinity of the hemocyanin. The tonometer was then evacuated and increments of air of O_2 added. Evacuation was performed three times to ensure that the deoxygenation was completed, judging from the UV spectrum. In cases where the hemocyanin is not fully saturated at 1 atm of air or 1 atm of O_2, 1/O.D. was plotted against $1/pO_2$ and extrapolated to obtain the O.D. at fully saturated state. All binding curves were made at 25 ± 0.1°C. For each condition, an

aliquot was taken from the same solution for a velocity sedimentation experiment at the same temperature.

Fluorescence Measurements

The quenching of the intrinsic fluorescence of hemocyanin upon oxygenation was measured by using the Hitachi-Perkin Elmer MPF-2A fluorescence spectrophotometer. A sample of a hemocyanin solution of about 0.3 mg/ml with or without 50 mM Mg^{2+} at pH 7.65 was placed in the tonometer and evacuated. At each oxygen pressure, the UV spectrum between 300 nm and 360 nm and the fluorescence spectrum were recorded. The excitation wave length was 280 nm.

Binding Studies of Mg^{2+} and Ca^{2+}

Binding of Mg^{2+} and Ca^{2+} by the hemocyanin was measured by the equilibrium dialysis method. Hemocyanin solutions eluted from a Bio-Gel A5m column were pooled and centrifuged at 80,000 g for 10 hrs. The pellet was dissolved into 0.1 I Tris buffer solution at pH 7.65. Thus concentrated material was diluted to about 30 mg/ml. Samples were then dialyzed against Tris buffers of desired pH and Mg^{2+} (or Ca^{2+}) concentrations for 20 to 24 hrs. Magnesium binding was determined in the presence of 0.1 mM EGTA. Although most of the experiments in this thesis were performed with the hemocyanin which was pretreated with EDTA, Mg^{2+} binding was the earliest experiment and at

that time samples were not treated with EDTA in advance. Instead, Mg^{2+} binding was determined with a buffer which contains 0.1 mM of EGTA in order to remove Ca^{2+} from the system. For Ca^{2+} binding measurement, samples were first dialyzed against 0.1 Tris buffer pH 7.65 with desired Ca^{2+} concentration. The Mg^{2+} (or Ca^{2+}) concentrations and copper content of solutions outside and inside of the dialysis tube were measured by atomic absorption spectroscopy, using a Perkin-Elmer Model 403 spectrometer. Preliminary experiments showed no measurable interference from the protein. Standard solutions were prepared with $CaCO_3$ (Mallinckrodt #4072), $MgCl_2$ $6H_2O$ (J. T. Baker Analytical #2444) and copper metal (Fisher Scientific Company #C-430) according to the Perkin-Elmer manual. Standard curves were linear up to 10 ppm for Ca^{2+} and Cu^{2+} and 1 ppm for Mg^{2+}. Samples were serially diluted into these concentration ranges for the measurement. In order to minimize the error upon dilution the weights of the samples were measured at each stage of dilution and the volumes were calculated from the density of the solution. The density of the hemocyanin solution was calculated from the relationship: $\rho = \rho_0 + (1 - \bar{v}_0)C$, where ρ_0 is the density of the pure buffer, $\bar{v}$ is the partial specific volume of the protein (0.724 ml/g in this case, Roxby et al., 1974) and C is the concentration of the protein.

The activities of Mg^{2+} and Ca^{2+} were calculated according to Davies' empirical formula which is based on the Debye-Hueckel theory (see Stumm and Morgan, 1970):

$$\log \gamma_{\pm} = -AZ_{\pm}^2 \left(\frac{\sqrt{I}}{1 + \sqrt{I}} - 0.3\ I\right) \qquad (27)$$

$$A = 1.82 \times 10^6 (\varepsilon T)^{-3/2}$$

at 20°C, $\varepsilon = 80.36$. (There is a typographical error on page 83 of Stumm and Morgan. The power of (εT) should read -3/2 instead of 2/3 as given in that text.) Equation (27) applies well in the range of the ionic strength employed; e.g. up to an ionic strength of 0.35. The equation is recommended for use below ionic strength of 0.5 by the same authors as above. The contribution of the protein to the ionic strength was neglected. In case of divalent cation binding studies, however, the protein concentration is a about 30 mg/ml which is rather high. The calculated $\gamma_{\pm}$ values in this case, therefore, should be taken as a convenient approximation, which might well contain errors of several percent.

The excluded volume of the protein was also taken into consideration. It turned out that the excluded volume of the hydrated protein cannot be ignored at Mg^{2+} concentrations of more than about five mM at this concentration of the protein. Accordingly, the Mg^{2+} concentration outside

the dialysis bag was multiplied by $1 - (\bar{v} + \delta v_0)c$ before subtracted from that of inside; where $\bar{v}$ is the partial specific volume, δ is the hydration assuming a typical value for proteins, $\delta = 0.3$ g/g (Kuntz and Kauzmann, 1974), v_0 is the specific volume of the solvent and c is the concentration of the protein (g/ml).

The protein concentration was determined from the copper content of the sample. Two copper atoms per 72,000 daltons was assumed (Roxby et al., 1974).

Magnesium binding in the absence of O_2 was also measured. In that case purified nitrogen was bubbled through buffer solutions during incubation. The blue color of hemocyanin disappeared within an hour.

Amino Acid Analysis

The amino acid analysis was carried out according to Spackman et al. (1958) using a modified Spinco 120B (Beckman) amino acid analyzer. Cysteine and cystine were determined as cysteic acid by treating 0.3 mg of protein with 30 µl of dimethyl sulfoxide and 3 ml of constant-boiling HCl (Spencer and Wold, 1969). Hydrolysis time was 21 hrs. Tryptophan was determined according to Hugli and Moore (1972).

RESULTS

Association Equilibria

The existence of a mobile equilibrium between tetramer (39S) and monomer (17S) was confirmed by measuring the fraction of tetramer as a function of the total concentration of hemocyanin at pH 7.65 in 0.1 I Tris buffer with 50 mM of $MgCl_2$. Fig. 4 shows the concentration dependence of the monomer-tetramer equilibrium. The solid line is calculated, assuming an apparent association constant of $7.7 \times 10^{21}\ M^{-3}$. The percentage of 39S was measured by velocity sedimentation as described in Materials and Methods.

Weight average sedimentation coefficients were measured at different pH values and magnesium ion concentrations. Hemocyanin was first dialyzed against 10 mM EDTA, 0.1 I Tris buffer pH 7.65 in order to remove all divalent cations. The solutions thus treated were dialized twice against the same buffer without EDTA to remove the EDTA and then dialyzed against the Tris buffer of the desired pH and Mg^{2+} concentration. The results are shown in Fig. 5. Above pH 7.65 the boundaries of the 17S form and the 39S form are clearly separated. Below pH 7.3, however, the boundary tends to be diffuse and appears to be a reaction boundary. In this case, weight average sedimentation coefficients were calculated from the second moment

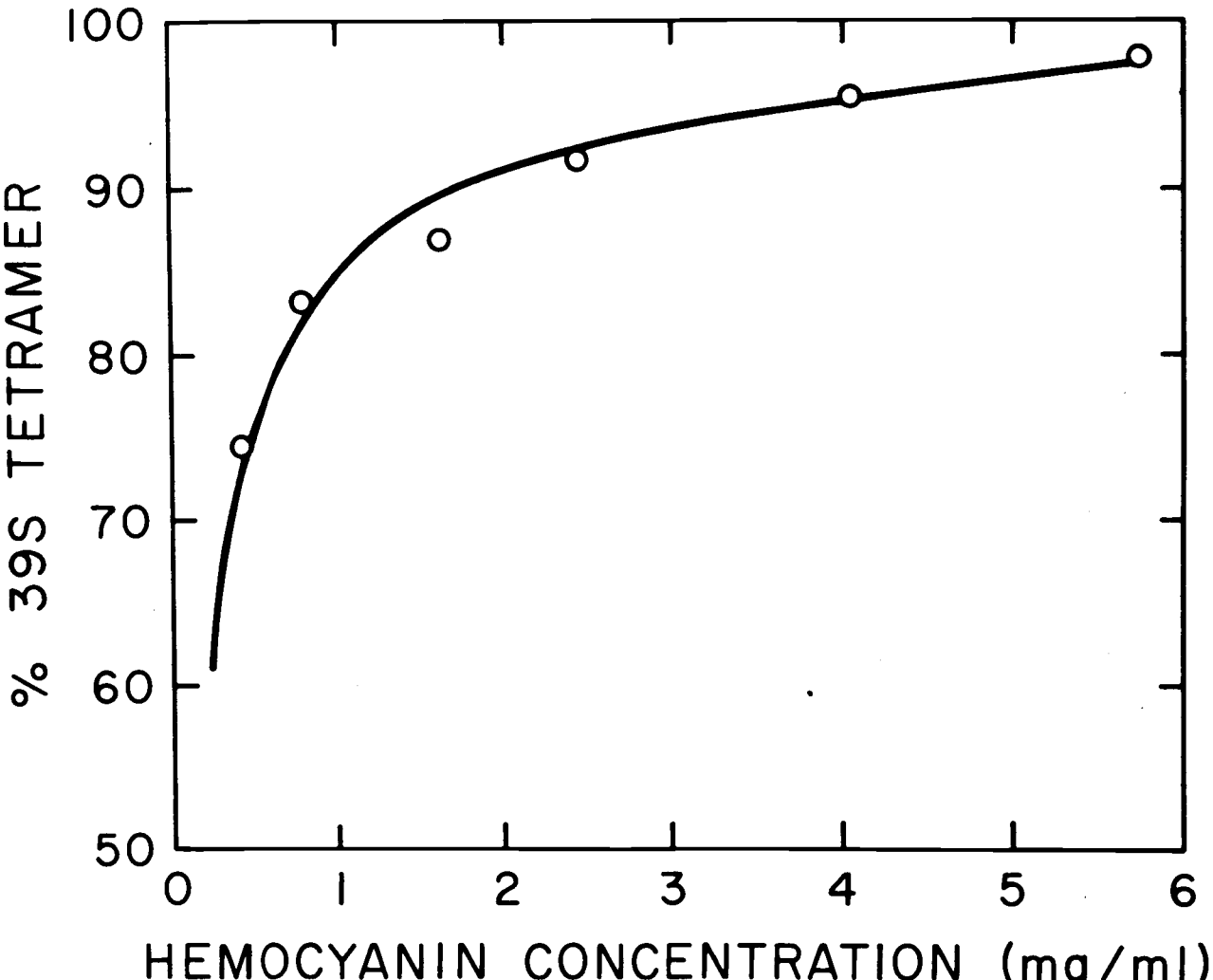

Figure 4. A test of the mass-action law for hemocyanin dissociation. Samples at pH 7.65, 50 mM, $MgCl_2$, and 20°C were diluted to the concentrations indicated. The solid line is a theoretical curve for a monomer-tetramer equilibrium.

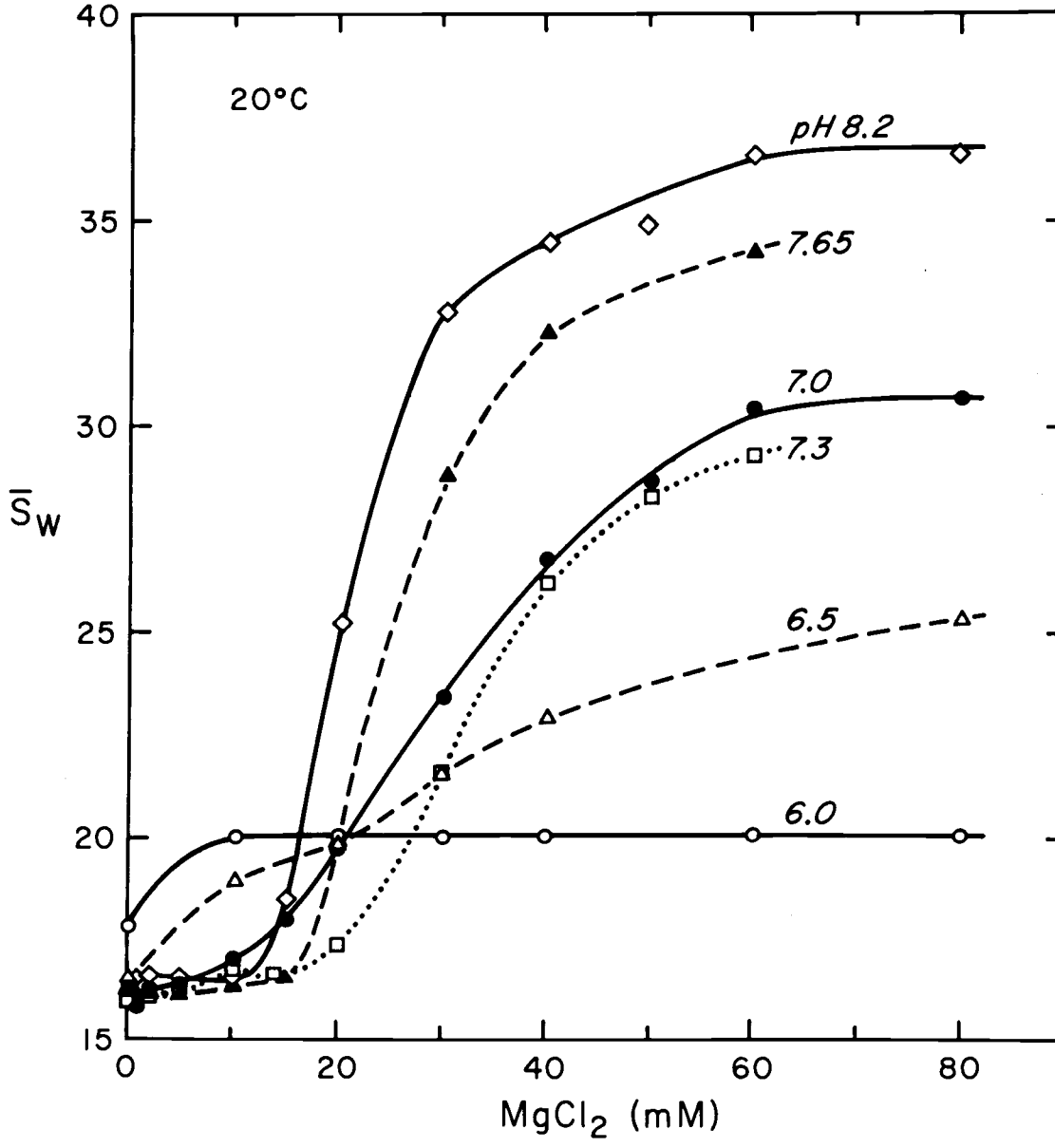

Figure 5. Weight average sedimentation coefficients as a function of Mg^{2+} concentration. All data at hemocyanin concentration of approximately 1 mg/ml. (See the text for details of calculations.)

of the boundary as described in Materials and Methods. As long as the second moment of the concentration gradient is calculated correctly, it will give the correct weight average sedimentation coefficient even for a reaction boundary (see H. Fujita, 1975). As seen in Fig. 5, lowering the pH generally favors dissociation. From pH 8.2 to 7.3 the curves appear to shift uniformly without changing shape. Below pH 7.3, however, another tendency appears; i.e. the hemocyanin tends to associate slightly at relatively low magnesium concentration, but does not associate much further as magnesium ion concentration increases. In Fig. 6, the association of apohemocyanin at pH 7.65 is shown as a function of Mg^{2+} concentration, comparing with the native hemocyanin. The curve is displaced considerably toward higher Mg^{2+} concentration, but the capacity for association is still evident. The sedimentation coefficient of apohemocyanin in the absence of Mg^{2+} is 16.7S, which is identical to that of native hemocyanin (16.6S) within the experimental error.

The effect of oxygen binding on the association equilibrium was measured at pH 8.0. After being dialyzed against the buffers of desired $MgCl_2$ concentration, the samples were placed in a glove bag, which was filled with either nitrogen or oxygen, for more than twelve hours and the cells were loaded in that bag. Weight average sedimentation coefficients were determined by velocity

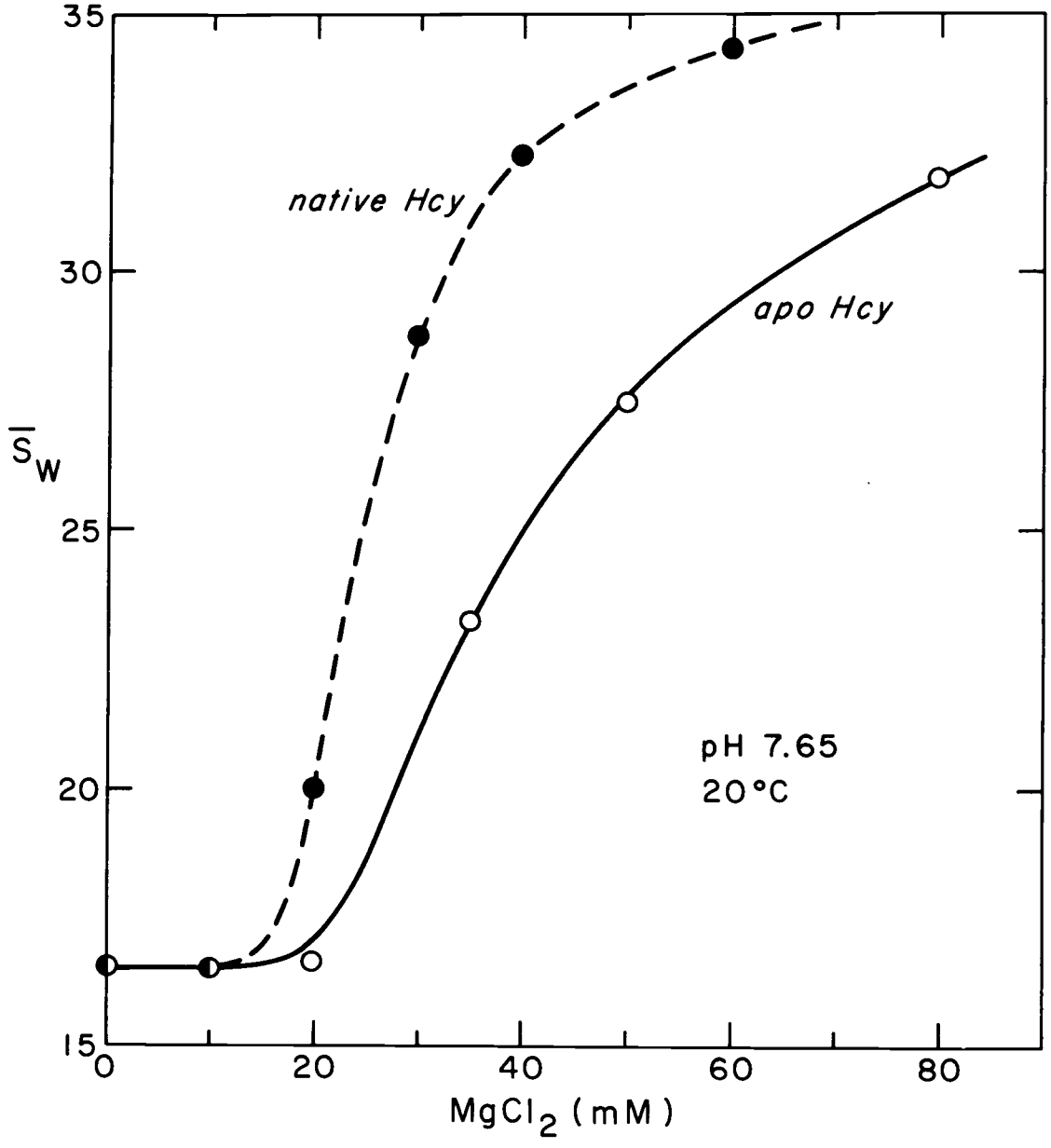

Figure 6. A comparison of the association profiles between the native and apo-hemocyanin. Conditions the same as in Figure 5.

sedimentation as described above. The data were corrected for radial dilution as described in Materials and Methods. The exact sedimentation coefficient values for 17S and 39S components were taken to be 16.5S and 38.8S respectively under the conditions (Roxby et al., 1974). Under these conditions the boundaries of monomer and tetramer are well resolved (see Fig. 21 at pH 8.0). The results are shown in Fig. 7. There is a significant shift of the association curve upon oxygenation. Apparently oxygenation favors association. The solid lines are calculated using a simplified reaction scheme:

$$4M + mMg^{2+} \rightleftarrows Te \quad ,$$

where M is the 17S form (monomer), Te is the 39S form (tetramer) and m is the number of Mg^{2+} involved in the reaction per tetramer. The equilibrium constant is defined as:

$$K'' = \frac{[Te]}{[M]\ a_B^m} \quad , \tag{28}$$

where a_B is the activity of Mg^{2+} which is calculated as in Materials and Methods. From eq. (28).

$$\ln \frac{[Te]}{[M]^4} = m \ln a_B + \ln K'' \tag{29}$$

m is thus obtained from the slope of the plot $\ln(Te/(M)^4)$ vs. $\ln a_B$. Oxy- and deoxyhemocyanin give m = 10.4 and 10.1

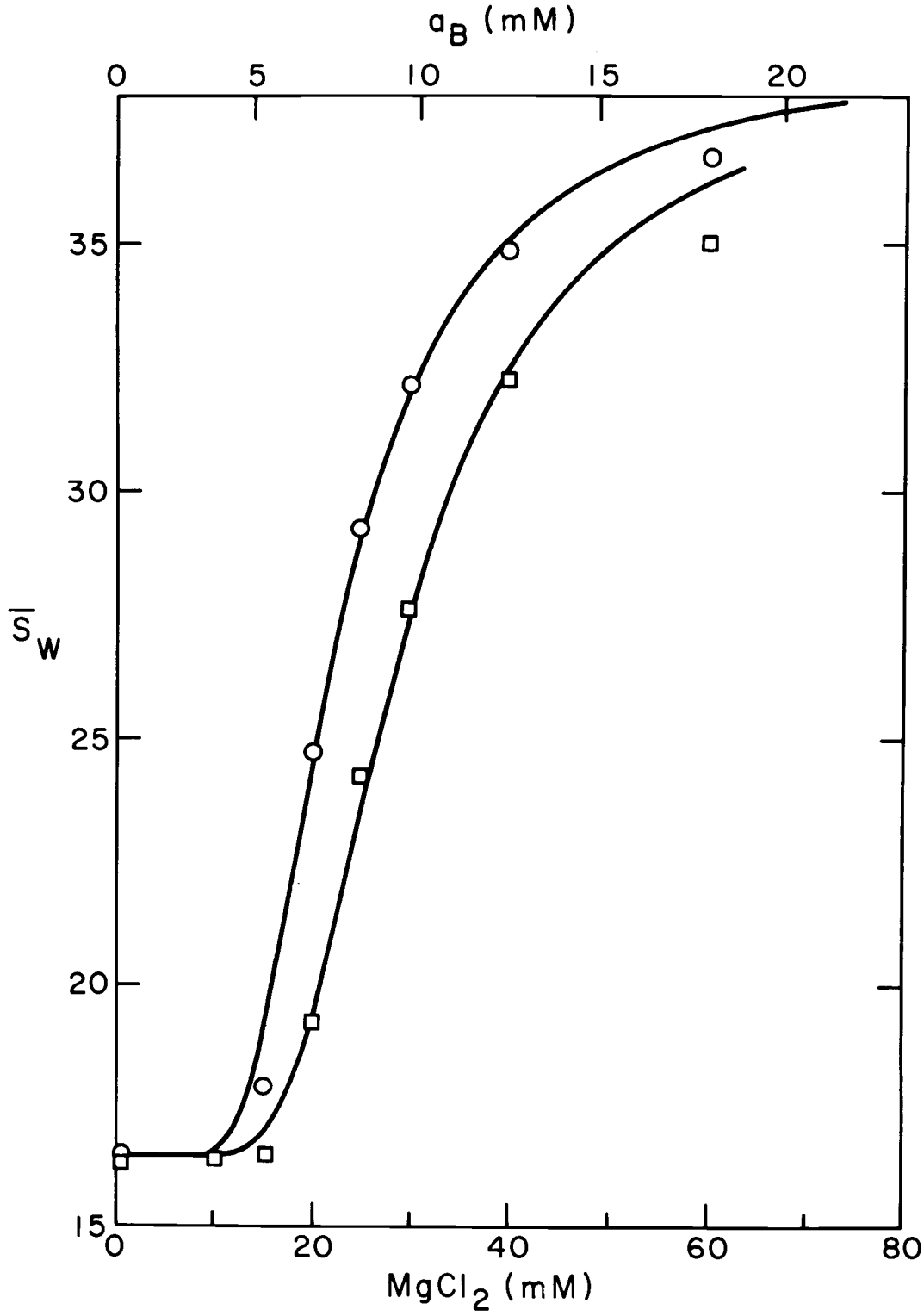

Figure 7. A comparison of association profiles between oxy (o) and deoxy (□) hemocyanin at pH 8.0. The smooth curves are theoretical ones based on eq. (28). Almost identical curves are obtained by using eq. (48).

respectively as shown in Fig. 8. The solid lines were calculated by eq. (48) in the discussion section. The difference of the free energy of the association reaction between oxy- and deoxyhemocyanin may be written as

$$\Delta G = -RT \ln \frac{K''(oxy)}{K''(deoxy)} \tag{30}$$

which gives -1.28 kcal/mol per tetramer at 20°C. More rigourously we could use the model given in the Theory section, where it was assumed that there are p Mg^{2+} binding sites per monomer involved in the association, each of which competes with two H^+. It was assumed that Mg^{2+} favors tetramer and H^+ favors monomer. From eq. (22-1) and (22-2), we have:

$$K_{deoxy} = K'(1+k_B a_B)^{4P} \tag{31-1}$$

$$K_{oxy} = K'\left\{\frac{1+L'_M+2\sqrt{L'_M/q}}{1+L'_{Te}+2\sqrt{L'_{Te}/q}} \cdot \frac{1+c^6L'_{Te}+2c^3\sqrt{L'_{Te}/q}}{1+c^6L'_M+2c^3\sqrt{L'_M/q}}\right\}^4 (1+k_B a_B)^{4P}$$

$$\simeq K'\left\{\frac{1+L'_M+2\sqrt{L'_M/q}}{1+L'_{Te}+2\sqrt{L'_{Te}/q}}\right\}^4 (1+k_B a_B)^{4P} , \tag{31-2}$$

where $K' = K_0/(1 + k_C a_C)^{8P}$; L'_M and L'_{Te} are defined in eq. (10) and (12), c (= 1.0 x 10^{-2} for the hemocyanin) is the ratio of the binding constant of oxygen for T and R states, k_T/k_R. $c^6L'_{Te}$, $c^6L'_M$, $2c^3\sqrt{L'_{Te}/q}$ and $2c^3\sqrt{L'_M/q}$ are considered to be negligible comparing to 1 ($L'_{Te} \sim 10^6$; see

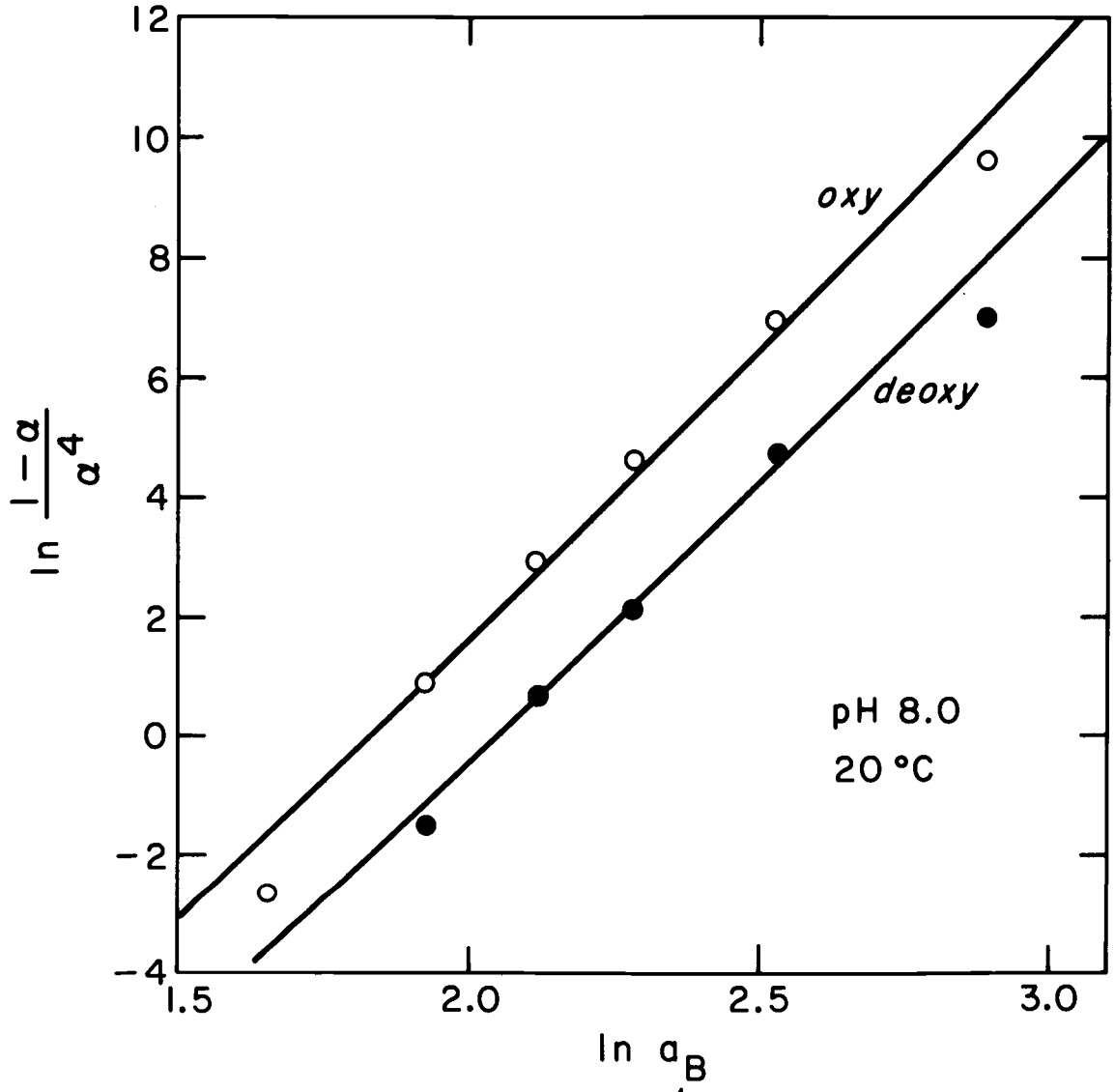

Figure 8. A graph of ln $(1-\alpha)/\alpha^4$ vs. ln a_B, where α denotes the degree of dissociation and a_B is the activity of Mg^{2+} (in mM) which was calculated by eq. (27).

the discussion of the oxygen binding study). From those equations, we obtain;

$$\ln K_{deoxy} = \ln \frac{[Te]}{[M]^4} = 4P \ln (1+k_B a_B) + \ln K' \qquad (32\text{-}1)$$

$$\ln K_{oxy} = \ln \frac{[Te]}{[M]^4} = 4P \ln (1+k_B a_B) + \ln K' \left\{ \frac{1+L'_M+2\sqrt{L'_M/q}}{1+L'_{Te}+2\sqrt{L'_{Te}/q}} \right\}^4$$

$$\simeq 4P \ln (1+k_B a_B) + \ln K' \left(\frac{L'_M}{L'_{Te}}\right)^4 \qquad (32\text{-}2)$$

The approximation $(1 + L'_M + 2\sqrt{L'_M/q})/(1+ L'_{Te} + 2\sqrt{L'_{Te}/q})$ L'_M/L'_{Te} is justified, because L'_M and L'_{Te} are both considered to be very large compared to one. For k_B we have the value of $2.28 \times 10^3\ M^{-1}$ from Mg^{2+} binding study. If we take this value as the binding constant for the Mg^{2+} which is involved in the association of monomer to tetramer (p binding sites per monomer), $k_B a_B >> 1$ within experimental error, since a_B has the range between 4×10^{-3} to 20×10^{-3}M (in activity). Then eq. (32-1) and (32.2) become:

$$\ln K_{deoxy} = 4P \ln k_B a_B + \ln K'$$

$$= 4P \ln a_B + \ln K'' \qquad (33\text{-}1)$$

$$\ln K_{oxy} = 4P \ln k\,a + \ln K' \left(\frac{L'_M}{L'_{Te}}\right)^4$$

$$= 4P \ln a_B + \ln K'' \left(\frac{L'_M}{L'_{Te}}\right)^4 , \qquad (33\text{-}2)$$

where $K'' = K'k_B^{4P}$. It is to be noted that (33-1) and (33-2) have the same form as eq. (29), m being 4P. The difference of the free energy of association between oxy- and deoxy-hemocyanin in eq. (30) has now a physical meaning in terms of the equilibrium constants of the allosteric transitions (see Fig. 1 and 2):

$$\Delta G = -RT \ln \left(\frac{L'_M}{L'_{Te}}\right)^4 \qquad (34)$$

Comparing eq. (30) and (34), we obtain $L'_M/L'_{Te} = 1.73$. From eq. (23-2) in the theory section,

$$\frac{\partial \ln K}{\partial \ln a_B} = \Delta\bar{B} + \delta'_B$$

$$\simeq 4P + \delta'_B \qquad (23\text{-}2)$$

As pointed out in that section $\delta'_B = 0$ for the deoxygenated hemocyanin. The difference of m(10.4 - 10.1 = 0.3) between oxy- and deoxyhemocyanin may correspond to the term $\delta'_B(\alpha\to\infty)$ in eq. (23-2). The difference, however, is very small and may be taken as an experimental error. In any event, $\partial \ln K/\partial \ln a_B$, essentially gives $\Delta\bar{B}$. The remaining parameter which we could evaluate from the association

equilibria study is K_0 in eq. (21). In the deoxygenated state eq. (21) is reduced to eq. (22-1):

$$K = K_0 \frac{(1 + k_B a_B)^{4P}}{(1 + k_C a_C)^{8P}} = \frac{1 - \alpha}{256\ \alpha^4 C_0^3}, \tag{35}$$

where α denotes the degree of dissociation, c_0 is the molar concentration of tetramer. We have the association profile of the deoxygenated hemocyanin at pH 8.0. For instance, $\alpha = 0.653$ at $a_B = 8.34$ mM (25 mM $MgCl_2$) and $c_0 = 6.9 \times 10^{-7}$ M. Substituting those into eq. (35), we obtain:

$$K_0 = 9.45 \times 10^5\ M^{-3}$$

(for the values of k_B and k_C, see Table V).

Although the monomer unit is rather stable in the presence of Mg^{2+} even at high pH values, it tends to dissociate further into 5S particles at low concentration of Mg^{2+} above pH 8.5. It appears that the dissociated 5S particles can associate to 17S particles, but for some reason not all of the 17S component thus obtained can further associate to 39S. The situation is depicted in Fig. 9. The upper curve is obtained, if we dialyze against pH 7.65 in the absence of Mg^{2+}, thus converting all to 17S, and then dialyze it against pH 8.8 buffer with

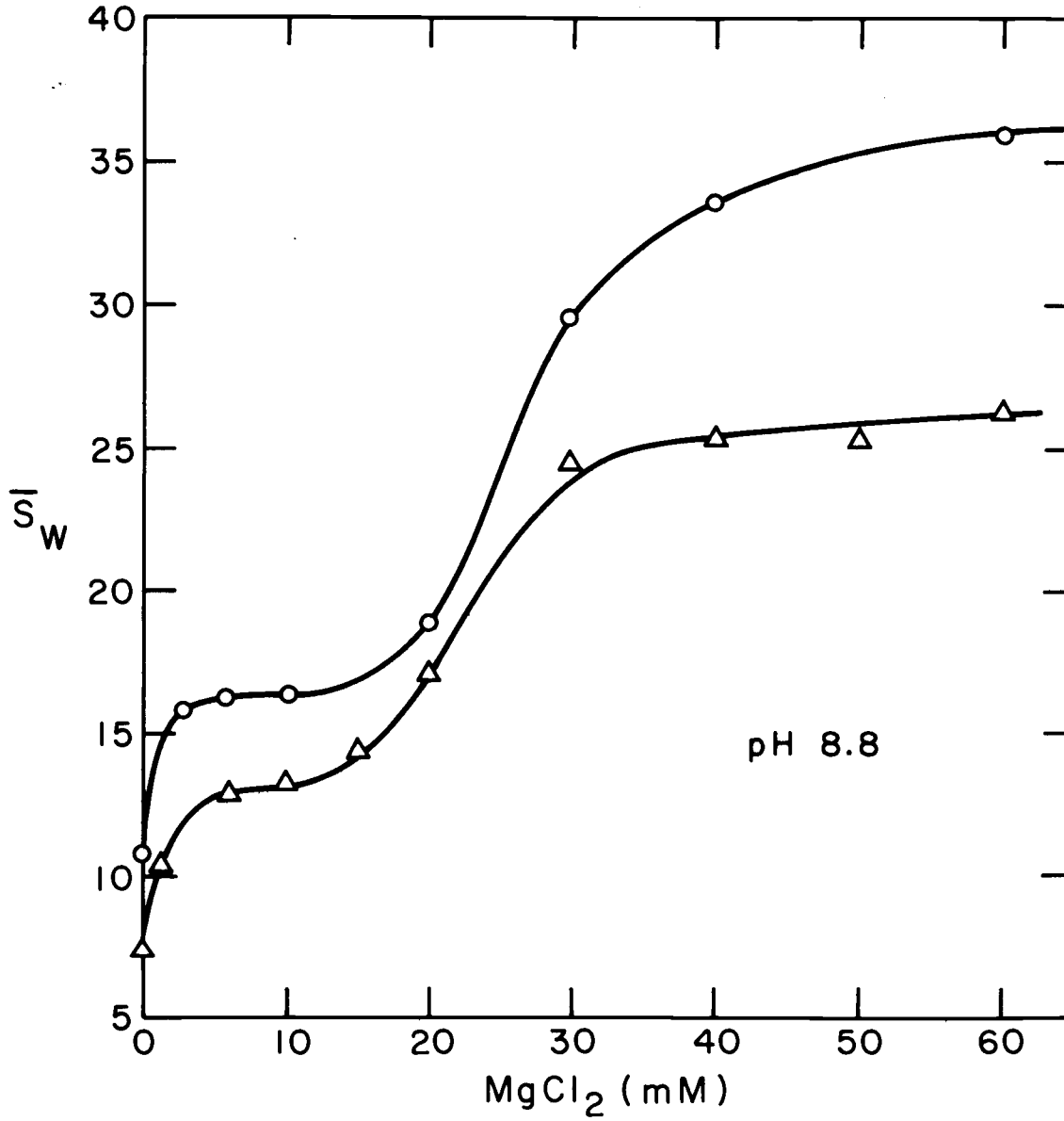

Figure 9. Weight average sedimentation coefficients as a function of Mg^{2+} concentration at pH 8.8. The hemocyanin was first dialyzed against a buffer at pH 7.65 without divalent cations, thus converted into the 17S component. The samples were then dialyzed against the buffer at pH 8.8 with the indicated Mg^{2+} concentration (upper curve). The lower curve is obtained, when the hemocyanin is dissociated into the 5S component, and Mg^{2+} is then added to yield the indicated concentrations (for details, see text).

each of the indicated concentrations of Mg^{2+}. The lower curve, on the other hand, was obtained by first dialyzing against pH 8.8 buffer without Mg^{2+}, which converts about 90 percent of the hemocyanin to the 5S component, then add Mg^{2+}. In either case only 17S and 39S components exist, but no intermediate forms such as a 25S component are observed in appreciable concentration.

Association-Dissociation Reaction

The association kinetics of the hemocyanin from monomer (17S) to tetramer (39S) was monitored by both sedimentation velocity and light scattering at pH 8.0 with four different concentrations of the hemocyanin. The results from sedimentation velocity were corrected for the radial dilution and shown in Fig. 10. Throughout the association process only 17S and 39S species were observed and the boundaries were well resolved. No intermediate species such as 25S was detected (Fig. 11). In order to resolve the initial stage of the reaction, the light scattering method, which has a shorter dead time, was also employed. The results are shown in Fig. 12. Under the conditions, the intensity of the scattered light should be proportional to the square of the molecular weight:

$$i = c'M_1^2 (N_1 + 4N_2 + 16N_4) ,$$

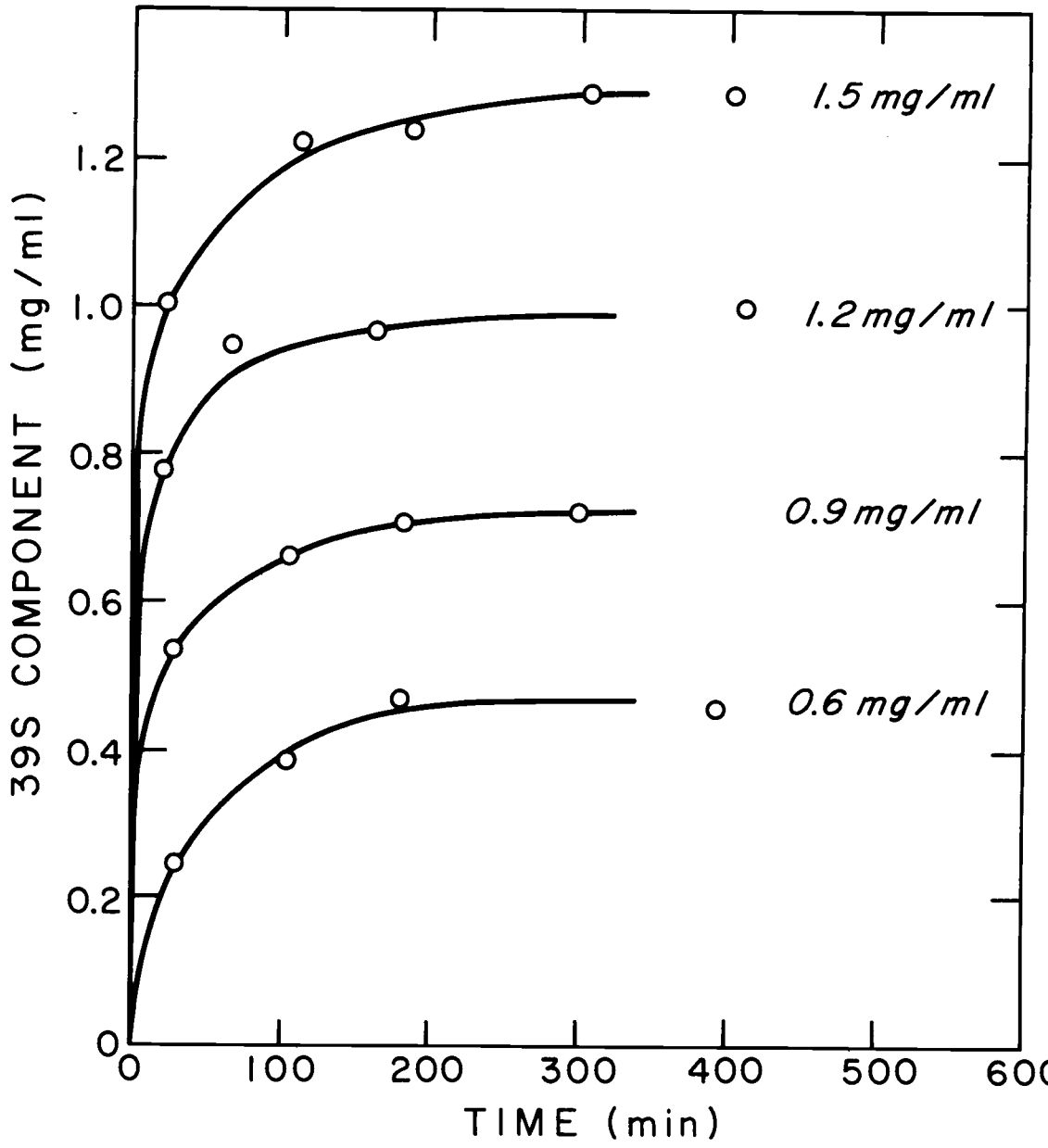

Figure 10. Association of monomer to tetramer as measured by velocity sedimentation at pH 8.0, 20°C. Magnesium was added at t = 0, to give a concentration of 50 mM.

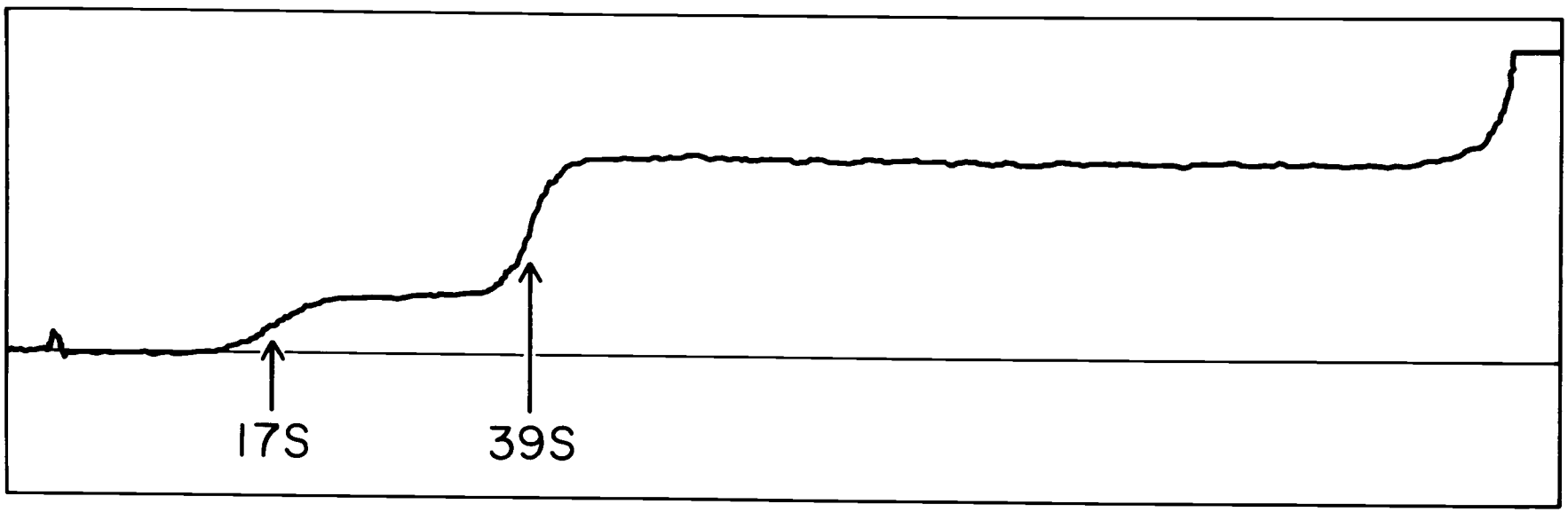

Figure 11. Scanning profile of the hemocyanin solution at t = 30 min after adding $MgCl_2$ to 50 mM, pH 8.0, 20°C. Hemocyanin concentration of 1.5 mg/ml. The reequilibrium process is slow enough that both boundariesare clearly separated. No intermediate species are observed.

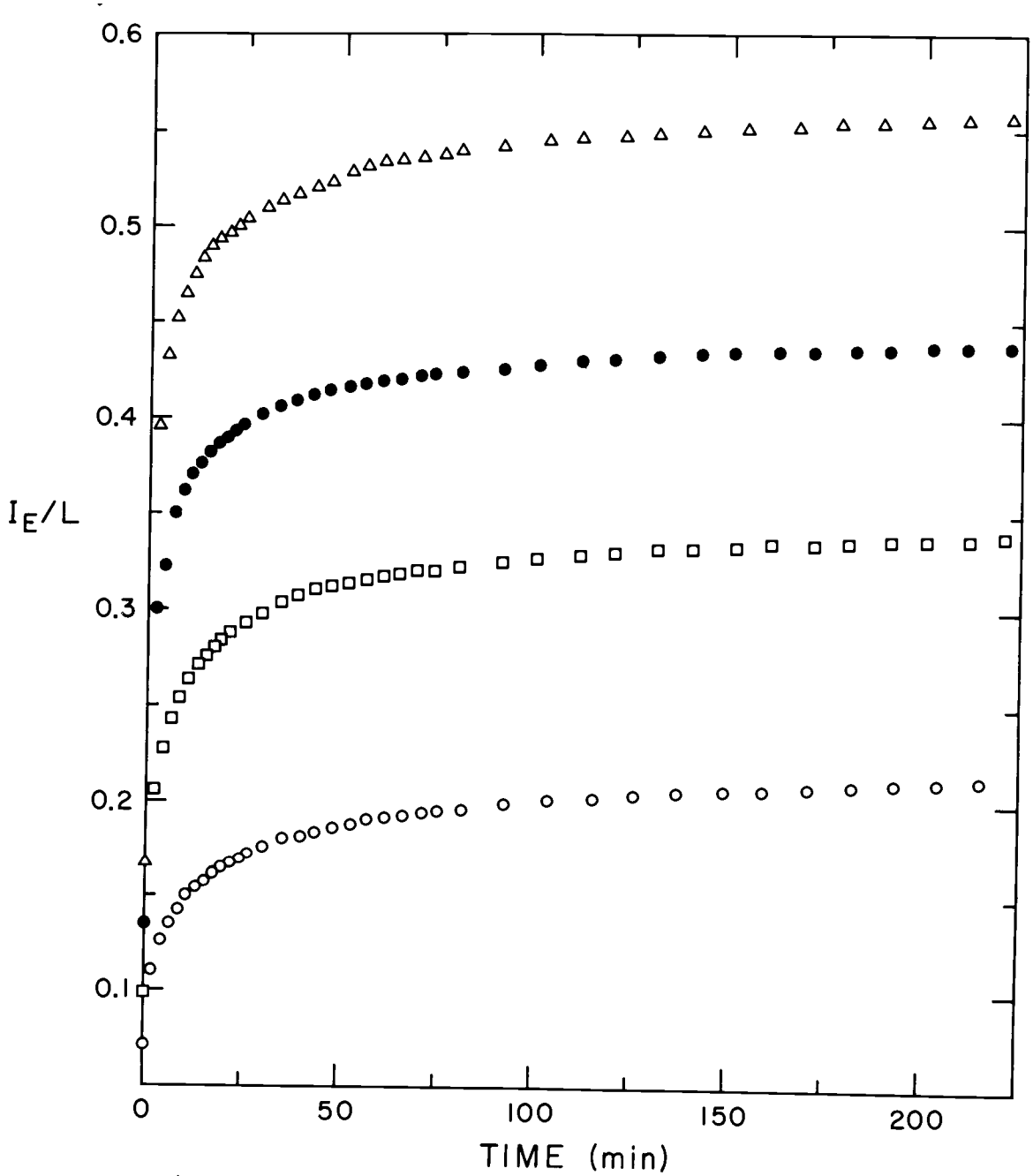

Figure 12. Association from monomer to tetramer measured by light scattering. The conditions are the same as in Figure 10; hemocyanin concentrations of 1.5 mg/ml (△), 1.2 mg/ml (•), 0.9 mg/ml (□) and 0.6 mg/ml (○).

where M_1 denotes the molecular weight of monomer (17S), N_i is the molar concentration of i-mer and c' is a constant. Since the dimer concentration is negligible as we see in Fig. 11, N_2 can be neglected. Thus we have:

$$i = c\ (N_1 + 16N_4)\ , \quad c = c'M_1^2 \tag{36}$$

Since total concentration of the hemocyanin,

$$N_0 = N_1 + 2N_2 + 4N_4 \simeq N_1 + 4N_4 \tag{37}$$

should be constant, eq. (36) becomes:

$$i = c\ (N_1 + 4N_0 - 4N_1) = 4cN_0\ (1 - 3N_1/4N_0) \tag{38}$$

or

$$i = c\ (N_0 - 4N_4 + 16N_4) = cN_0\ (1 + 12N_4/N_0) \tag{39}$$

From eq. (39), we obtain:

$$N_4 = (N_0/12)(i/i_0 - 1) \tag{40}$$

or

$$C_{Te} = C_0/3\ (i/i_0 - 1)\ , \tag{41}$$

where C_{Te} ($= N_4 \cdot M_4$) and C_0 ($=N_0 \cdot M_1$) are the weight concentrations of tetramer and total hemocyanin. In Fig. 13 C_{Te} is plotted against t (min) with the velocity sedimentation data under the same conditions. The agreement of the reaction time course between the two experiments is satisfactory. A relatively slow process, lasting six

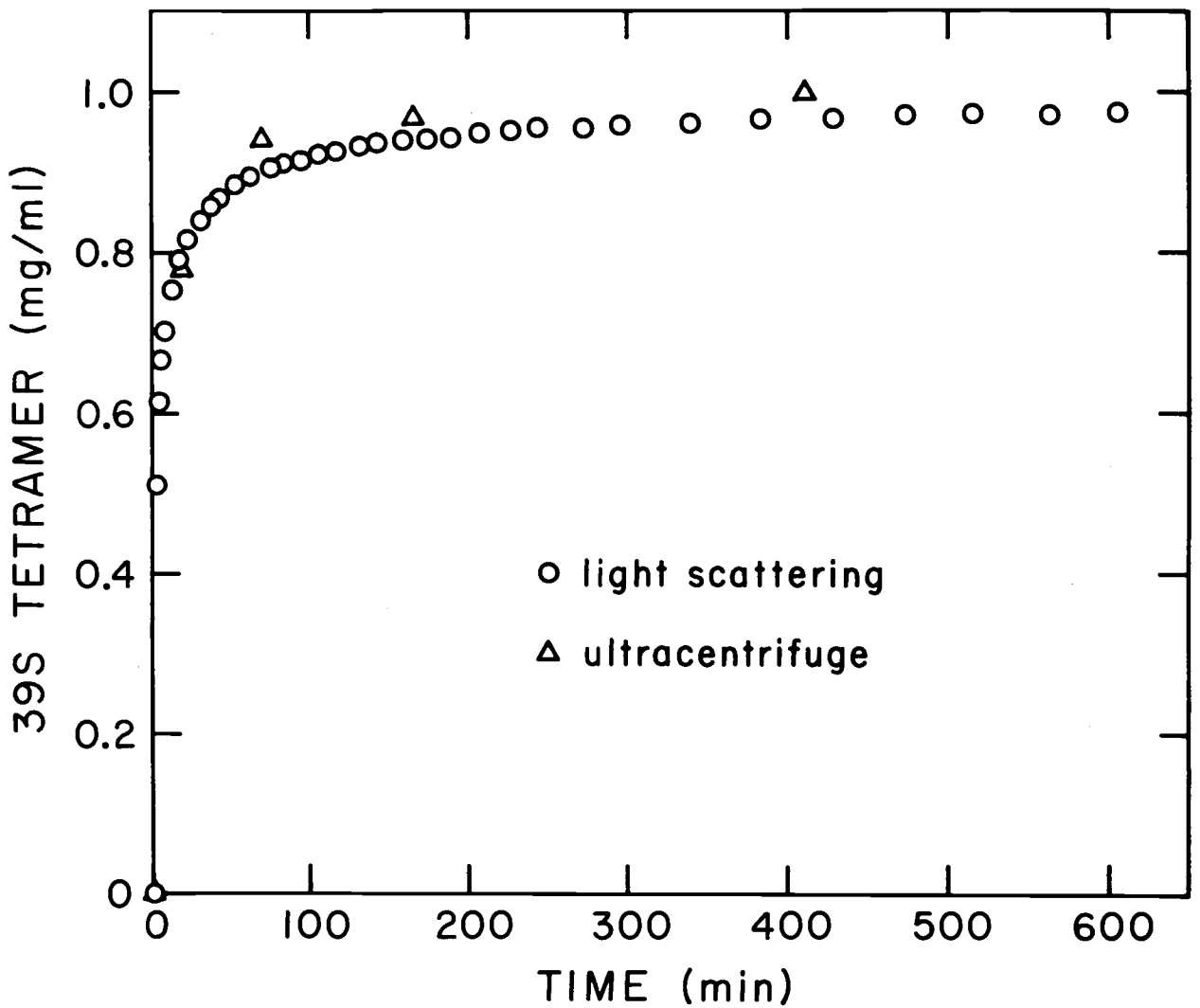

Figure 13. A comparison of the association kinetics data as obtained by the ultracentrifuge and by light scattering. Light scattering data were converted to mg/ml of 39S component by eq. (41).

hours or so, following the initial fast reaction. In any case this confirms that the equilibration time of more than twelve hours which was employed in association equilibrium experiments was sufficient for those experiments. The dissociation process of tetramer (39S) into monomer (17S) upon removal of divalent cations by EDTA was too fast to observe with these methods.

As we saw in Fig. 9, the monomer (17S) tends to dissociate into subunits (5S) at low concentration of Mg^{2+} at high pH. The time course of the dissocation of monomer (17S) into 5S subunits at pH 8.8 in the absence of Mg^{2+} was also monitored by velocity sedimentation experiment. An aliquot of the hemocyanin solution of 16 mg/ml at pH 8.2 was added to a buffer solution of pH 8.8 so that the final concentration of hemocyanin would be about 0.8 mg/ml. In the course of time aliquots were taken from the solution and the fraction of the 17S form was measured by velocity sedimentation. The result is shown in Fig. 14(a) through (c). Evidently, the dissociation is sufficiently slow that the sedimentation velocity method can be used to measure its rate, although early time points are possibly inaccurate because of appreciable dissociation during the experiment. In Fig. 14(c), y is the fraction of 17S and y_0 is the value of 48 hrs later. Two phases, i.e. the first fast decay and the second long decay are observed.

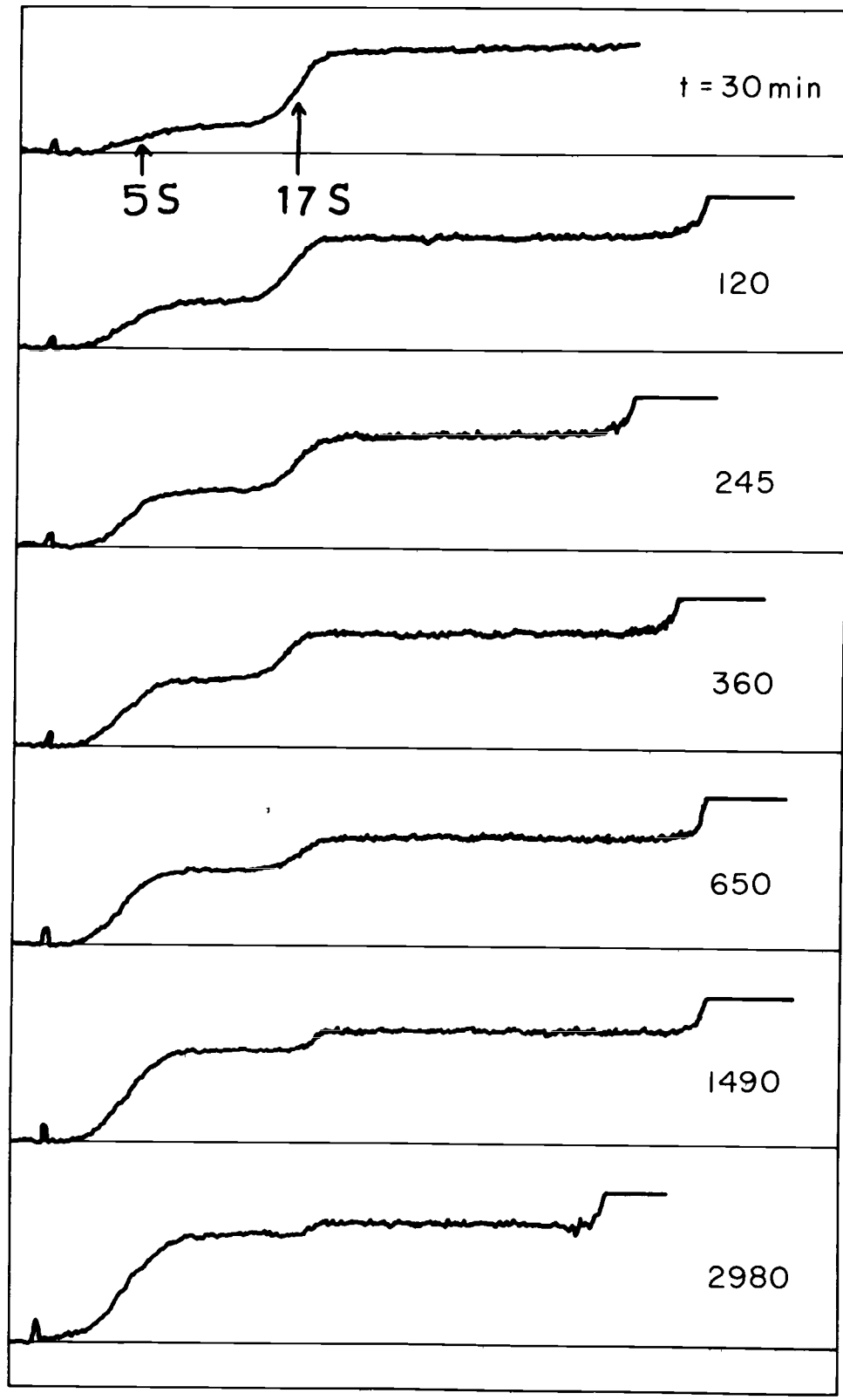

Figure 14(a). Scanning profiles of the time course of the dissociation process from 17S component into 5S particles. Boundaries are clearly separated and no intermediate species are observed.

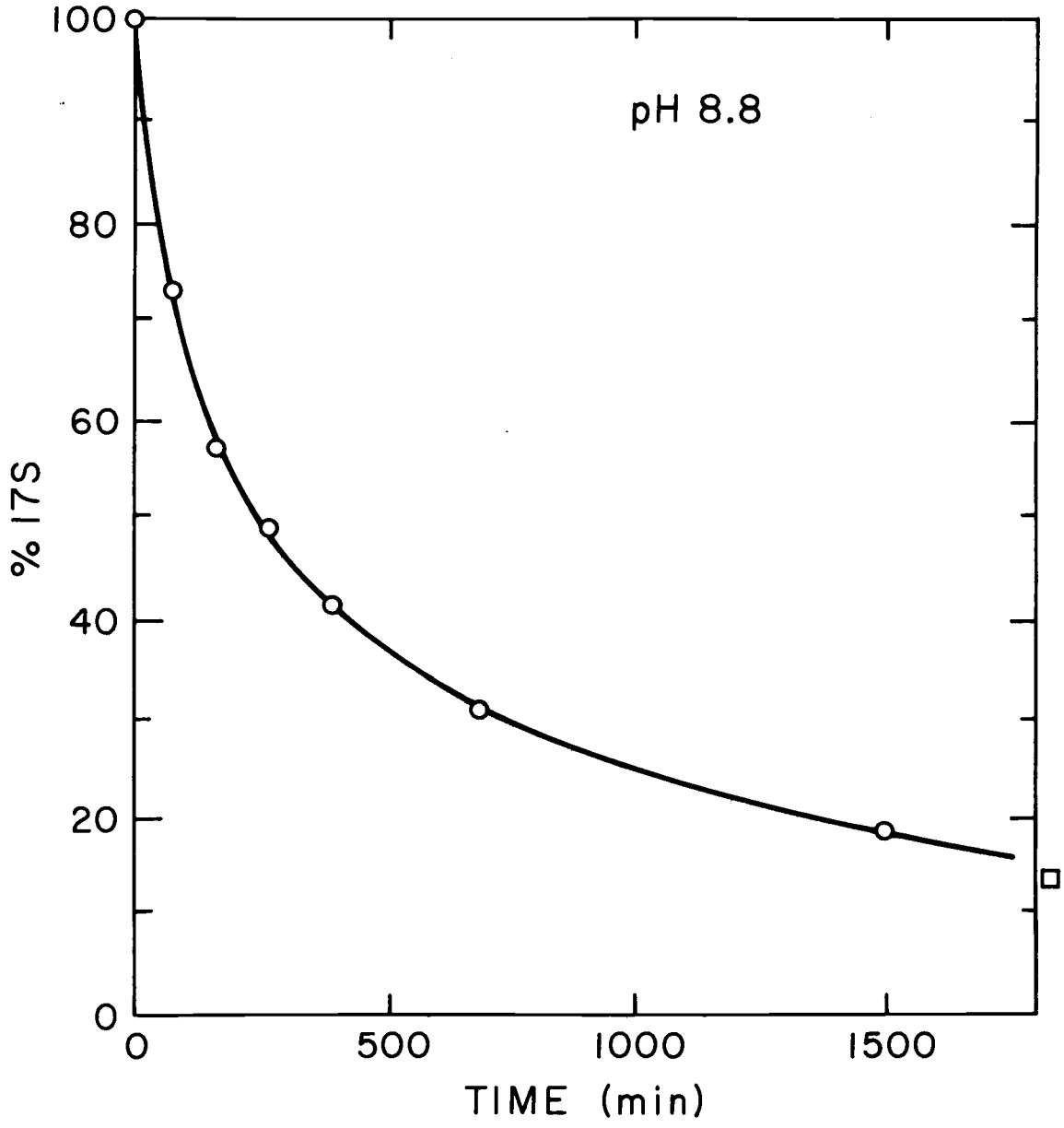

Figure 14(b). Dissociation of 17S particles to 5S subunits at pH 8.8, as measured by velocity sedimentation, □: t = 2980 min.

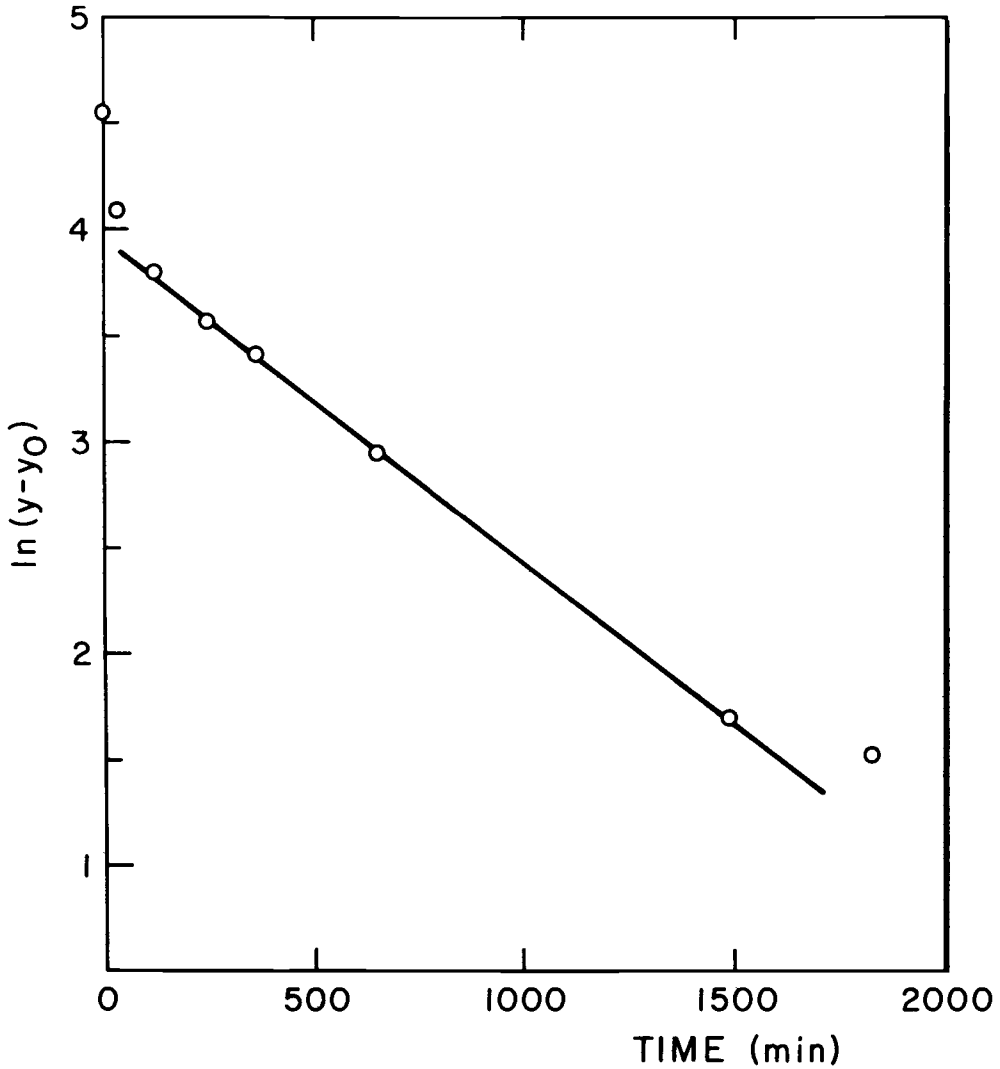

Figure 14(c). A semilog plot of the data in Figure 14(b), where y and y_o are the percentage of 17S at time t = t and t = 3000 min respectively.

Oxygen Binding Study

Oxygen binding was measured at a number of pH values and Mg^{2+} concentrations in order to clarify the role of H^{+} and Mg^{2+} as allosteric effectors of the hemocyanin. A pH range was chosen where the hemocyanin exists in equilibrium between the 17S form and the 39S form, but no 5S component exists. Prior to the experiments hemocyanin was treated with 10 mM EDTA to remove all divalent cations. The fraction of 39S component was measured for the same samples in oxy and deoxy states by velocity sedimentation. Hill plots of some of the data are shown in Fig. 15. In Fig. 15, the two straight lines with slope unity (R & T) have p50 values corresponding to the intercepts at the abscissa in Fig. 17. The smooth curves were drawn based on the hybrid model which is described in the Theory section (eq. (19a)). The parameters, c and q, were set 1.04×10^{-2} and 7.5 respectively as determined in the Discussion section and L' values were adjusted to fit the data points at each pH. In Fig. 16, log L' values, which were determined by curve fitting as mentioned agove, are plotted against pH and log a_B, a_B being the activity of Mg^{2+}. For the sake of simplicity, let us assume that the effector Mg^{2+} (h binding sites per allosteric unit as assumed in the Theory

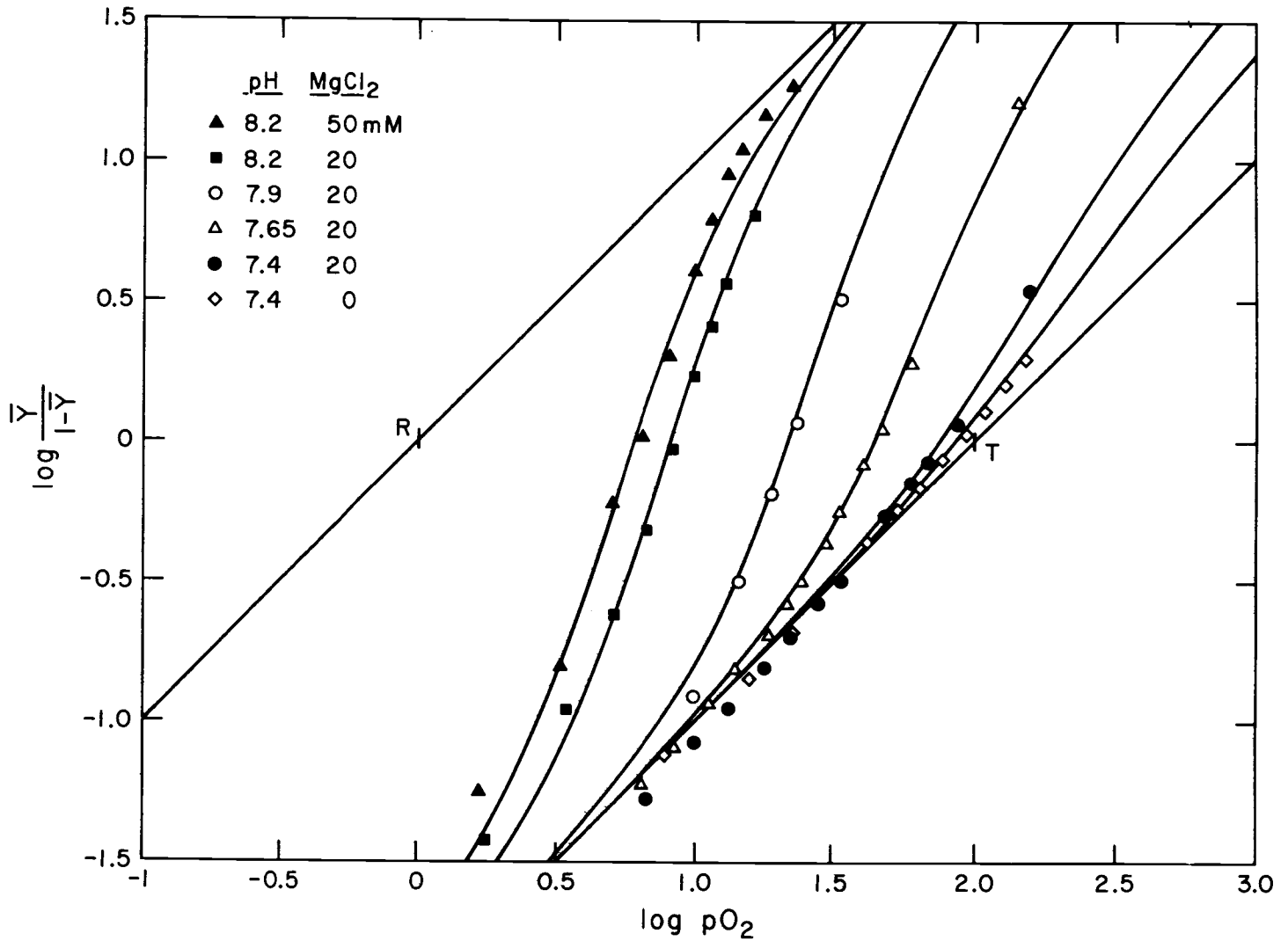

Figure 15. Hill plots of the binding of O_2 by hemocyanin C at 25°C. Two straight lines with slope unity (T and R) are placed according to data in Figure 17.

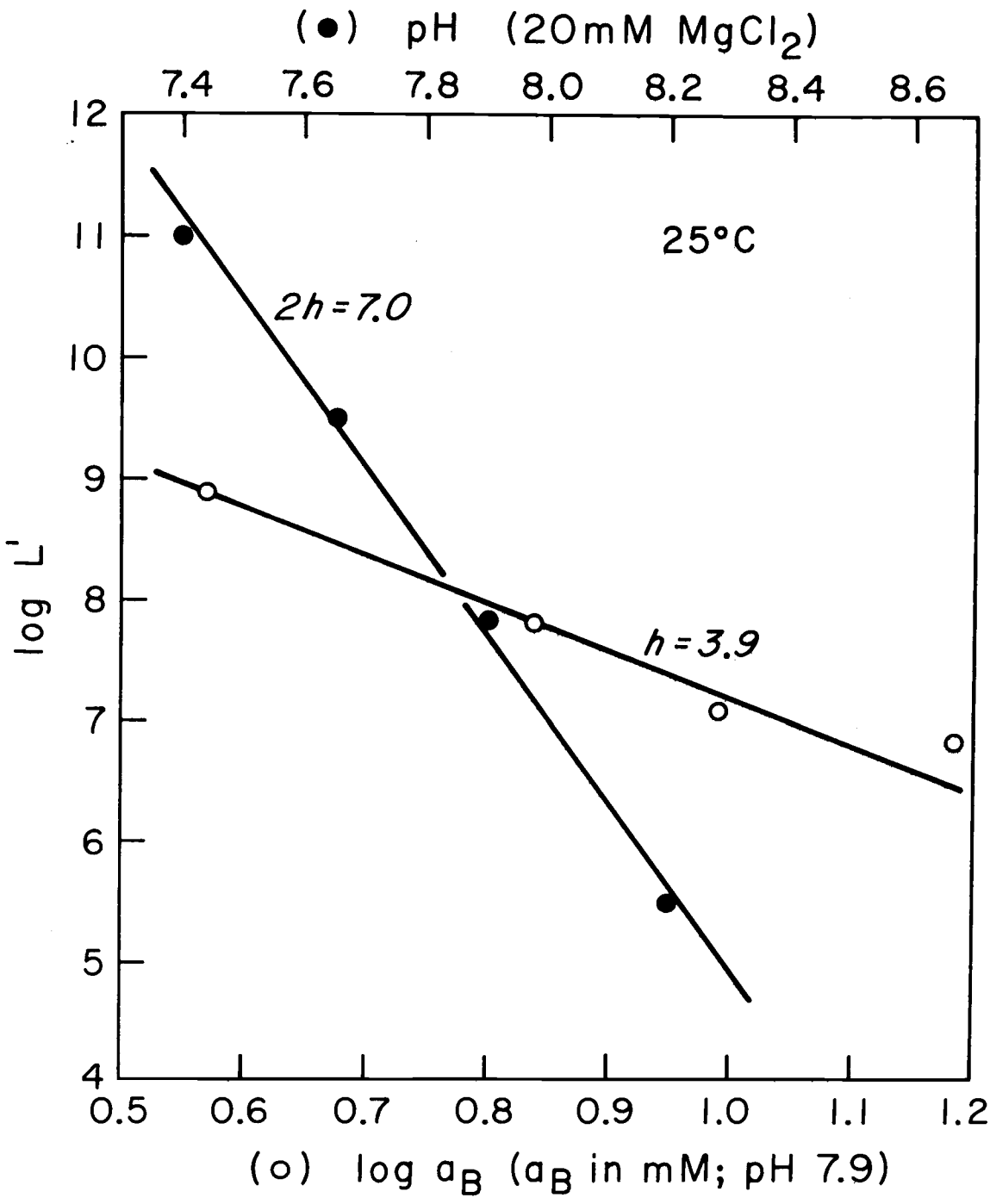

Figure 16. A graph of log L' vs. pH and log a_B, where a_B is the activity of Mg^{2+} calculated by eq. (27). The parameter h is the number of the binding sites of Mg^{2+} which are linked to oxygen binding.

section) has much stronger affinity for R state ($d << 1$) than for T state and H^+ for the same sites has much stronger affinity for T state than for R state ($e << 1$). Then, from eq. (10):

$$L' \simeq \frac{(1+\gamma)^{2h}}{(1+\beta)^{h}} L^0 \qquad (42)$$

which gives:

$$\log L' = 2h \log (1+\gamma) - h \log (1+\beta) + \log L^0 \qquad (43)$$

Eq. (10) was derived for a concerted model, but it holds regardless of the presence of hybrid molecules. Under the conditions where $\gamma >> 1$ or $\beta >> 1$, the plot of log L' vs. pH or log L' vs. log a_B should give a straight line with a slope of -2h or -h respectively. The slopes in Fig. 16 give $2h = 7.0$ and $h = 3.9$ respectively, which implies that among the magnesium binding sites about four per monomer corresponds to the sites for the Mg^{2+} which are the effectors of the oxygen binding (see Table V). Also, those slopes support the conclusion drawn earlier (see Association Equilibrium, in this section) that two H^+ compete with one Mg^{2+} for these sites.

The summary of the results are shown in Table III(a) through (c) and the Hill coefficients are plotted with respect to log p50 (in this case it incidentally coincides with log $\alpha_{\frac{1}{2}}$ in Fig. 17. Although the data are somewhat scattered

Table I. Oxygen binding and association equilibrium.

		7.4	7.65	7.9	8.2
n_H					
0		1.1	1.4	1.6	1.9
10		1.4	1.5	2.3	3.3
20		1.5	1.9	2.8	3.3
30		1.9	2.8	3.2	3.1
50		1.9	2.9	2.9	3.0
P_{50} (mmHg)					
0		82	73	53	39
10		76	66	36	15
20		75	47	22	8
30		73	30	15	7
50		64	30	16	6
% of 39S					
0	(oxy)	0	0	0	0
	(deoxy)	0	0	0	0
10	(oxy)	0	0	0	0
	(deoxy)	0	0	0	0
20	(oxy)	52[a]	54	59	66
	(deoxy)	52[a]	53[a]	48	64
30	(oxy)	81	82	85	86
	(deoxy)	77	72	75	84
50	(oxy)	85	91	93	93
	(deoxy)	84	-	88	91

[a]Boundaries diffuse.

Conditions: 25°C, hemocyanin 3 mg/ml.

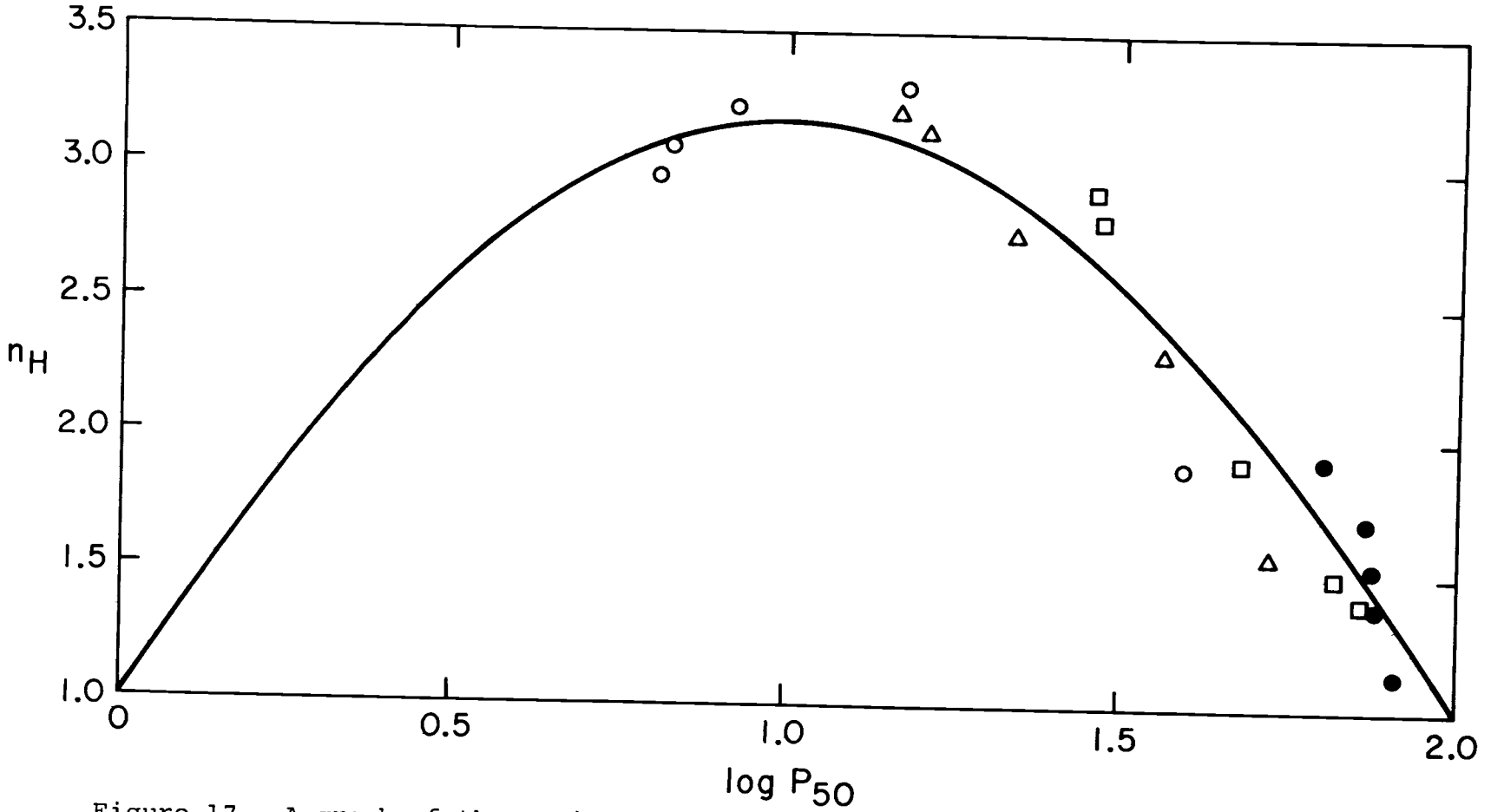

Figure 17. A graph of the maximum Hill coefficient, n_H, vs. log P50 or log $\alpha_{1/2}$ at pH 7.4 (●), pH 7.65 (□), pH 7.9 (△) and pH 8.2 (○).

all data points fall on the same curve as expected from non-exclusive (or extended non-exclusive) MWC model (see eq. (72) in the Discussion section). From Table I we see that even in the case where no appreciable amount of 39S component is present, the hemocyanin still shows rather high cooperativity as judged by the Hill coefficient n_H. In particular, it should be noted that a Hill coefficient as large as are ever observed for this system ($n_H = 3.3$) is observed for the non-associated 17S components. This shows that the 17S particle can itself act as an allosteric assembly.

It has been known that oxygen binding quenches the intrinsic fluorescence of a molluscan hemocyanin (Shaklai and Daniel, 1970). In order to examine the possibility to use the fluorescence quenching as a tool of measuring the oxygen binding of our hemocyanin, the quenching effect of our hemocyanin from Callianassa (which is an Arthropod species) was measured. It can be seen from Fig. 18 that the quenching effect was not in this case a linear function with respect to the oxygen saturation. It has not seemed profitable to carry this line of research further.

Binding Studies of Mg^{2+} and Ca^{2+}

Magnesium binding was measured at a number of pH values. The data are shown in Table II. Fig. 19 is a Scatchard plot of these data. The symbol $\bar{\nu}$ denotes the

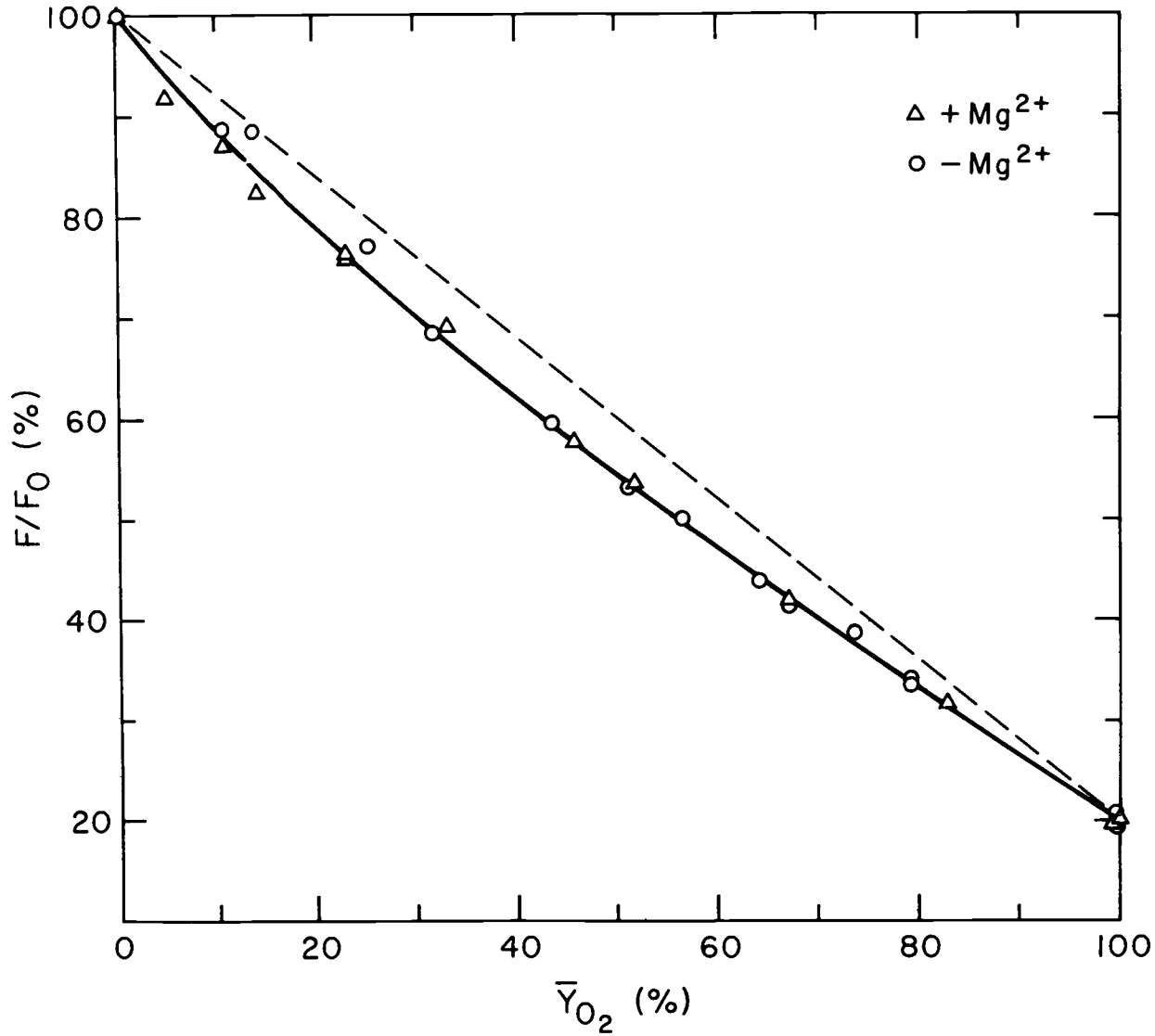

Figure 18. Fluorescence quenching as a function of oxygen saturation.

Table II. Mg^{2+} binding to hemocyanin.

pH 7.0		pH 7.65		pH 8.2		pH 8.8	
$MgCl_2$ (mM)	$\bar{\nu}$	$MgCl_2$ (mM)	$\bar{\nu}$	$MgCl_2$ (mM)	$\bar{\nu}$	$MgCl_2$ (mM)	$\bar{\nu}$
0.257	0.22	0.232	0.44	0.250	0.907	0.276	1.65
0.272	0.24	1.04	1.80	1.41	3.63	1.27	5.27
1.20	0.86	1.67	2.46	4.14	6.48	1.32	5.33
1.23	0.99	2.78	3.32	9.96	9.75	4.01	8.97
4.06	2.45	3.93	4.07	19.78	11.65	4.09	8.95
4.10	2.09	9.59	6.53	33.7	14.40	9.55	10.80
9.57	3.63	9.79	6.68			18.9	14.17
9.88	3.69	18.51	9.58			19.0	15.38
19.22	5.19	45.9	15.20				
32.8	6.56	47.1	15.25				
45.0	7.90						

$\bar{\nu}$ denotes the number of bound Mg^{2+} per polypeptide chain. All values are the average of the duplicate samples.

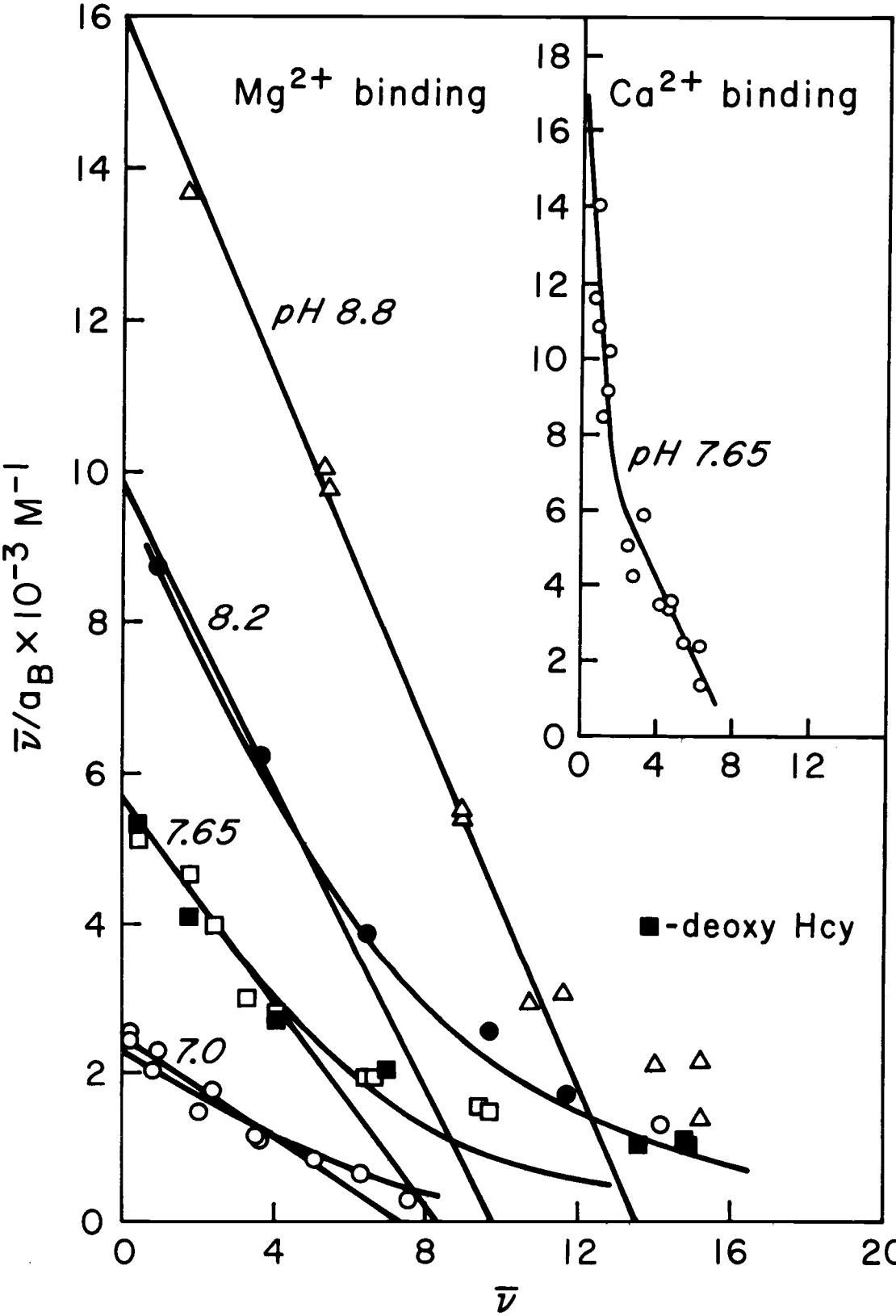

Figure 19. Scatchard plots of the Mg^{2+} and Ca^{2+} binding to hemocyanin C.

number of bound Mg^{2+} per subunit (72,000 dalton), a_B is the activity of Mg^{2+}, calculated as described in Materials and Methods. Activity values, rather than concentrations, were used for the plot, because in the case of a strong electrolyte the activity differs significantly from its concentration and is a function of the ionic strength, which changes from about 0.1 to 0.35 in this experiment. Each data point is the average of two duplicate samples. Higher pH favors stronger binding, suggesting competitive binding between Mg^{2+} and H^+. There are at least two kinds of binding sites and about seven of them (see the Discussion section) are strong binding sites up to pH 8.2. The other binding sites appear to be non-specific. However, at pH 8.8, where most of the hemocyanin molecules tend to dissociate the 5S particles in the absence of Mg^{2+}, there appear to be more strong binding sites. There is some uncertainty concerning the number of the binding sites because of the fact that the intercepts at the abscissa do not coincide well.

Mg^{2+} binding of the deoxygenated hemocyanin was also measured as shown in Fig. 19. No significant difference from the binding of the oxygenated hemocyanin was observed. The number of the magnesium binding sites which are linked to the oxygen binding is presumably too small compared to the total number of binding sites to detect with this method.

If Mg^{2+} and H^+ bind to the same sites competitively, does one H^+ compete with one Mg^{2+} or two H^+ with one Mg^{2+}? Suppose that one H^+ competes with one Mg^{2+}. Then we may write (neglecting the electrostatic interaction),

$$\bar{\nu}_B = \frac{(s/6)k_B a_B}{1+k_B a_B+k_C a_C} , \qquad (44)$$

where $\bar{\nu}_B$ denotes the number of bound Mg^{2+} per subunit, s is the number of binding sites per monomer (six subunits), k_B is the binding constant, a_B is the molar activity of Mg^{2+} (C. Tanford, 1961). Eq. (44) yields:

$$\frac{\bar{\nu}_B}{a_B} = \frac{sk_B}{6(1+k_C a_C)} - \frac{k_B \bar{\nu}_B}{1+k_C a_C}$$

$sk_B/6(1+k_C a_C) = d$ should be the intercept of the Scatchard plot. Since $d = sk_B/6 - k_C a_C d$, a plot of d vs. $a_C d$ will give a straight line. On the other hand, if two H^+ compete with one Mg^{2+} (suppose that each Mg^{2+} binding site consists of a pair of groups capable of binding ligand C), we may write (eq. (13) in the Theory section):

$$\bar{\nu}_B = \frac{(s/6)k_B a_B}{k_B a_B + (1+k_C a_C)^2} \qquad (45)$$

which gives:

$$\frac{\bar{\nu}_B}{a_B} = \frac{sk_B}{6(1+k_C a_C)^2} - \frac{k_B}{(1+k_C a_C)^2} \bar{\nu}_B$$

The intercept of the Scatchard plot, therefore should be $sk_B/6(1+k_Ca_C)^2 = d$. Since $\sqrt{d} = \sqrt{sk_B/6} - k_Ca_C\sqrt{d}$, a plot of $\sqrt{d}$ vs. $a_C\sqrt{d}$ will give a straight line. The two graphs are shown in Fig. 20(a) and (b). The fact that the plot of $\sqrt{d}$ vs. $a_C\sqrt{d}$ appears to be more straight line than the plot d vs. a_Cd suggests competition between two H^+ and one Mg^{2+} (the closed circles in Fig. 20(a) and (b) are for pH 8.8, where the hemocyanin partially dissociates into 5S subunits, which will cause some complication. Hence these values have not been weighted heavily. Compare Table II at pH 8.8 and Fig. 20. From the intercept and the slope of the plot in Fig. 20(b), we obtain $k_B = 1.6 \times 10^3\ M^{-1}$ and $k_C = 1.6 \times 10^7 M^{-1}$, assuming s = 42 (7 x 6). The dissociation constant $k_C = 1/k_C = 6.1 \times 10^{-8} M$, which gives $pK_C = 7.21$, suggesting the involvement of histidine residues. There are 36 hestidine residues in a polypeptide chain (see next section: Amino Acid Composition). Note that the value of k_C is not affected by the choice of the value of s.

As an insert in Fig. 19, Ca^{2+} binding data are plotted. There appear to be about eight binding sites, but because of the scattered data there is still considerable uncertainty. It is to be noted, however, that in the case of Ca^{2+} a few of them have distinctively high affinity.

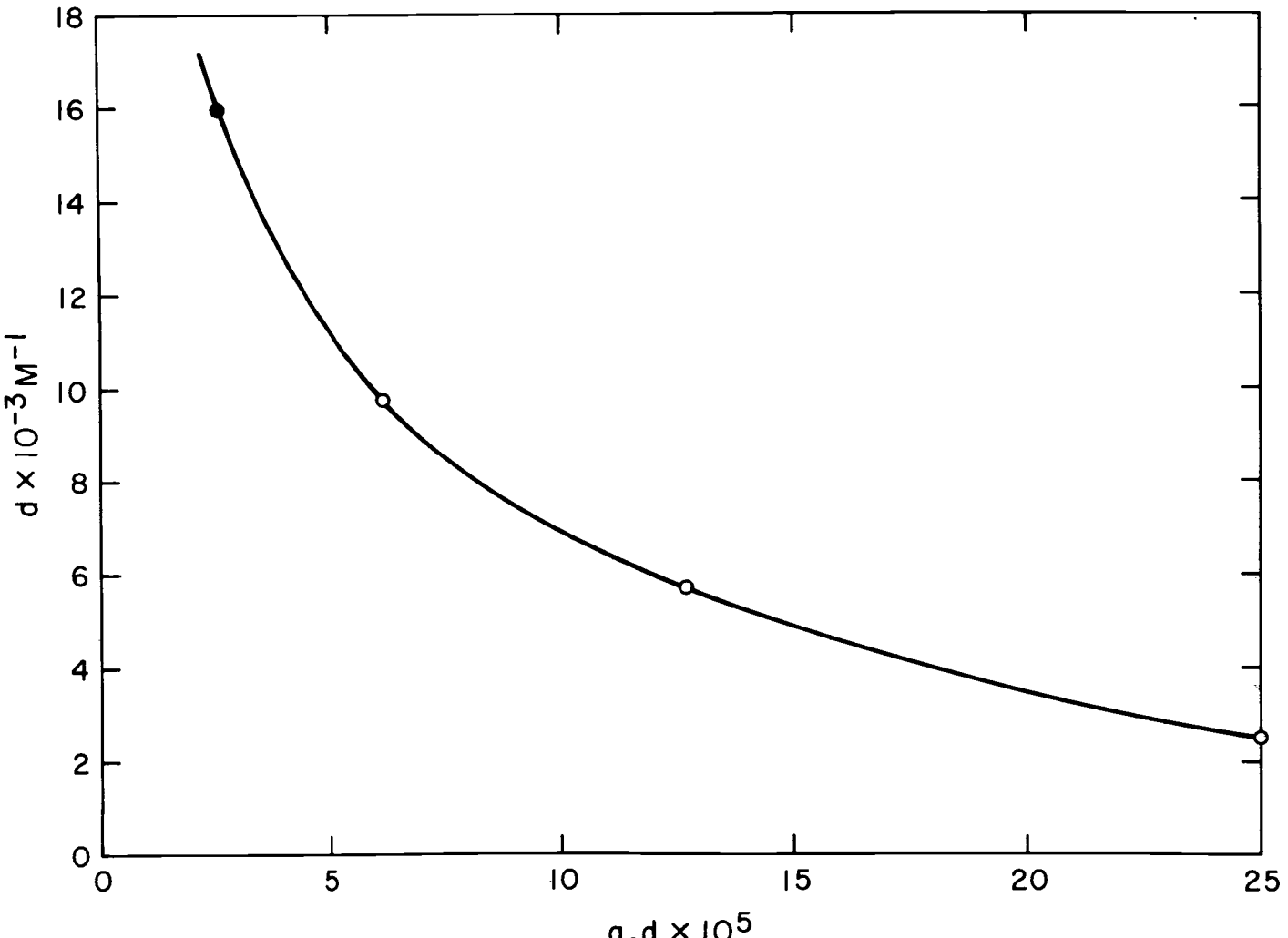

Figure 20(a). A graph of d vs. $a_C d$, where a_C is the activity of H^+, d is defined in the test.

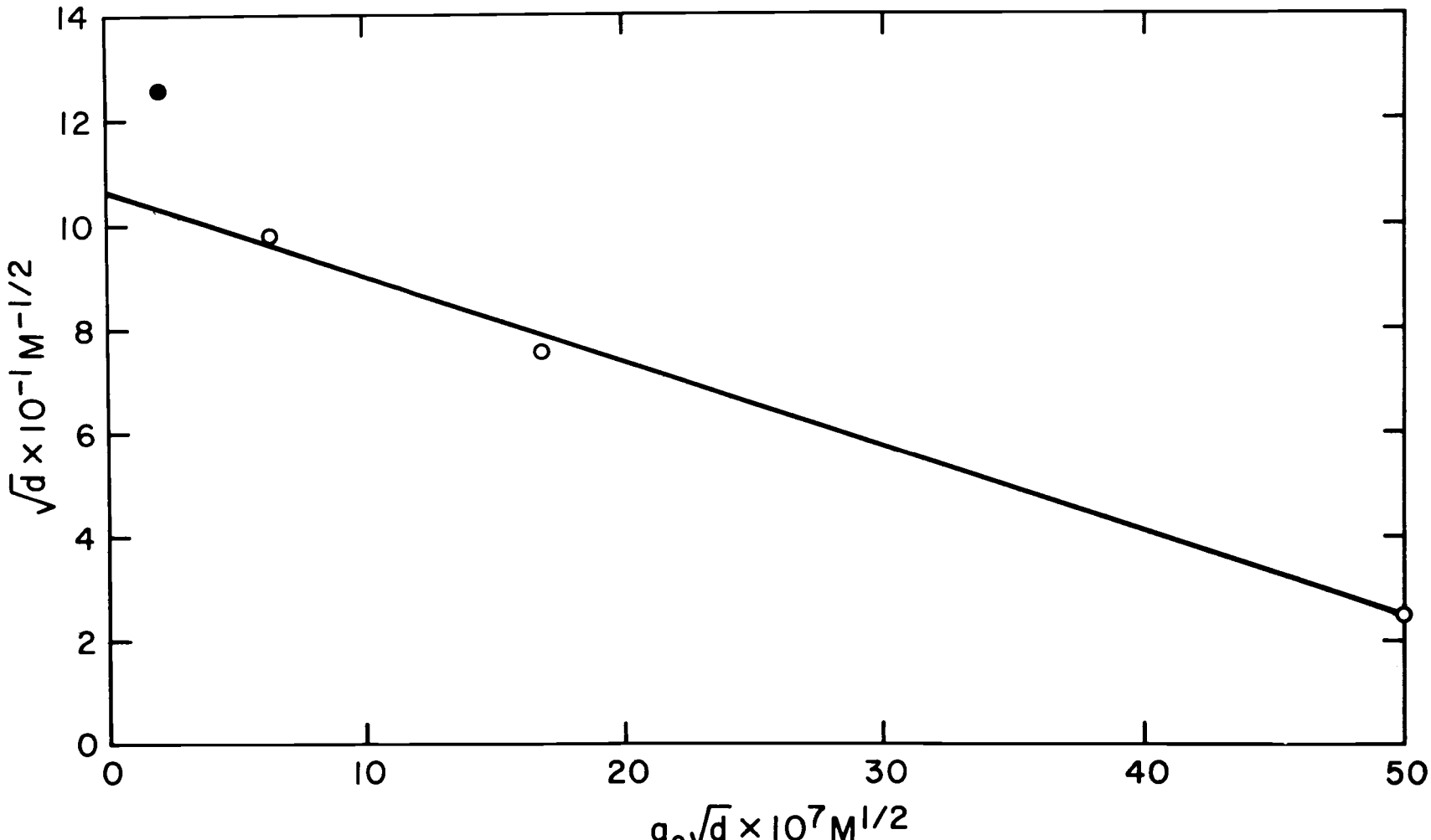

Figure 20(b). A graph of $\sqrt{d}$ vs. $a_c\sqrt{d}$, where a_c is the activity of H^+, d is defined in the text.

Amino Acid Composition

Table III presents the amino acid composition data of Callianassa hemocyanin. Since this hemocyanin is known to be microheterogeneous (Miller et al., 1976), these numbers are taken as the average values. Among the values given in Table III, the number of methionine is the least reliable value because of the lability of these residues. The specific volume as calculated from amino acid analysis and residue volumes (Cohn and Edsall, 1943) was found to be 0.720 ml/g. This is in good agreement with the value for both 17S and 37S forms as found from density measurements, 0.724 g/cm^3 (Roxby et al., 1974).

In Table IV, amino acid compositions of a number of hemocyanins are compared. Callianassa hemocyanin has a fairly average amino acid composition except relatively high content of glutamic acid.

Table III. Amino acid composition of hemocyanin from Callianassa californiensis.[a]

Amino Acid	Hours of Hydrolysis mol 20	48	72	Av[b]	Wt %	Amino Acid Residues/ 72,000g of Protein	Nearest Integer/ 72,000g
Lysine	0.0468	0.0455	0.0431	0.0451	4.63	26.0	26
Histidine	0.0635	0.0613	0.0605	0.0618	6.78	35.6	36
Ammonia	0.0807	0.0879	0.1095				
Arginine	0.0491	0.0462	0.0457	0.0470	5.87	27.1	27
Aspartic acid	0.1428	0.1399	0.1468	0.1432	13.19	82.6	83
Threonine	0.0534	0.0514	0.0470	0.0570[c]	4.61	32.9	33
Serine	0.0584	0.0521	0.0435	0.0644[c]	4.49	37.1	37
Glutamic acid	0.1508	0.1480	0.0949	0.1494[e]	15.43	86.0	86
Proline	0.0549	0.0528	0.0493	0.0523	4.06	30.2	30
Glycine	0.0709	0.0790	0.0781	0.0760	3.47	43.8	44
Alanine	0.0658	0.0651	0.0711	0.0673	3.83	38.8	39
Cysteine				0.0119	0.98	6.9	7
Valine	0.0634	0.0671	0.0608	0.0638	5.06	36.8	37
Methionine	0.0314	0.0225	0.0017	0.0314[d]	3.30	18.1	18
Isoleucine	0.0396	0.0457	0.0460	0.0460[d]	4.16	26.5	27
Leucine	0.0745	0.0756	0.0729	0.0743	6.73	42.9	43
Tyrosine	0.0342	0.0377	0.0326	0.0348	4.54	20.1	20
Phenylalanine	0.0609	0.0554	0.0555	0.0573	6.75	33.0	33
Tryptophan				0.0142	2.12	8.2	8

[a]A small amount of hexosamine was present in all hydrolysates; [b]Data were averaged, extrapolated to zero time(c), or value at maximum recovery used (d). Cystine and cysteine was determined as cysteic acid after oxidation by Me_2SO. Trypotphan was determined by alkaline hydrolysis according to Hugli and Moore (1972); [2]Value at 72 hr not used in average.

Table IV. Amino acid composition of hemocyanins. *

Source of hemocyanin	Lys	His	Arg	Try	Asp	Thr	Ser	Glu	Pro	Gly	Ala	Cys	Val	Met	Ileu	Leu	Tyr	Phe
Arthropoda:																		
Callianassa californiensis	4.6	6.8	5.9	2.1	13.2	4.6	4.5	15.4	4.1	3.5	3.8	1.0	5.1	3.3	9.2	6.7	4.5	6.8
Callinectes sapidus	4.6	5.8	4.7	1.2	13.4	5.0	4.6	10.9	4.7	6.5	6.8	0.9	6.7	2.4	4.8	7.3	4.0	5.5
Eriphia spinifrons	4.1	7.1	4.8	1.6	13.3	5.4	5.6	10.2	4.6	5.9	6.2	0.5	6.7	2.6	4.4	7.4	3.8	6.1
Homarus vulgaris	4.8	6.6	4.8	1.2	13.1	6.1	4.3	11.3	4.6	6.0	6.0	0.8	6.6	2.3	5.0	7.5	3.5	5.6
Limulus polyphemus	5.9	7.5	5.1	-	11.6	5.1	4.9	11.4	4.2	5.9	4.9	1.6	6.7	2.4	5.4	8.4	3.6	5.2
Palinurus vulgaris	4.5	6.7	4.9	1.3	14.9	4.9	4.0	11.1	4.8	6.2	5.6	0.8	6.4	3.0	5.1	7.2	3.3	5.6
Mollusca:																		
Cymbium neptuni	4.7	4.7	4.7	3.0	11.2	5.1	5.9	11.0	4.7	6.1	6.6	0.5	5.6	2.3	4.2	8.9	4.4	6.3
Eledone moschata	4.6	6.0	3.9	1.7	12.1	5.1	5.5	9.6	5.3	5.8	6.5	2.1	5.8	2.4	5.3	8.9	4.1	5.5
Helix pomatia(α)	4.4	5.7	4.4	1.5	11.4	5.4	5.4	9.9	5.4	5.9	6.9	1.5	5.9	1.0	4.9	9.6	4.9	5.9
Helix pomatia(β)	4.7	5.7	4.4	1.5	11.9	5.7	5.4	9.9	4.9	5.9	6.7	1.7	5.7	1.2	4.9	8.9	4.9	5.7
Murex brandaris	4.2	6.8	4.7	1.6	11.9	5.1	4.7	11.2	5.1	6.1	6.5	1.6	5.6	2.1	4.0	8.7	3.7	6.3
Murex trunculus	4.6	6.4	4.6	1.6	11.9	5.0	4.8	11.2	5.0	6.2	6.6	1.4	5.7	2.3	4.1	8.7	3.9	6.2
Octopus macropus	4.8	5.5	4.4	1.4	11.2	6.0	5.3	9.8	5.3	5.7	6.4	1.8	5.5	2.3	5.5	9.2	4.4	5.5
Octopus vulgaris	4.8	5.2	3.8	1.7	11.7	5.2	5.0	9.5	5.7	5.2	6.7	2.4	6.2	2.6	5.2	9.0	4.3	5.7
Pila leopoldillensis	3.2	4.1	5.3	3.0	11.0	5.0	5.7	11.5	6.2	6.0	7.6	1.1	6.0	1.1	4.4	8.7	3.9	5.5
Strophocheilus terrestris	3.9	4.4	4.4	2.8	11.8	5.6	6.0	10.7	5.6	5.8	6.5	0.9	5.6	0.5	4.9	9.0	4.6	5.8

*Values given in mole percent of amino acids. All the data except *Callianassa* are from Van Holde and van Bruggen (1971).

DISCUSSION

In the hemolymph of the shrimp, Calianassa californiensis, 85 percent of the hemocyanin is present in a form with $s^0_{20,w}$ = 38.8S, which is referred to as hemocyanin C. Attention has been focused in the present study to the hemocyanin C, which reversively dissociates into 17S particles (actually, 16.8S) when the divalent cations (Mg^{2+} or Ca^{2+}) are removed. An attempt was made to interpret the experimental results and characterize the system in terms of a thermodynamic model, which interrelates the association-dissociation reaction, cooperative oxygen binding, and the binding of the ligands Mg^{2+} and H^+. This model is developed in the Theory section.

The principal result in the Theory Section is eq. (21):

$$K=K_0\left\{\frac{1+L'_M+2\sqrt{L'_M/q}}{1+L'_{Te}+2\sqrt{L'_{Te}/q}}\cdot\frac{(1+\alpha)^6+L'_{Te}(1+c\alpha)^6+2\sqrt{L'_{Te}/q}(1+\alpha)^3(1+c\alpha)^3}{(1+\alpha)^6+L'_M(1+c\alpha)^6+2\sqrt{L'_M/q}(1+\alpha)^3(1+c\alpha)^3}\right\}^4\frac{(1+k_Ba_B)^{4P}}{(1+k_Ca_C)^{8P}} \tag{21}$$

where the equilibrium constant of monomer (6 subunits) and tetramer (24 subunits), K, is expressed as a function of the activities of the substrate (oxygen), α (= k_Aa_A), and two effectors, a_B and a_C, which are Mg^{2+} (or Ca^{2+}) and H^+ respectively. It is assumed that two H^+ and one Mg^{2+} compete for the same binding sites, the former favoring monomer and the latter favoring tetramer; this assumption

is based on the qualitative features of the Mg^{2+} binding and association equilibria studies. The parameters in the above equation were determined by the experimental studies, as described in Results, and are summarized in Table V. Although there are some limitations of the analysis which are discussed below, the model seems to give a reasonably consistent description of the system.

Association Equilibria

Although the weight average sedimentation coefficient can be obtained even from the poorly resolved boundaries as long as the second moment of the concentration gradient is used as the boundary, we cannot necessarily calculate the association constant of the monomer-tetramer equilibrium. In Fig. 21 a number of scanning profiles at pH 7.3, 7.65 and 8.0 are shown. At pH 8.0 the boundaries are clearly resolved and the plateau regions are reasonably horizontal. Under these conditions re-equilibration must be so slow that the sedimentation pattern reflect accurately the distribution of components existing at the beginning of the experiment. The boundaries are still well resolved at pH 7.65, but there is some indication at the plateau region between the two boundaries that some intermediate species are present and/or slight reequilibration reaction is going on. At pH 7.3, the boundaries are rather diffuse and the weight average sedimentation coefficient has to be

Table V. Numerical values of the parameters in eq. (21) determined from the experiments.

		Definition	Comments
k_B	$1.6 \times 10^3 M^{-1}$	eq. (44)	from mg^{2+} binding study[a]
k_C	$1.6 \times 10^7 M^{-1}$	eq. (44)	from Mg^{2+} binding study[a]
S	42 per monomer	eq. (44)	from Mg^{2+} binding study
P	2.5 per monomer	eq. (44)	from association equilibrium
h	3.7 per monomer	eq. (10)	from oxygen binding study
L'_M/L'_{Te}	1.7	eq. (32-2)	from association equilibrium
q	7.5	eq. (19)	from oxygen binding study
c	1.0×10^{-2}	eq. (11)	from oxygen binding study
K_O	$9.5 \times 10^5 M^{-3}$	eq. (21)	from association equilibrium

[a]It is assumed that the binding constant which is obtained from Mg^{2+} binding study applies also for the binding sites which are involved in the association of the hemocyanin.

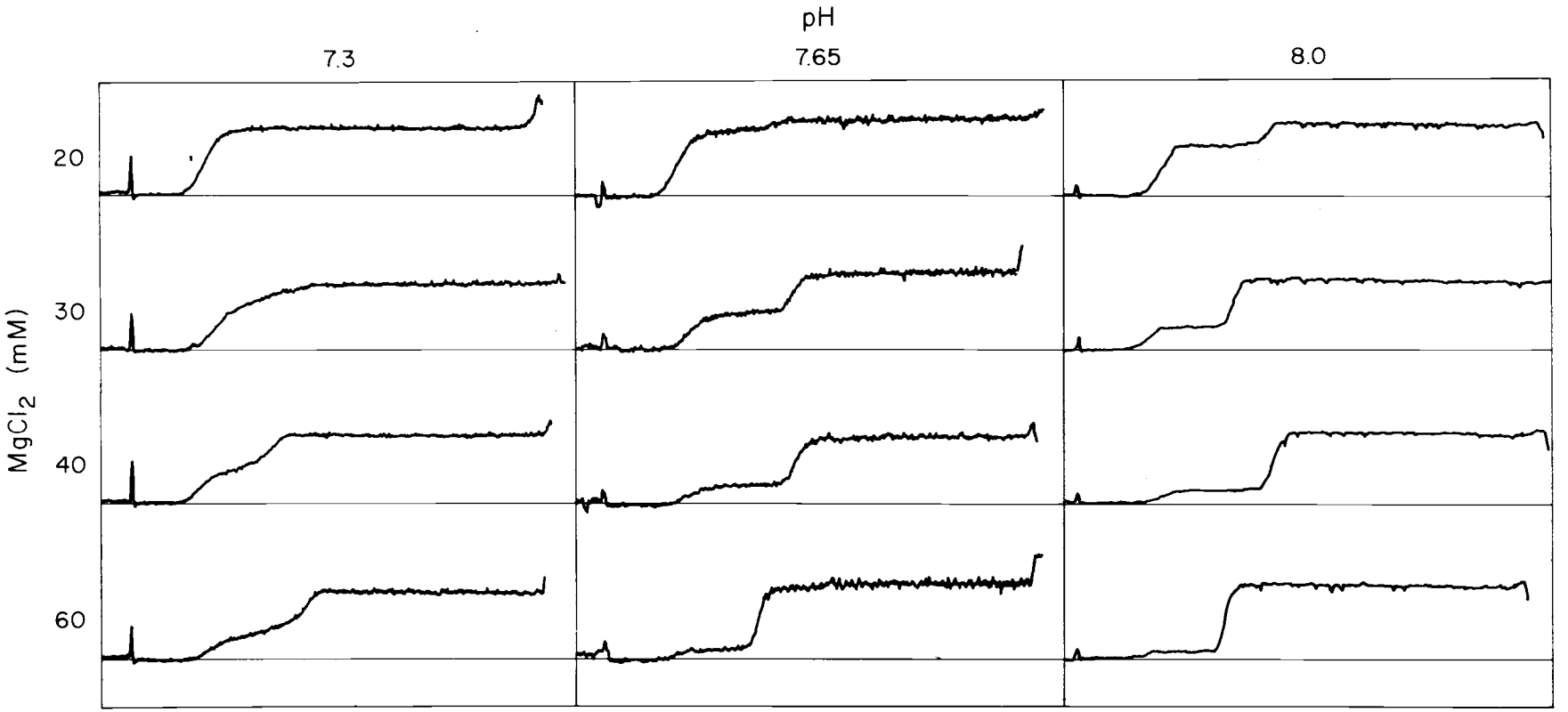

Figure 21. Scanning profiles of the velocity sedimentations at 40,000 r.p.m. At pH 8.0, the boundaries are well resolved; they are nearly so at pH 7.65.

from the second moment of the concentration gradient. The resolution at pH 7.0 is even poorer. Under these conditions, where re-equilibration is clearly occurring during the experiment, the distribution of components may be effected by the hydrostatic pressure in the ultracentrifuge cell (Roxby, et al., 1974). For that reason, the rigorous thermodynamic analysis has been carried out in the Results Section only at pH 8.0. Although the data at pH 7.3 are used in the following discussion, the above situation should be kept in mind and will be treated only qualitatively.

As we see in Fig. 5 and in the following discussion, the association profiles above pH 7.3 are similar and as expected from eq. (21):

$$K = K' \frac{(1+k_B a_B)^{4P}}{(1+k_C a_C)^{8P}} \tag{46}$$

$$K' = K_0 \left\{ \frac{1+L'_M+2\sqrt{L'_M/q}}{1+L'_{Te}+2\sqrt{L'_{Te}/q}} \cdot \frac{(1+\alpha)^6+L'_{Te}(1+c\alpha)^6+2\sqrt{L'_{Te}/q}(1+\alpha)^3(1+c\alpha)^3}{(1+\alpha)^6+L'_M(1+c\alpha)^6+2\sqrt{L'_M/q}(1+\alpha)^3(1+c\alpha)^3} \right\}^4$$

As we saw in the Theory section, $K' = K_0$ if $\alpha = 0$ (deoxy state). Also under the normal conditions where the system is in contact with air, the hemocyanin is almost fully saturated with O_2. In that case from eq. (22-2)

$$K'_{\alpha\to\infty} = K_0\{\frac{1+L'_M+2\sqrt{L'_M/q}}{1+L'_{Te}+2\sqrt{L'_{Te}/q}} \cdot \frac{1+c^6L'_{Te}+2c^3\sqrt{L'_{Te}/q}}{1+c^6L'_M+2c^3\sqrt{L'_M/q}}\}^4$$

$$\simeq K_0\{\frac{1+L'_M+2\sqrt{L'_M/q}}{1+L'_{Te}+2\sqrt{L'_{Te}/q}}\}^4 \qquad (47)$$

$$\simeq K_0(\frac{L'_M}{L'_{Te}})^4 = K_0(\frac{L^0_M}{L^0_{Te}})^4$$

The first approximation comes from the fact that $c^6L'_{Te}$, $c^6L'_M$, $2c^3\sqrt{L'_{Te}/q}$ and $2c^3\sqrt{L'_M/q}$ are much smaller than 1. The second approximation is justified, because both L'_M and L'_{Te} are considered to be much larger than 1. $L'/L'_{Te} = L^0_M/L^0_{Te}$ from the definition. Thus, although L'_M and L'_{Te} are functions of the concentrations of Mg^{2+} and H^+, K' is essentially a constant under the conditions where the association equilibria are studied. Instead of eq. (37), we have:

$$K = K' \frac{(1+k_Ba_B)^{4P}}{(1+k_Ca_C)^{8P}} = \frac{1-\alpha}{256\,\alpha^4C_o^3} \qquad (48)$$

The curves in Fig. 22 are calculated by eq. (48). There $K'c_0^3$ was set $10^{-11.2}$ and the activity coefficient of a_B was held constant 0.325, which is the average activity coefficient under the conditions for the sake of simplicity. Other numerical values of the parameters were taken from

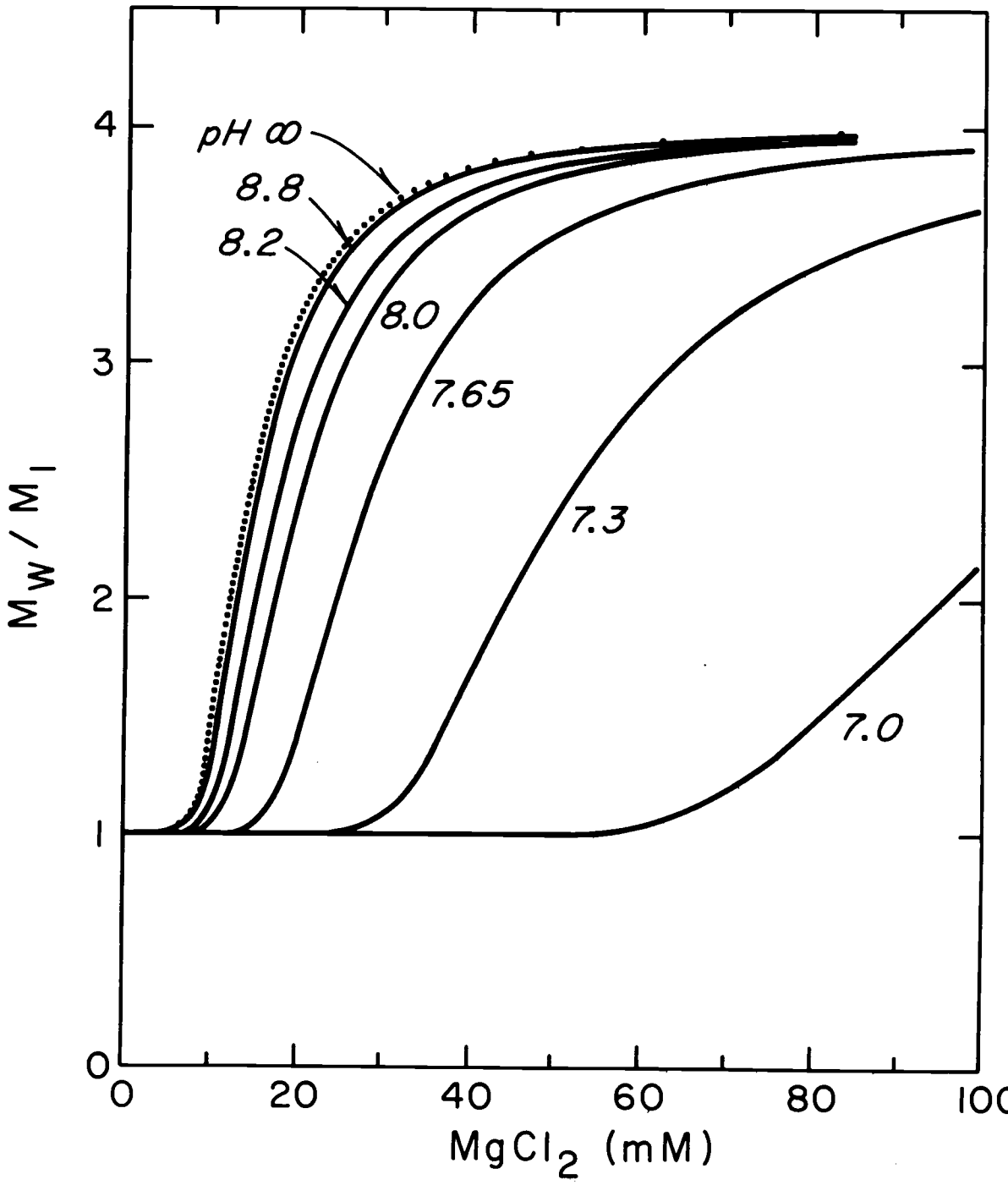

Figure 22. Theoretical association profiles at a number of pH values based on eq. (48).

Table V. Apparently the experimental results at low pH do not fit the expected profile based on eq. (48). The disagreement between the experimental results and the calculation under these conditions may be discussed in terms of the possibility of the dimer formation. As a matter of fact at around pH 5.0 the formation of a stable dimer has been observed (Fig. 23). The dimer formed under these conditions is insensitive to the presence of divalent cations (Eldred, unpublished results). If dimer formation is taking place, the theoretical treatment itself does not apply. The slope of the association curve close to zero Mg^{2+} concentration in Fig. 5 increases as the pH decreases. A possibility to explain this tendency is shown in Fig. 24, where the dimerization process is plotted with different hypothetical number of Mg^{2+} which is involved in the association process; the association constant being defined as:

$$K = K' \frac{(1+k_B a_B)^n}{(1+k_C a_C)^{2n}} = \frac{1 - \alpha}{4 \alpha^2 Co} , \qquad (48a)$$

where the parameters are defined as in eq. (48). It may be suggested that the effect of Mg^{2+} at low pH is overcome by H^+ and around pH 6.0, Mg^{2+} starts to play the same role as H^+ to form the dimer. The competition between Mg^{2+} and H^+ has been discussed in the Result Section. The low pH dimer may be a different species from the dimer at low

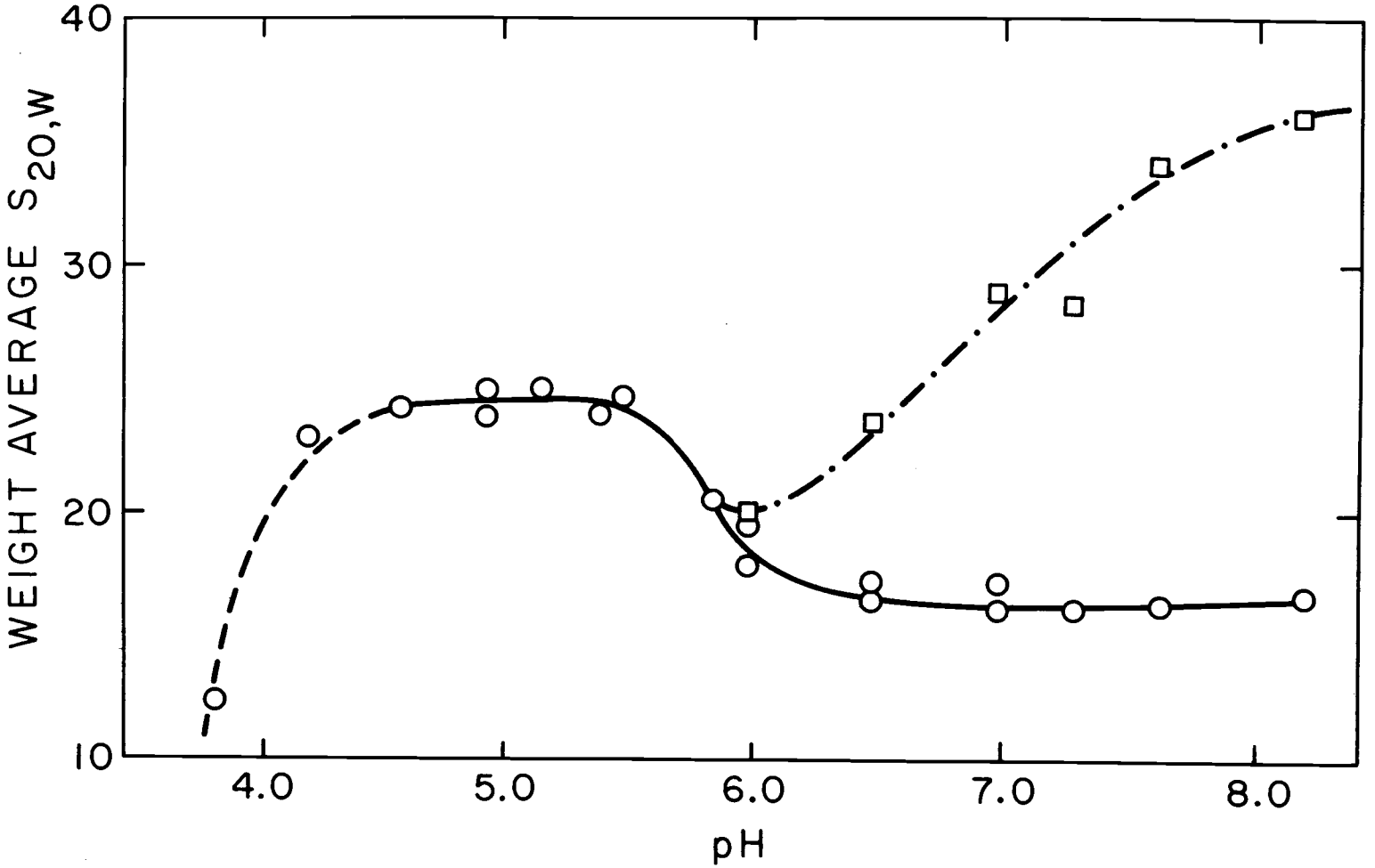

(From Van Holde et al., 1976)

Figure 23. Weight average sedimentation coefficients as a function of pH. Open circles show results in the absence of divalent cations, squares in 0.05M $MgCl_2$.

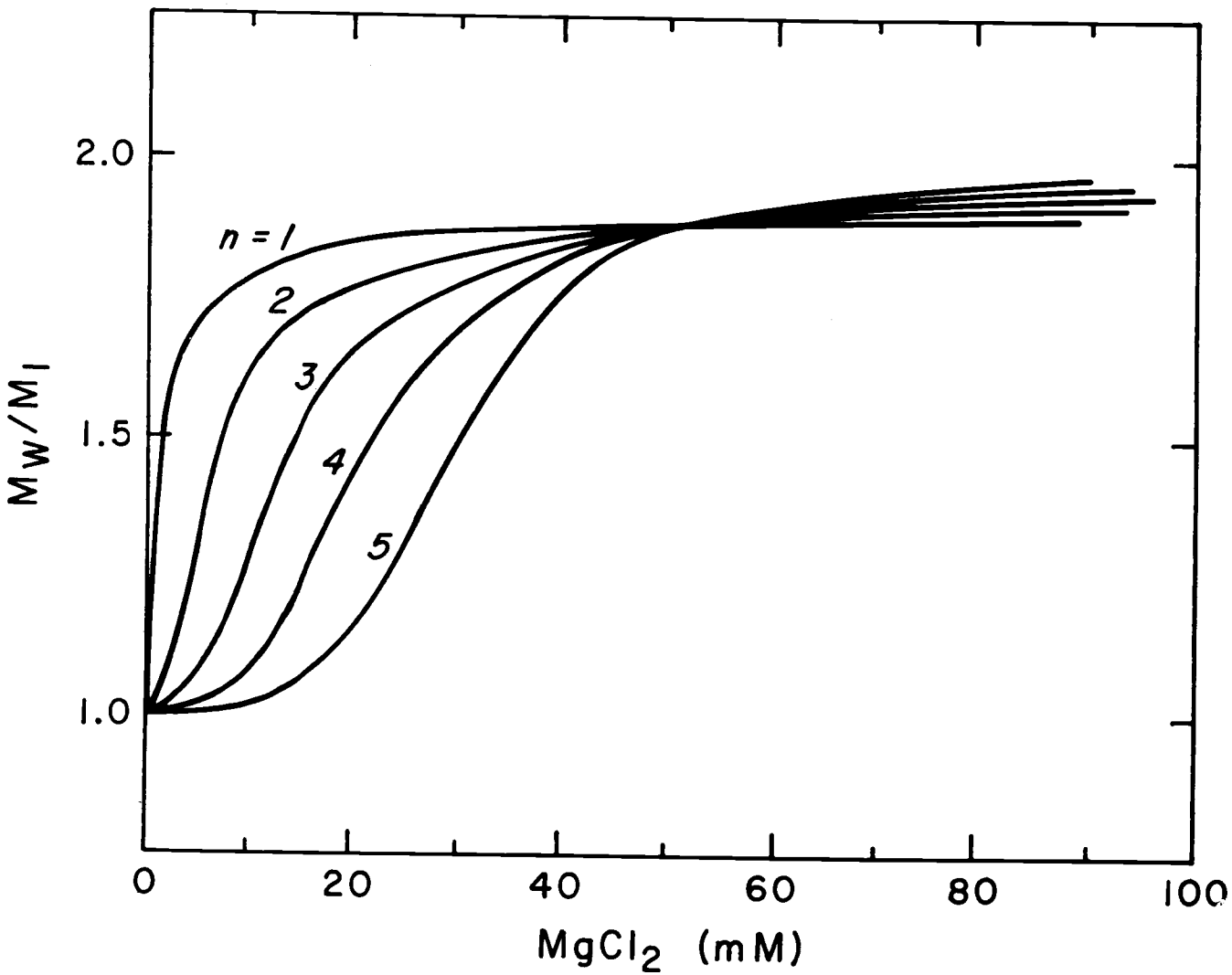

Figure 24. Hypothetical monomer-tetramer association profiles based on eq. (48a). K' values were chosen so that 90 percent of the hemocyanin associates at 0 mM Mg^{2+}.

temperature with the physiological pH (Blair and van Holde, 1976) which is discussed later.

In order to look at the difference between the experimental results and the theoretically expected features of the profiles of the association process more closely, the data in Fig. 7 are replotted in Fig. 25(a) and 26(a), where $\ln(1-\alpha)/\alpha^4$ (= ln K - ln 256 c_0^3) or log $(1-\alpha)/\alpha^4$ is plotted with respect to ln a_B or pH. The points at pH 8.0 were taken from the upper curve in Fig. 11. The expected curves from eq. (48) are plotted in Fig. 25(b) and 26(b). Although all the data points at each pH, except at pH 7.3, fall on a straight line with a common slope which gives the 4p value (eq. (23-2)), they are different from the calculated profiles in that the straight line does not go upward monotonously and approach to a limit as the pH goes up, but instead it starts to go down at around pH 8.2. The discrepancy is also reflected in Fig. 26(a) and (b). Each curve in (a) has a maximum around pH 8.1, while the theory predicts that it reaches a plateau at high extreme pH values. The disagreement at high pH may be attributed to the charge effect of the protein which has been neglected in the theoretical treatment. The increasing negative charge at high pH is presumably not negligible and may cause some electrostatic repulsion between monomer units. Alternatively, the titration of some specific groups at pH > 8.1 may specifically interfere with the association.

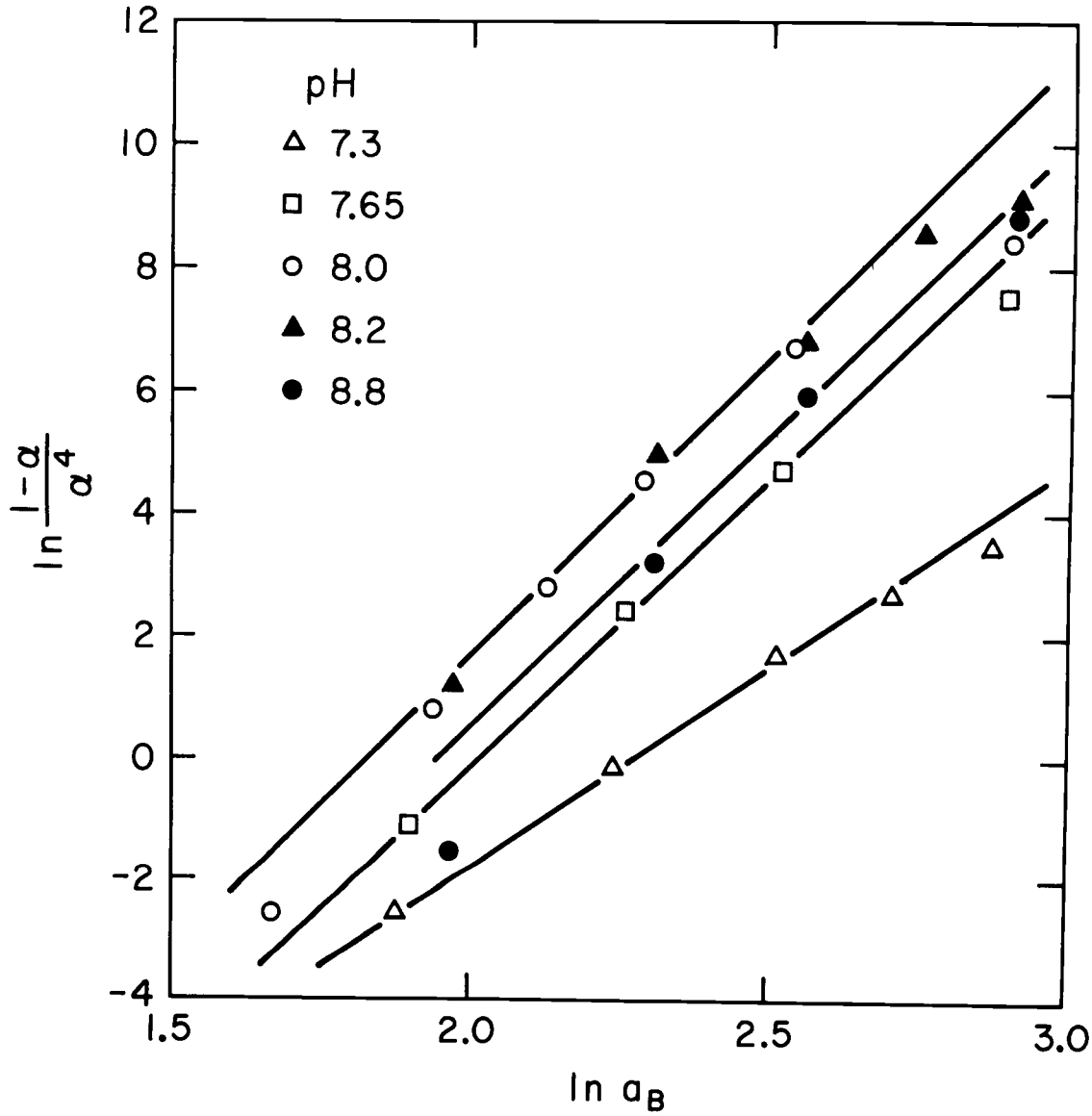

Figure 25(a). A graph of ln $(1-\alpha)/\alpha^4$ vs. a_B, where α denotes the degree of dissociation. The data were taken from Fig. 5.

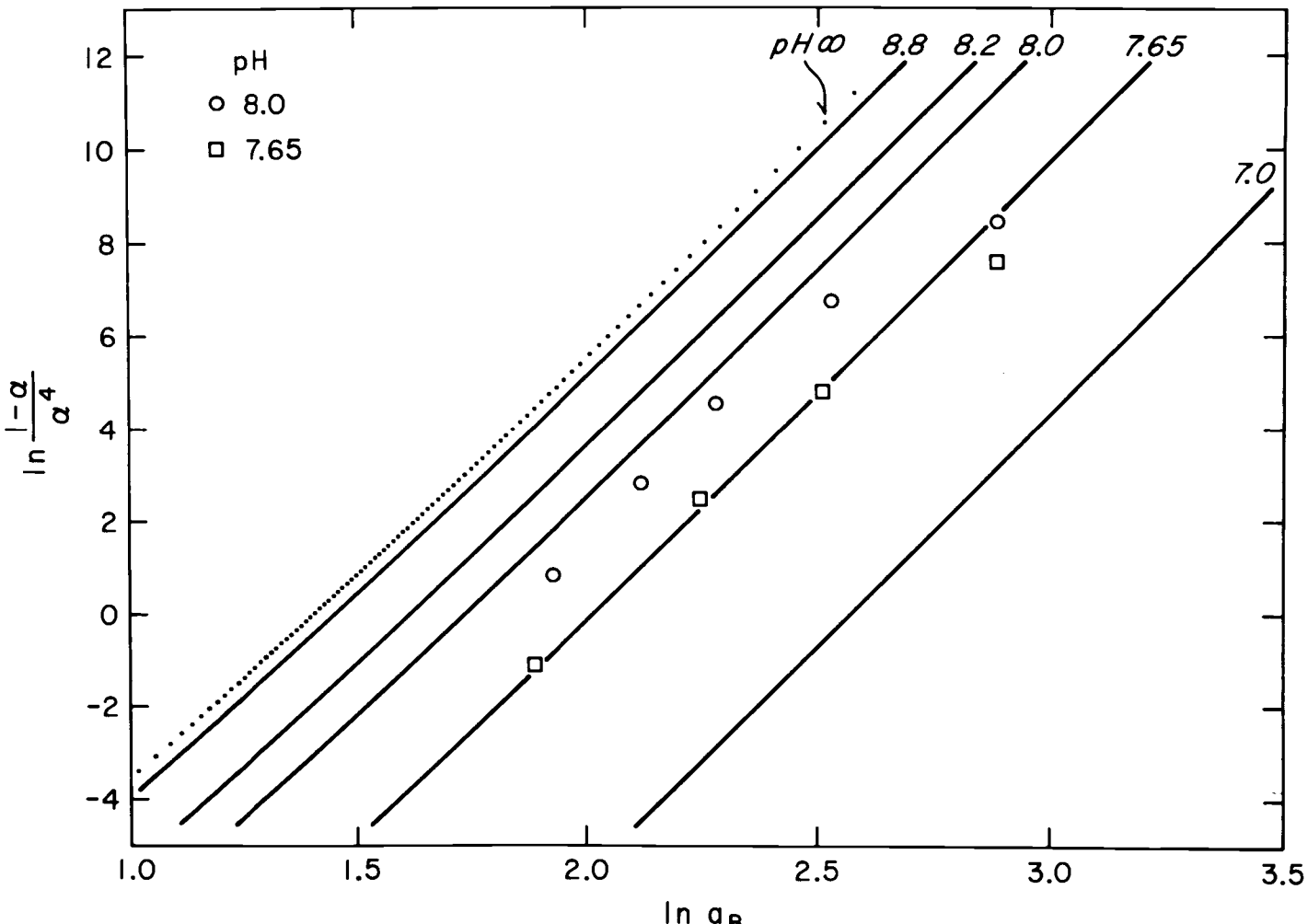

Figure 25(b). Theoretical curves of ln $(1-\alpha)/\alpha^4$ vs. ln a_B based on eq. (48).

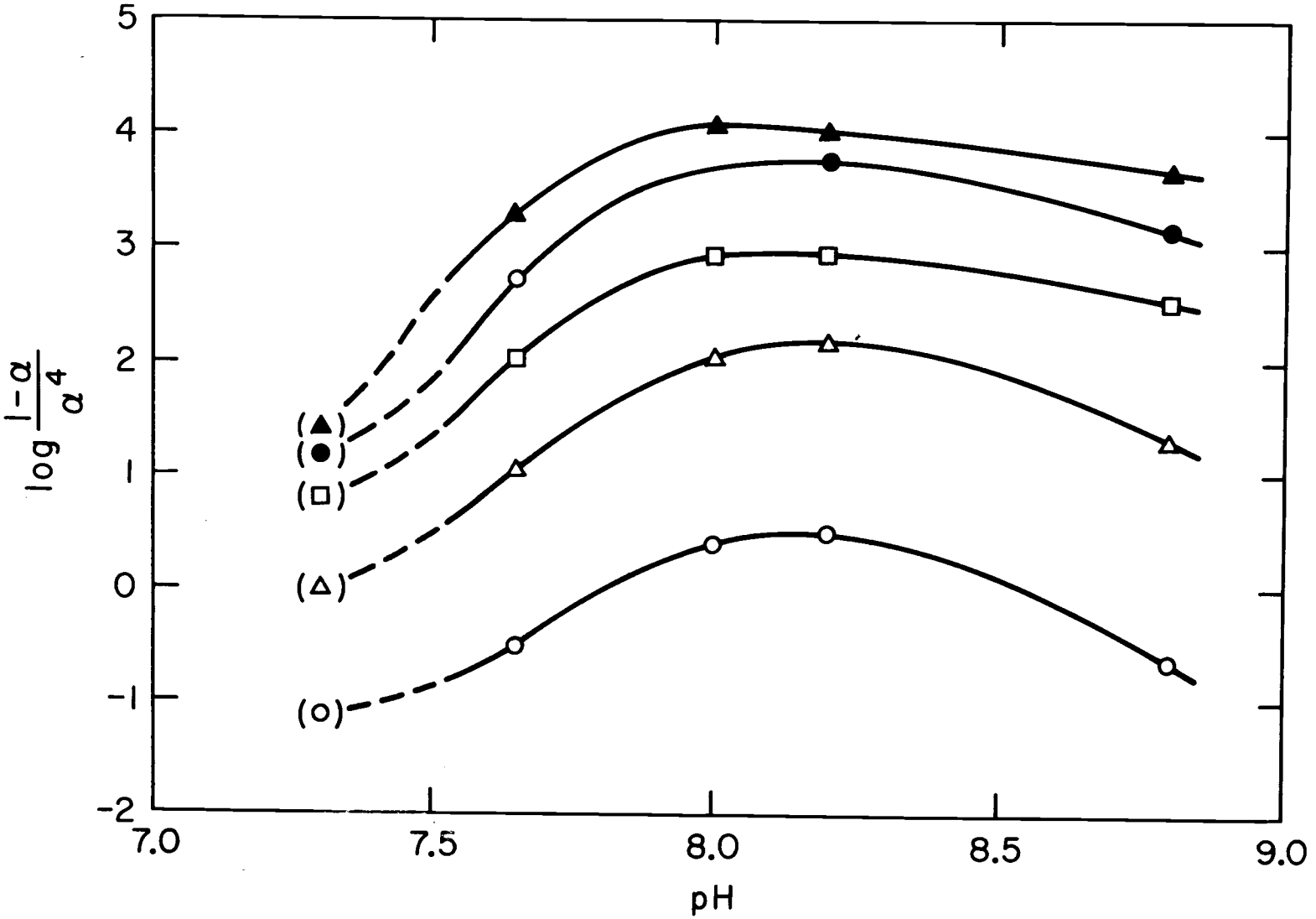

Figure 26(a). A graph of log $(1-\alpha)/\alpha^4$ vs. pH. The data were taken from Figure 5.

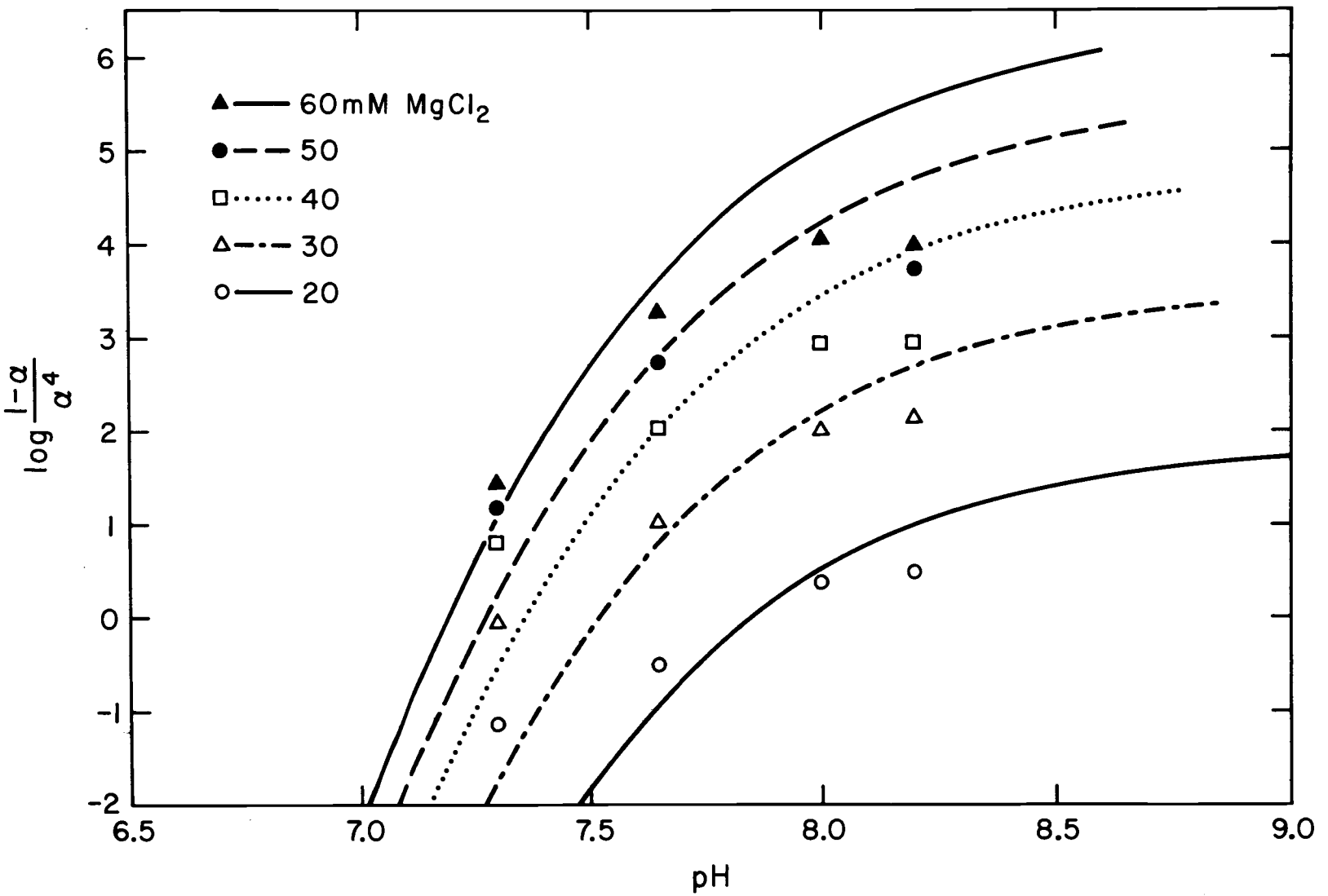

Figure 26(b). Theoretical curves of log $(1-\alpha)/\alpha^4$ vs. pH based on eq. (48).

In principle we should be able to estimate the value of 8P (eq. 23-3) by measuring the slope of the curve as we did for Mg^{2+}:

$$\frac{\partial \ln K}{\partial \ln a_C} = -\frac{\partial \log K}{\partial pH} = \frac{-8P\, k_C a_C}{1 + k_C a_C} + \delta'_c$$

$$\simeq \frac{-8P\, k_C a_C}{1 + k_C a_C}$$

As the calculated curves in Fig. 26(b) indicate, however, H^+ activity in the pH range were monomers associated to tetramer is not so high that one in the denominator cannot be neglected compared to $k_C a_C$. Thus the plot of ln K vs. ln a_C is not a straight line in this region and the slope is smaller than 8P. For example, the large slope, at pH 7.5 with 60 mM $MgCl_2$, gives 8P 14.0. This value turns out to be another confirmation that one Mg^{2+} compete with more than one H^+, because 8P from the above observation certainly exceeds the value 10.4 (=4P).

Looking at the data in Fig. 25(a) and also in Fig. 8 closely, we may observe slight curvature (upward convex) or deviation especially from the straight line at the extreme right. Considering that the data points at the extreme ends are the least reliable, this may be the result of experimental error. We could, however, expect those deviations on the following basis. We have assumed that 4P Mg^{2+}

binding sites have affinity for Mg^{2+} only in tetrameric state. Suppose that they have slight affinity in monomer state also. Then we may write:

$$\frac{\partial \ln K}{\partial \ln a_B} = \frac{4P\ k_B a_B}{1 + k_B a_B} - \frac{4P\ k_B' a_B}{1 + k_B' a_B} , \qquad (49)$$

where $k_B >> k_B'$. As long as a_B is reasonably small, the second term on the right hand side is negligible and the slope of the straight line will give the value of 4P (if $1 << k_B a_B$). As a_B increases, however, the second term will not be negligible any more and the slope will eventually become zero. This situation may reflect on the slight curvature or the deviation at the upper extreme region in Fig. 25(a) or Fig. 8. If this is the case, the estimated 4P is smaller than the actual value.

If the hydration of the hemocyanin changes upon association significantly, it will also affect the slope of the curve of ln K vs. ln a_B. According to Tanford (1969):

$$\frac{d \ln K}{d \ln a_x} = \Delta\bar{\nu}_x - \frac{n_x}{n_w} \Delta\bar{\nu}_w , \qquad (50)$$

where a_x is the activity of the ligand X, n_x and n_w are the moles of the ligand X and water in that system. In the present case, eq. (50) becomes:

$$\left(\frac{\partial \ln K}{\partial \ln a_B}\right)_{a_A, a_C} = \Delta\bar{\nu}_B - \frac{n_B}{n_w} \Delta\bar{\nu}_w \qquad (51)$$

If $n_B \sim 50$ mM, $n_B/n_w \sim 10^{-3}$. Although this value is very small, $\Delta\bar{\nu}_w$ may well be close to -10^3 in the present case because of the high molecular weight of the protein, i.e. 1.7×10^5 for tetramer. Suppose that the protein has 30 percent hydration, which is a usual value (Kuntz and Kauzmann, 1974), and 5 percent of the bound water mosecules are released. Then $\Delta\bar{\nu}_w$ amounts to -1.5×10^3. 4P, which is determined from the slope of the curve of ln K vs. ln a_B may be one or two larger than the actual value. In any case the estimated 4P has some uncertainty, of the order of ±2.

Sedimentation equilibrium studies of the same hemocyanin by Blair and Van Holde (1976) have revealed that the association proceeds in two steps: (1) a monomer-dimer association which is sensitive to Mg^{2+} concentration and insensitive to temperature, and (2) a dimer-tetramer association which is highly temperature dependent but insensitive to Mg^{2+}. They analyzed their data according to the simple reaction scheme:

$$2M + nMg^{2+} \rightleftarrows D \qquad (52)$$

and

$$4M + mMg^{2+} \rightleftarrows Te \qquad (53)$$

The values of n = 6.6 and m = 12.7 which correspond to 4P in eq. (38) were obtained. The value of m = 12.7 is reasonably close to the present result of 4P = 10.4. The scatter in the data of Blair and Van Holde is such that the difference should not be taken as significant.

As Miller and Van Holde (1974) have observed, oxygen binding significantly affects the monomer-tetramer equilibrium of Callianassa hemocyanin. In the present study, the effect of oxygenation was quantitated (Fig. 7) and analyzed based on the model which was given in the Theory section. One of the conditions which the model must satisfy is the fact that the allosteric unit is a monomer (six subunits). This requirement comes from the experimental result that the highest observed Hill coefficient, n_H, is 3.3 and that the monomer alone can show significant cooperativity, with Hill coefficient as high as 3.3 (Table I). The shift of the monomer-tetramer equilibrium upon oxygenation is essentially explained in the model by the difference of the allosteric equilibrium constant L'_M and L'_{Te} (compare equations (22-1) and (22-2)). Because of the difference between L'_M and L'_{Te}, the population of R state in tetramers is higher than in monomers. Oxygenation thus favors the tetramer state, thereby shifting the equilibrium toward tetramer. It is to be noted that a relatively small difference in L', a ratio of 1.7, can explain the shift of the association curve shown in Fig. 7. The oxygen-linked association or dissociation such as this has also been observed in some Gstropod hemocyanins. In most cases oxygenation favors larger association state, especially dimerization of half molecules (DePhillips, et al., 1970; Wood and Dalgleish,

1973), but in some cases oxygenation facilitates dissociation (van Driel and van Bruggen, 1974).

Morimoto and Kegeles (1971) have obtained the value of n = 5 (eq. (52)) for the dimerization process of lobster 17S hemocyanin, which is also close to the present results (per monomer). The peculiar difference between our results and theirs is that not only divalent cations but also H^+ favors the dimerization of the lobster hemocyanin. Since their experiments were performed at rather high pH (9.6), it may be possible that the conditions in which their experiments were done correspond to the pH region higher than 8.2 in our case where the curve of ln K vs. pH starts to go down.

It may be appropriate here to comment on the consequence of the present treatment of the association reaction, eq. (48), compared with the simple reaction scheme such as eq. (53). For simplicity, let us consider the effect of Mg^{2+} only. From eq. (46), we have:

$$\frac{[Te]}{[M]^4} = K'' (1 + k_B a_B)^m \qquad (54)$$

$$K'' = \frac{K'}{(1+k_C a_C)^{8P}}, \qquad m = 4P$$

For the reaction (53), the association constant K"' may be defined as:

$$K''' = \frac{[Te]}{[M]^4 a_B^m} ,$$

where a_B is the activity of Mg^{2+}.

$$\therefore \quad \frac{[Te]}{[M]^4} = K''' \cdot a_B^m \tag{55}$$

The above equation assumes simple chemical reaction and any tetramer has m Mg^{2+}. On the other hand, eq. (54) basically assumes preexisting monomer-tetramer equilibrium where Mg^{2+} preferentially but statistically binds to tetramer thus shifts the equilibrium just as in allosteric transition. Although eq. (54) assumes m independent binding sites, it is easily rewritten to incorporate any kind of site-site interaction. For example, the general expression of eq. (54) can be written as:

$$\frac{[Te]}{[M]^4} = K''(1 + k_1 a_B + k_2 a_B^2 + \text{---} + k_m a_B^m) \tag{56}$$

$\sum = 1 + k_1 a_B + \text{---} + k_m a_B^m$ is the binding polynomial of Mg^{2+}. If the binding sites are all independent, it reduces to eq. (54). If the binding is completely cooperative so that no intermediate species such as $Te(Mg^{2+})_{n-i}$ $(1 \leq i \leq n - 1)$ are present, eq. (56) reduces to:

$$\frac{[Te]}{[M]^4} = K'' \ (1 + k_m a_B^m) \tag{57}$$

This equation again reduces to eq. (55) when $K_m a_B^m >> 1$. Can we distinguish the two cases (eq. (54) and (55)) from the results of the association equilibria? As we have seen, both schemes give almost identical association profiles and the qualitative distinction is difficult. Although it is not practical at the present stage, the association equilibrium at low concentration of Mg^{2+} will give us some information, if we have some way to measure a small amount of tetramer precisely.

Association-Dissociation Reaction

The original purpose of the measurement of the association kinetics was to determine the time required for the equilibration of the reaction. The data shown in Figs. 12 and 13 demonstrate that the reaction, while slow at high pH, is essentially at equilibrium in about ten hours. These data can be used, moreover, to determine, in principle, the overall rate constants of the reaction. The following is an effort along that line. Since the association process takes place by two steps, i.e. the Mg^{2+} dependent dimerization and the temperature dependent dimer-tetramer equilibrium (Blair and Van Holde, 1976), we may write:

$$2M \underset{k_2}{\overset{k_1}{\rightleftarrows}} D \qquad (58\text{-}1)$$

$$2D \underset{k_4}{\overset{k_3}{\rightleftarrows}} Te \qquad (58\text{-}2)$$

For those reactions, the rate equations can be written as below:

$$\frac{dN_1}{dt} = -2k_1N_1^2 + 2k_2N_2 \qquad (59\text{-}1)$$

$$\frac{dN_2}{dt} = k_1N_1^2 - k_2N_2 - 2k_3N_2^2 + 2k_4N_4 \qquad (59\text{-}2)$$

$$\frac{dN_4}{dt} = k_3N_2^2 - k_4N_4 \ , \qquad (59\text{-}3)$$

where N_i denotes the molar concentration of i-mer. Since the dimer concentration is very small under the conditions throughout the reaction (dimer is not detectable in the sedimentation velocity experiment, Fig. 11), we may assume a low, steady-state concentration of N_2:

$$\frac{dN_2}{dt} = 0 \qquad (60)$$

or

$$N_2 = \text{const.} \qquad (60a)$$

From eq. (59-1),

$$\frac{dN_1}{dt} = -2k_1(N_1^2 - B) \qquad (61)$$

$$B = \frac{k_2}{k_1} N_2 = \text{const.} \tag{61a}$$

Integrating eq. (61), we obtain:

$$\frac{1}{2\sqrt{B}} \ln \frac{N_1 - \sqrt{B}}{N_1 + \sqrt{B}} = -2k_1 t + C \tag{62}$$

where C is an integration constant. Since $N_1 = N_0$ (the total molar concentration of monomer units in the system), when $t = 0$,

$$C = \frac{1}{2\sqrt{B}} \ln \frac{N_0 - \sqrt{B}}{N_0 + \sqrt{B}} \tag{63}$$

Substituting (63) into eq. (62),

$$\ln \frac{N_1 - \sqrt{B}}{N_1 + \sqrt{B}} \cdot \frac{N_0 + \sqrt{B}}{N_0 - \sqrt{B}} = -4k_1 \sqrt{B}\, t ,$$

from which we obtain:

$$N_1 = \sqrt{B} \cdot \frac{1 + Re^{-4k_1\sqrt{B}\, t}}{1 - Re^{-4k_1\sqrt{B}\, t}} \tag{64}$$

$$R = \frac{N_0 - \sqrt{B}}{N_0 + \sqrt{B}} \tag{64a}$$

It can be seen that the quantity N_1 in eq. (64) satisfies the conditions; $N_1 = N_0$ at $t = 0$ and that in the limit as

$t \to \infty$,

$$N_1 = B = \sqrt{\frac{k_2}{k_1} N_2} \tag{65}$$

i.e.,

$$\frac{N_2}{N_1^2} = \frac{k_2}{k_1} . \tag{65a}$$

Putting eq. (64) into eq. (38), we obtain an equation for the intensity of the scattered light as a function of time:

$$i = 4cN_0 \{1 - \frac{3\sqrt{B}}{4N_0} \cdot \frac{1 + Re^{-4k_1\sqrt{B}\ t}}{1 - Re^{-4k_1\sqrt{B}\ t}} \} \tag{66}$$

From eq. (66), we obtain an expression of a quantity whose value can be experimentally determined:

$$\frac{i_\infty}{i_0} = 4(1 - \frac{3}{4} \frac{\sqrt{B}}{N_0}) \tag{67}$$

where i_0 and i_∞ are the intensities of the scattered light at $t = 0$ and $t = \infty$ respectively. At short times:

$$e^{-4k_1\sqrt{B}\ t} \simeq 1 - 2k_1\sqrt{B}\ t$$

This approximation gives, from eq. (66):

$$i \simeq CN_0 \{1 + \frac{6k_1(N_0^2 - B)}{N_0} t\} \tag{68}$$

From the initial slope of the light scattering data, therefore, we could determine:

$$6\ Ck_1(N_0^2 - B)$$

from which k_1 is determined, since B is available from eq. (67) and N_0 is known. Thus, we can determine all the necessary parameters in eq. (64), i.e., $k_1 = 3.0 \times 10^7\ M^{-1}min^{-1}$ and $B = 5.0 \times 10^{-19}M^2$. In Fig. 27 the light scattering data and the calculated light scattering are compared. The agreement is not very satisfactory. There are two parameters in eq. (66); i.e. k_1 and $\sqrt{B}$ (R is a function of $\sqrt{B}$). Qualitatively, k_1 affects the initial slope and $\sqrt{B}$ affects both the initial slope and the equilibrium value of the scattering intensity. It was not possible to choose those parameters so as to fit the whole data set. It may be possible that the separation of the reassociation process into an initial fast reaction which lasts for about an hour and a subsequent slow reaction which lasts for six hours or so arises from the heterogeneous population of the hemocyanin molecules. In fact, some microheterogeneity of monomer molecules (17S) has been found in this system (Eldred, unpublished results). It appears that there are electrophoretically distinguishable kinds of 17S molecules, which most probably result from different combinations of the set of polypetidide chains.

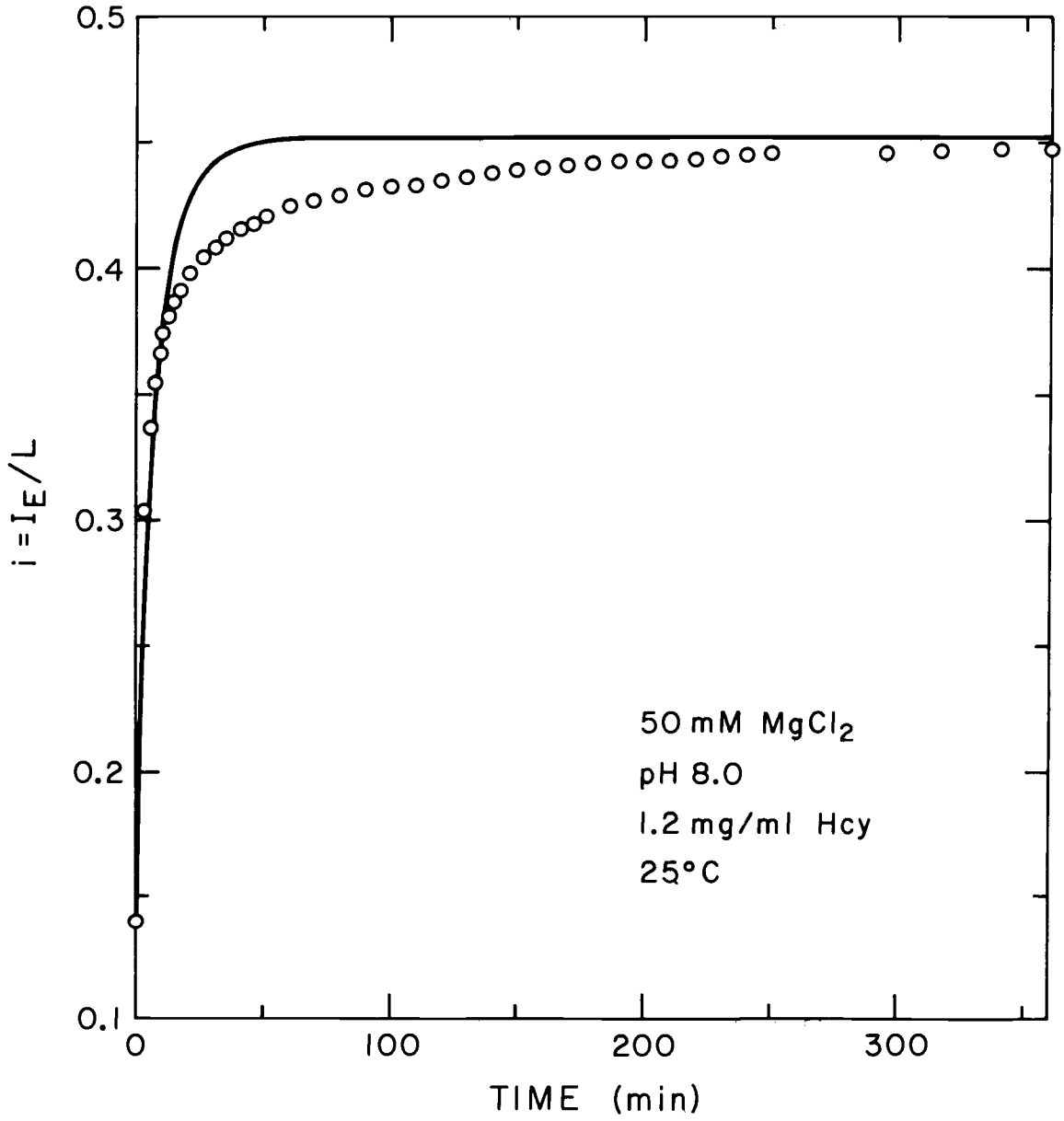

Figure 27. Time course of the change in light scattering in association process. A comparison between the experimental data and the calculation based on eq. (66).

Obviously the overall rate constants we have observed may involve contributions from a number of kinds of reaction steps, such as the ligand binding, conformational change and macromolecular interactions. Recently Tai and Kegeles (1975) have employed concentration jump relaxation kinetics to elucidate more detailed reaction mechanism of the monomer-dimer association of lobster hemocyanin. Their analysis strongly suggested the "ligand-mediated" dimerization in which the binding of four calcium ions was required before dimerization took place.

As we saw in Fig. 9, some of the monomer molecule (17S) which was reassociated from 5S subunits cannot associate to tetramer (39S). Conceivably this also stems from the microheterogeneity of the subunit polypeptide chains. Five or six bands have been found in polyacrylamide gel electrophoresis of the polypeptide chains (Miller et al., 1977). Attempts have been made to find any conditions in which 39S molecules could be reconstituted from 5S subunits, but they have not been successful. In some cases we found very diffuse boundaries whose weight average sedimentation coefficient was between 17S and 39S at pH 8.0. Presumably, some combination of subunits which is necessary for the tetramerization is not realized when monomer (17S) is associated from subunit molecules. It is to be noted that although 5S subunits which were once separated seem to have some difficulty in finding its

original combination or configuration in monomer unit, it certainly retains its oxygen binding capacity (Miller and Van Holde, 1974). Marimoto and Kegeles (1971) have found similar situations in lobster hemocyanin. In their case the dissociated 5S subunits partially associated to monomer (17S) and some ill-defined species which have sedimentation coefficients between 5S and 17S were found at pH 9.6 with 14 mM Ca^{2+}, but no dimers (25S) were observed.

A major remaining problem in the study of arthropod hemocyanins lies in the separation and purification of individual polypeptide chains, and the study of their association. Some progress toward this goal has been achieved with Limulus hemocyanin by Sullivan et al. (1974). However, the separation techniques they have employed for Limulus hemocyanin have not been successful with other hemocyanins, including that of Callianassa. It is recognized that the existence of such microheterogeneity in the population of monomer particles is an impediment to more detailed analysis of the behavior of this, and other arthropod hemocyanins. The reader of this thesis should recognize the full implications of this microheterogeneity: many of the properties described herein may represent average quantities for a microheterogeneous population. It is precisely in the kinetic analysis that such microheterogeneity becomes most obvious.

Oxygen Binding Study

The effect of divalent cations, Mg^{2+} or Ca^{2+}, and H^{+} on the affinity of oxygen binding of Callianassa hemocyanin has already been reported by Miller and Van Holde (1974). They found that Mg^{2+} and Ca^{2+} increase the affinity for oxygen, whereas H^{+} decreases it. A positive Bohr effect is defined as oxygen binding behavior in which the affinity for oxygen (represented by P50) increases as pH increases. Wyman (1948) has explained the Bohr effect in terms of the change in the affinity of Bohr proton upon oxygenation. For the sake of simplicity, assume that one H+ is linked to oxygen binding. Then the equation derived by Wyman reduces to:

$$\log P50 = \text{constant} + \log \frac{k' + a_C}{k'' + a_C} \qquad (69)$$

where k" and k' denote the dissociation constants of the Bohr proton for the oxy and deoxy hemocyanin respectively and a_C is the activity of hydrogen ion. This treatment has been shown to explain the experimental results of hemoglobin very well. If Δpk (= pk" - pk') < 0, the system shows a positive Bohr effect. On the other hand, if $\Delta pk > 0$, it shows a negative Bohr effect. In terms of the allosteric model, k" and k' roughly correspond to $1/k''_R$ and $1/k''_T$, respectively, where k''_R and k''_T (= $\frac{k''_R}{e}$, e < 1) are the binding

constants of the proton which is linked to oxygen binding. The expression of the relationship between P50 and a_C (or pH) in terms of the allosteric model can, in principle, be derived by combining the relationships between L' vs. $\alpha_{\frac{1}{2}}$ and L' vs. a_C. The expression, however, turns out to be rather complicated and not very practical especially for the hybrid model. Since eq. (69) is considered to be a reasonably good approximation for the present analysis, let us rewrite eq. (69) for our present case. We observed in the Results section that two H^+ are likely to compete with one Mg^{2+}. Taking this result into account, eq. (69) becomes:

$$\log P50 = \text{const.} + \log \frac{d\beta + (1+\gamma)^2}{\beta + (1+e\gamma)^2} \qquad (70)$$

$$\simeq \text{const.} + 2 \log (1+\gamma) - \log(1+\beta) \qquad (70a)$$

where $\beta = k'_R a_B$ and $\gamma = k''_T a_C$. The approximation that "non exclusive binding coefficients d and e for Mg^{2+} and H^+ are much smaller than unity was used for simplicity. In Fig. 28(a) and (b), log P50 is plotted against pH and ln a_B (a_B denotes the activity of Mg^{2+} whose activity coefficient is calculated from eq. (27)). Although eq. (70a) explains qualitative features of those plots, eq. (70) in which d and e are not neglected is seemingly necessary to be employed for the quantitative analysis. In order to employ eq. (70), d and e must be determined in some way.

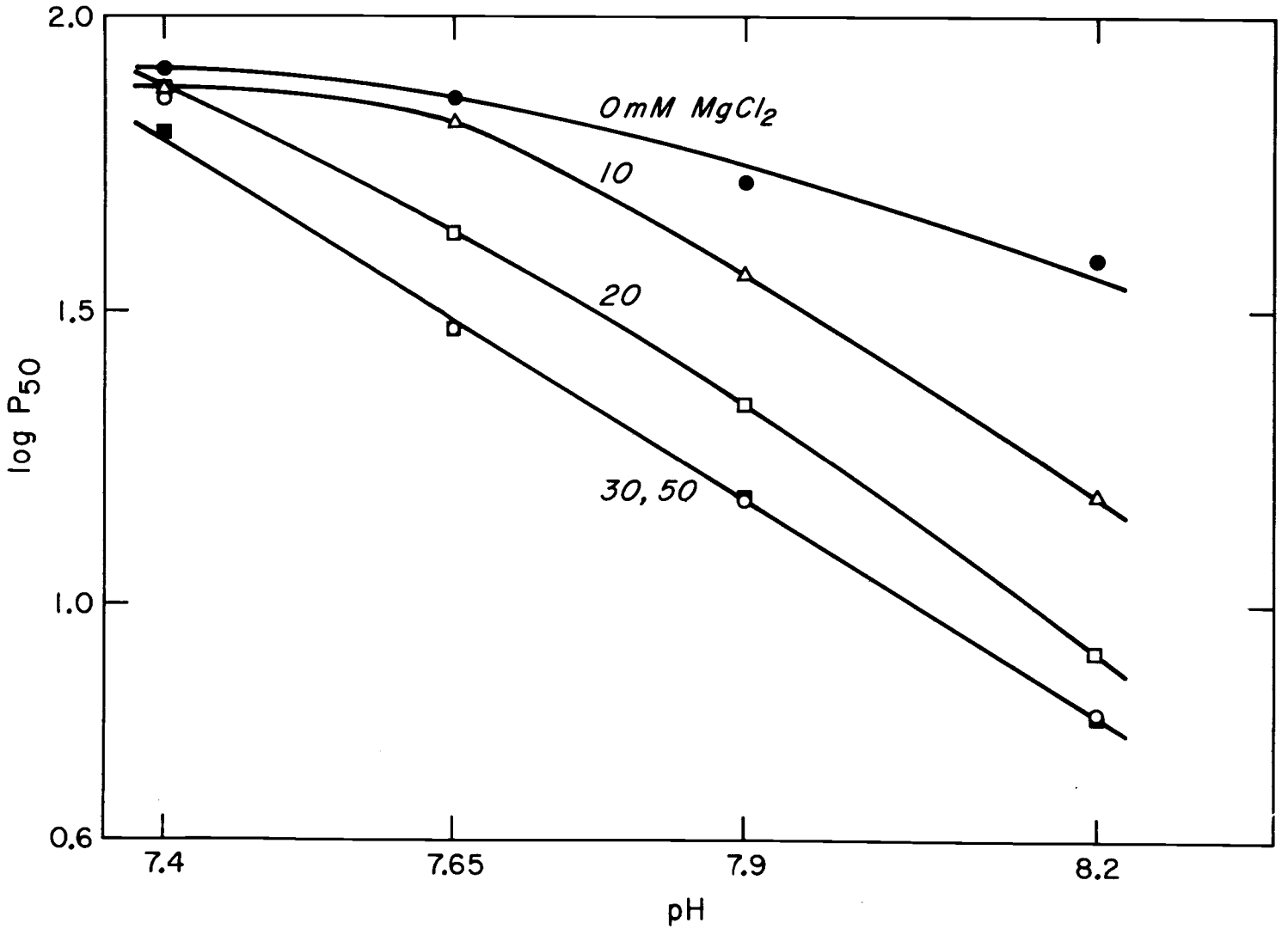

Figure 28(a). A graph of log P50 vs. pH. The data were taken from Table I.

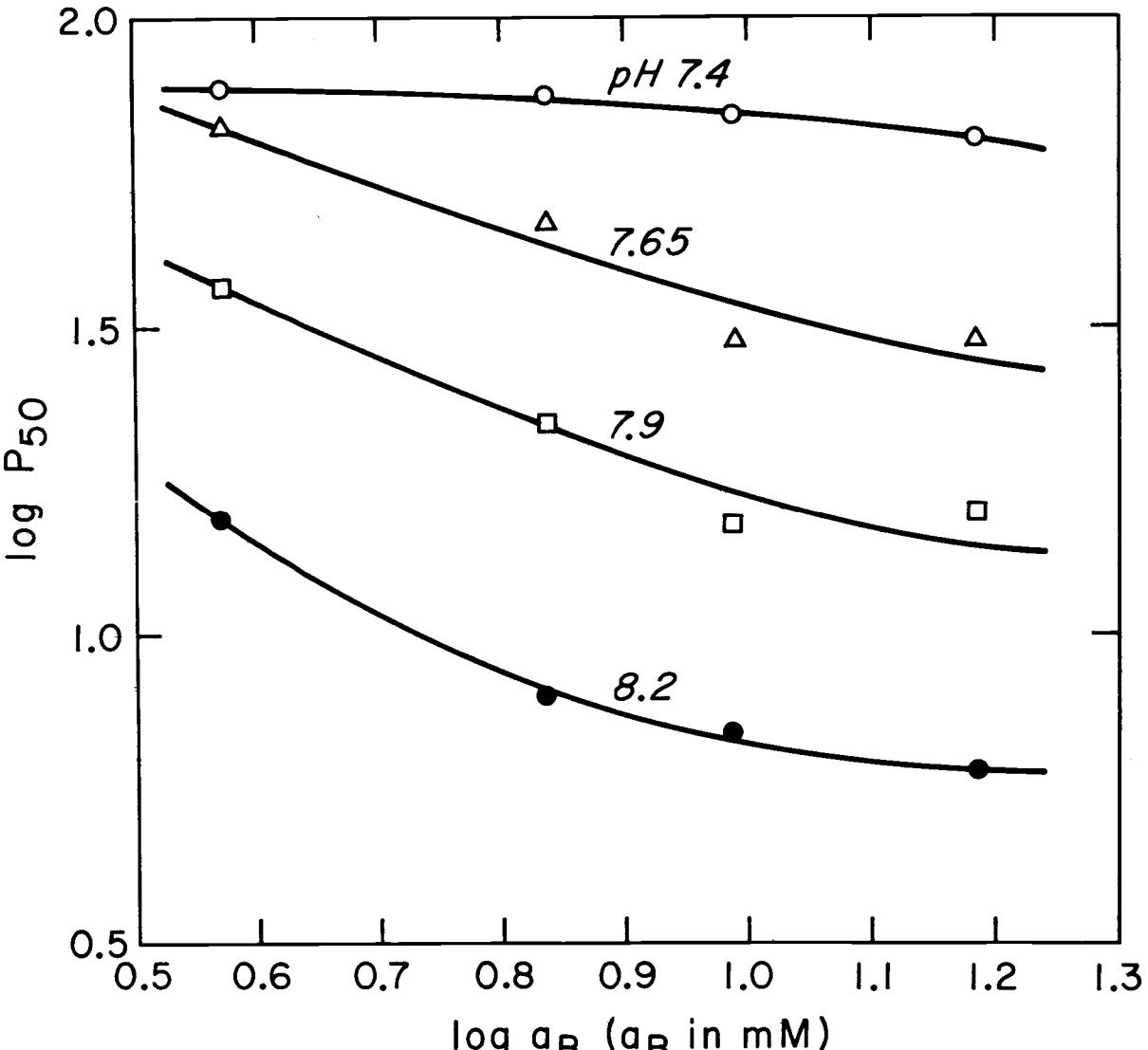

Figure 28(b). A graph of log P50 vs. log a_B. The data were taken from Table I.

The positive Bohr effect or alkaline Bohr effect is common in hemocyanins, though there are some gastropod molluscs, such as Helix pomatia (β hemocyanin) and Busycon canaliculatum, whose hemocyanins exhibit negative Bohr effects. Interestingly, hemocyanin from Limulus polyphemus, which is taxonomically arthropod, has also negative Bohr effect under physiological conditions (Table VI).

Miller and Van Holde have also suggested that the allosteric unit consists of six polypeptide chains and that the oxygen binding of the hemocyanin fits the hybrid model proposed by Buc et al. (1973) better than the concerted model extended by Rubin and Changeux (1967). The suggestion that the allosteric unit is a monomer (17S) which consists of six subunits is supported by the present data (Table I) on the grounds that the hemocyanin shows high cooperativity under the conditions where no appreciable amount of tetramer (39S) is present. The hybrid model which was suggested by Miller and Van Holde for this system is also supported by curve fitting of the experimental data with the model. From eq. (19a), we have:

$$\bar{Y}= \frac{\alpha(1+\alpha)^5+c\alpha L'(1+c\alpha)^5+\sqrt{L'/q}\{\alpha(1+\alpha)^2(1+c\alpha)^3+c\alpha(1+\alpha)^3(1+c\alpha)^2\}}{(1+\alpha)^6+L'(1+c\alpha)^6+2\sqrt{L'/q}(1+\alpha)^3(1+c\alpha)^3}$$

which gives:

Table VI.

	pH	Divalent Cations	n_{max}	P50 (mmHg)	Bohr Effect	References
Arthropoda:						
Callianassa californiensis	7.65	Yes	3.3	26	+	Miller & Van Holde, 1974
	7.65	No	1.0	100	+	Miller & Van Holde, 1974
Panulirus interruptus	7.6	Yes	2.7	23	+	Kuiper *et al.*, 1975
	7.6	No	1.4	10	+	Kuiper *et al.*, 1975
Cupiennius salei	7.6	Yes	5.3	25	+	Loewe and Linzen, 1975
	7.6	No	3.3	9	+	Lowew and Linzen, 1975
Procambarus simulans	7.6	Yes	3.4	4	+	Larimer and Riggs, 1964
	7.6	No	1.9	10	+	Larimer and Riggs, 1964
Carcinus maenas	7.6	Yes	-	17	+	*Truchot, 1975
	7.6	No	-	32	+	Truchot, 1975
Lymulus polyphemus	7.43	No	1.0	2.1	-	From Van Holde and van Bruggen,
Cardisoma guahumi	7.55	Yes	2.64	3.5	+	1971
Homarus americannus	7.7	Yes	3.6	2.5	+	
Mollusca:						
Buccinum undatum	7.8	Yes	1.78	13.5	-	Wood *et al.*, 1977
	7.8	No	1.20	3.5	-	Wood *et al.*, 1977
Helix pomatia(α)	7.6	Yes	2.1	11	Small +	From Van Holde and van Bruggen, 1971
	7.6	No	1.1	10	+	"
Helix pomatia(β)	7.6	Yes	4.6	21	-	"
	7.6	No	1.1	5	-	"
Loligo paelei	7.36	Yes	3.9	150	+	"
Busycan canaliculatum	8.77	No	1.0	2.5	-	"
	8.2	Yes	2.0	7.9	?	"

* P50 calculated from his experimental formula.

$$\log \frac{\bar{Y}}{1 - \bar{Y}} = \log$$

(71)

$$\left[\frac{\alpha(1+\alpha)^5+c\alpha L'(1+c\alpha)^5+\sqrt{L'/q}\{\alpha(1+\alpha)^2(1+c\alpha)^3+c\alpha(1+\alpha)^3(1+c\alpha)^2\}}{(1+\alpha)^5+L'(1+c\alpha)^5+\sqrt{L'/q}(1+\alpha)^2(1+c\alpha)^2(2+\alpha+c\alpha)}\right]$$

The "non-exclusive binding coefficient" C and the allosteric transition parameter which determines the population of the hybrid state can be determined as shown below. According to Buc *et al.* (1973), the Hill coefficient will be given by

$$n_H = 1 + \{n(\sigma^2/\sigma_m^2) - 1\} \frac{(\alpha_{\frac{1}{2}}-1)(1-c\alpha_{\frac{1}{2}})}{(\alpha_{\frac{1}{2}}+1)(1+c\alpha_{\frac{1}{2}})} \qquad (72)$$

where $\alpha_{\frac{1}{2}}$ is the ligand concentration at half-saturation normalized to the binding constant in the R state. In our case $\alpha_{\frac{1}{2}} = P50/P50_R$. The determination of C and n (σ^2/σ_m^2) has already been described by Miller and Van Holde (1974). With the same procedure, we obtain $c = 1.04 \times 10^{-2}$ and $\sigma^2/\sigma_m^2 = 0.73$. For the latter value, we assume n = 6, which has been justified above. Buc *et al.* (1973) also gave an expression for σ^2. At $\alpha_{\frac{1}{2}} = c^{-\frac{1}{2}}$, where the highest Hill coefficient is obtained:

$$\sigma^2 = \frac{1}{4}\left(1 - \frac{1}{\sqrt{q} + 1}\right) \qquad (73)$$

Using the value of $\sigma^2/\sigma_m^2 = 0.73$ and $\sigma_m^2 = 0.25$, we obtain $q = 7.5$. Because of the fact that σ^2 is a function of $\alpha_{\frac{1}{2}}$,

eq. (72) is somewhat complicated. The complete expression of σ^2 is given in eq.(A11) of Buc et al. (1973). The smooth curve in Fig. 17 was calculated by eq. (72) using that complete expression of σ^2. Using the values of c and q we now are able to calculate eq. (71). For the smooth curves in Fig. 15, L' values were chosen so as to best fit the data points at each pH and Mg^{2+} concentration. For the non-exclusive concerted model (Rubin and Changeux, 1967), eq. (71) is simplified to:

$$\log \frac{\bar{Y}}{1-\bar{Y}} = \log \left[\frac{\alpha(1+\alpha)^5+c\alpha L'(1+c\alpha)^5}{(1+\alpha)^5+L'(1+c\alpha)^5}\right] \qquad (73)$$

This equation did not fit the data very well. In Fig. 29, eq. (71) and eq. (73) are compared at L' values of 10^6. The difference at the extreme ends are obvious.

Concerning the value of the "nonexclusive binding coefficient" $c = 1.0 \times 10^{-2}$, Miller and Van Holde obtained a somewhat smaller value, 4×10^{-3}. Apparently, the distance between the two straight lines for R and T states observed in these newer studies (Fig. 15) is shorter than found in the earlier work (see Fig. 4 of Miller and Van Holde). The obvious difference is that in their studies 10 mM $CaCl_2$ was present as well as 50 mM $MgCl_2$. However, even in the absence of Ca^{2+}, Miller and Van Holde obtained the same small c value (Mg^{2+} series). In this case the only difference is that the hemocyanin in the present experiments was treated

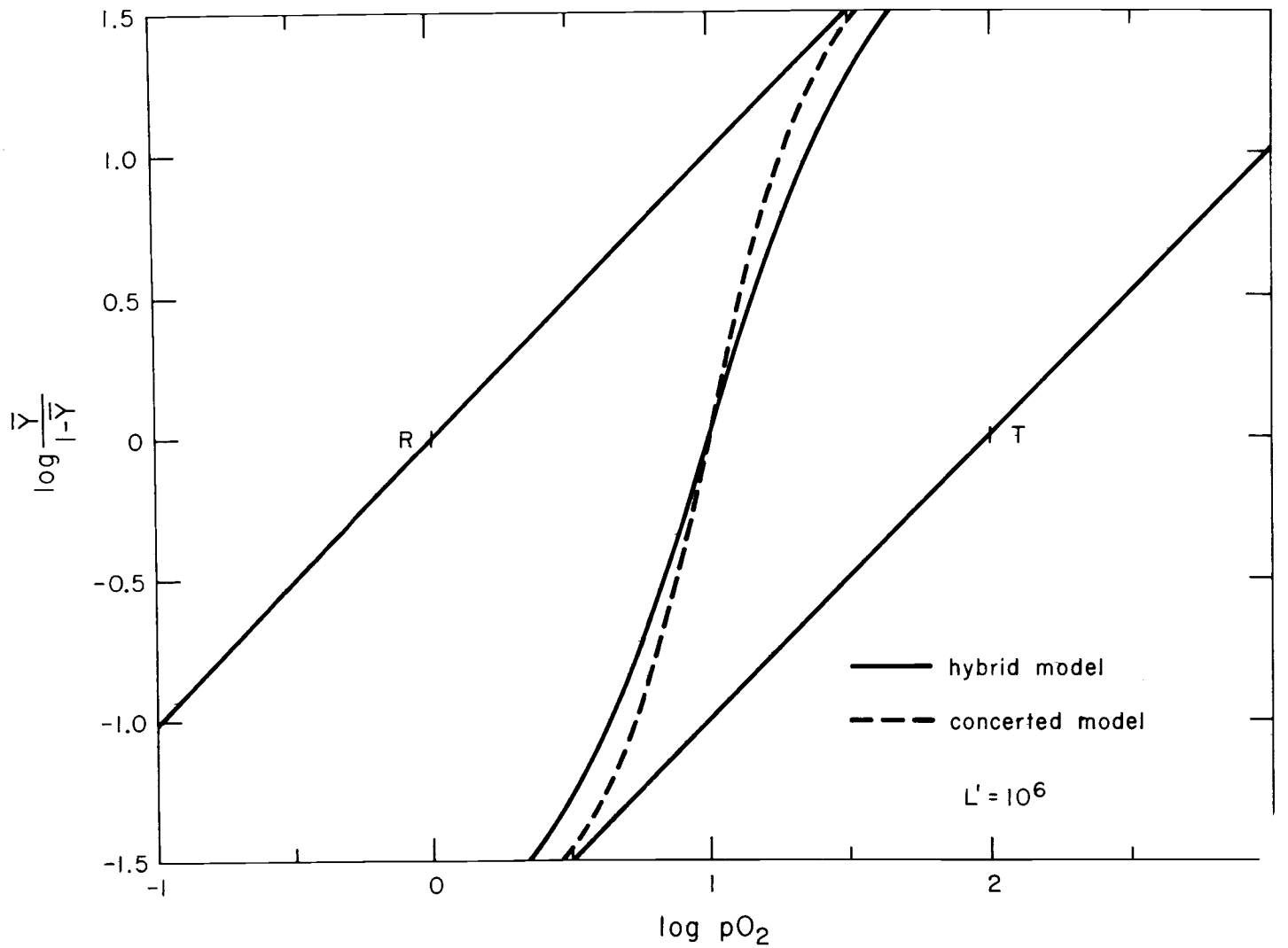

Figure 29. A comparison between the hybrid model (q = 7.5) and concerted model ($q \to \infty$).

with EDTA prior to the oxygen binding measurement. It may be possible that the hemocyanin which is not treated with EDTA retains some strongly bound Ca^{2+} even though it is dyalyzed against buffer without divalent cations several times. In any event, the small differences in parameters found in the two studies are unimportant in comparison with the observation that both sets of investigations indicate nonexclusive binding involving hybrid states.

As we observe in Table I or Fig. 17, the effect of Mg^{2+} tends to reach a plateau and increases of Mg^{2+} further does not decrease P50 any more (Compare at 30 mM and 50 mM of $MgCl_2$, also see Fig. 28(b)). This observation can be explained in terms of the Mg^{2+} activity dependence of the allosteric conformational equilibrium constant L':

$$L' = \{\frac{d\beta + (1+\gamma)^2}{\beta + (1+e\gamma)^2}\}^h L^0 \qquad (10)$$

From the above expression, we obtain:

$$d^h L^0 \leq L' \leq e^{-2h} L^0 \qquad (74)$$

Eq. (74) implies that there is a maximum and minimum value of L'. That is to say, from the consequence of the "non-exclusive binding coefficient" d, Mg^{2+} does not completely shift the equilibrium toward R state.

Although divalent cations increase the cooperativity of oxygen binding in any hemocyanin system to the author's

knowledge, increasing the oxygen affinity as in Callianassa is not necessarily a common case as can be seen in Table VI. In arthropod species there are both cases; e.g., Callianassa, Procambarus and Carcinus have lower P50 values in the presence of divalent cations, whereas Punubirus and Cupiernius show higher P50 values in the present of divalent cations. All molluscs listed in Table VI have higher P50 values in the presence of divalent cations. There is no obvious relation to the Bohr effect. In terms of the allosteric model, both divalent cations and H^+ behave as negative effectors for the latter case. In that case, instead of eq. (10), we may write:

$$L' = \{\frac{d\beta + (1+e\gamma)^2}{\beta + (1+\gamma)^2}\}h_L 0 \qquad (75)$$

where $d < 1$ and $e < 1$. Whether the Bohr effect is positive or not may be independent of whether divalent cations decrease P50 or not, because the former is determined by the sign of pK (= pK'-pK" is the difference of pK values of Bohr proton), while the latter is determined by whether the divalent cations have higher affinity to R state or not.

What is the effect of the association equilibrium of the hemocyanin molecule on the oxygen binding curve? For instance, as to the oxygen binding at pH 7.9 with 20 mM $MgCl_2$, the percentage of tetramer increases from 48 percent to 59 percent from deoxygenated state to oxygenated state

(Fig. 15 and Table I). From the association equilibrium experiment of the oxy and deoxy hemocyanin, we obtained $L'_M/L'_{Te} = 1.7$. In Fig. 30, oxygen binding curves with $L' = 10^6$ and 1.7×10^6 are compared. Because of the relatively small difference of the L' value, the shift of the binding curve is small. Furthermore, considering that the change in the association only amounts to 20 percent, the effect of the shift in association equilibrium is small; it may be considered to be within experimental errors. In other words, although oxygenation affects the association enough to be experimentally observable, the shift of equilibrium will not affect the oxygen binding curve enough to detect by other than very precise measurements. Recently Imai and Yontani (1977), using a somewhat different analysis, reached a similar conclusion: the dissociation of hemoglobin under normal conditions (about 20 percent upon oxygenation) will only slightly affect the oxygen binding curve. The difference between those two cases should be pointed out. In the case of hemoglobin, the allosteric unit, which consists of four polypeptide chains (two α chains and two β chains) dissociates into two α-β dimers which do not exhibit cooperative binding, whereas the Callianassa hemocyanin monomer (17S) which is dissociated from tetramer (39S) still contains the whole allosteric unit (six polypeptide chains).

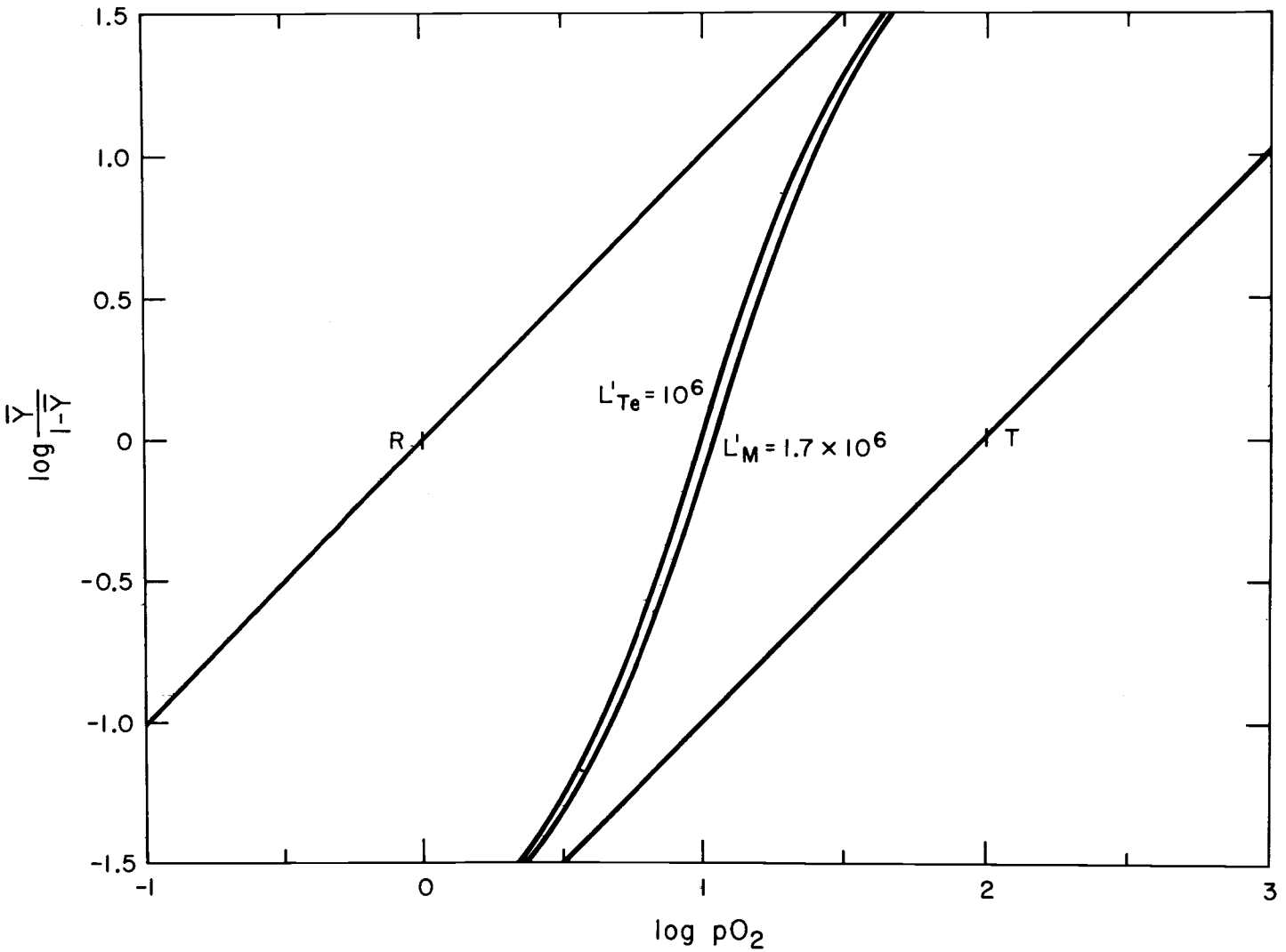

Figure 30. Calculated Hill plots for L' = 10^6 and 1.7 x 10^6 (q = 7.5).

Binding Studies of Mg^{2+} and Ca^{2+}

Based on the fact that no significant difference of the Mg^{2+} binding between the oxy- and deoxyhemocyanin was detected, the number of the Mg^{2+} binding sites which is linked to oxygen binding is considered to be very small compared with the total number of binding sites. The situation seems to be parallel to that of the Bohr protons which represent over one or a few of the many titratable hydrogens of the protein.

The fact that the intercepts of the Scatchard plot at the abscissa at different pH values do not coincide well makes the precise determination of the number of the Mg^{2+} binding sites difficult. The intercept of the extrapolation of the stronger (specific) binding moves slightly toward the right as the pH value goes up. At pH 8.8 there appears to be distinctively more strong binding sites. Suppose that there are m non-specific binding sites per subunit, which have the binding constant k'_B for Mg^{2+} and k'_C for H^+. Two H^+ compete with one Mg^{2+} for the same sites. Then we may write (neglecting the electrostatic interaction):

$$\bar{\nu}_B = \frac{(s/6)k_B a_B}{k_B a_B + (1+k_C a_C)^2} + \frac{m\, k'_B a_B}{k'_B a_B + (1+k'_C a_C)^2} \qquad (76)$$

where the second term on the right hand side corresponds to that for the nonspecific binding. The smooth curves for pH 7.0, 7.65 and 8.2 in Fig.19 have been generated by a computer program for equation (76). The numerical values of the parameters are chosen as follows: $s = 42$, $k_B = 1.5 \times 10^3 M^{-1}$, $k_C = 1.6 \times 10^7 M^{-1}$, $m = 15$, $k_B' = 1.0 \times 10^2 M^{-1}$ and $k_C' = 4.5 \times 10^7 M^{-1}$. It turned out that k_C' must be larger than k_C in order that the intercept of the extrapolation of the plots for the specific (stronger) binding increases as the pH increases. There is no way to choose the values of the parameters so that the calculation also fits the data at pH 8.8. The deviation at pH 8.8 may possibly stem from the partial dissociation of the hemocyanin into 5S particles, which cause some complications (compare Table II at pH 8.8 and Fig. 9). In this case k_B is fifteen times k_B', a relatively small difference. The extrapolation from the points of the low concentrations of the ligand, in this kind of a situation, does not necessarily coincide with the straight line for the stronger binding as shown in Fig. 31. Three curves were copied from Fig. 4 and the three straight lines were calculated by setting $k_B' = 0$ in eq. (76). The number of bound Mg^{2+} is replotted with respect to the pH values in Fig. 32. Smooth curves, each of which corresponds to the concentration of the free Mg^{2+}, are calculated by eq. (76) with the same numerical constants as above. As expected, the data points at pH 8.8 deviate from the curve to a large extent.

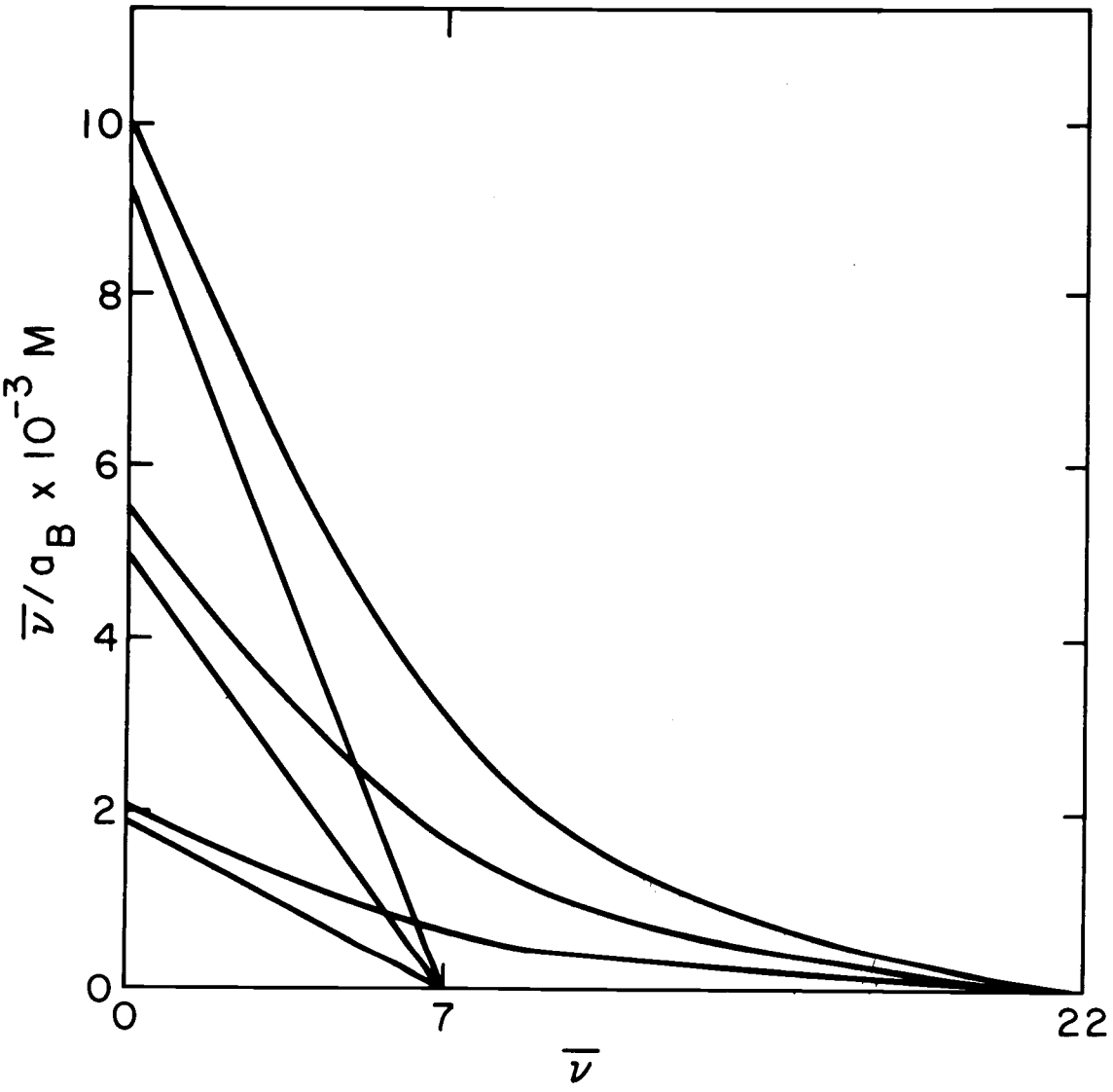

Figure 31. Scatchard plots calculated by eq. (76). Straight lines correspond to those of m = 0.

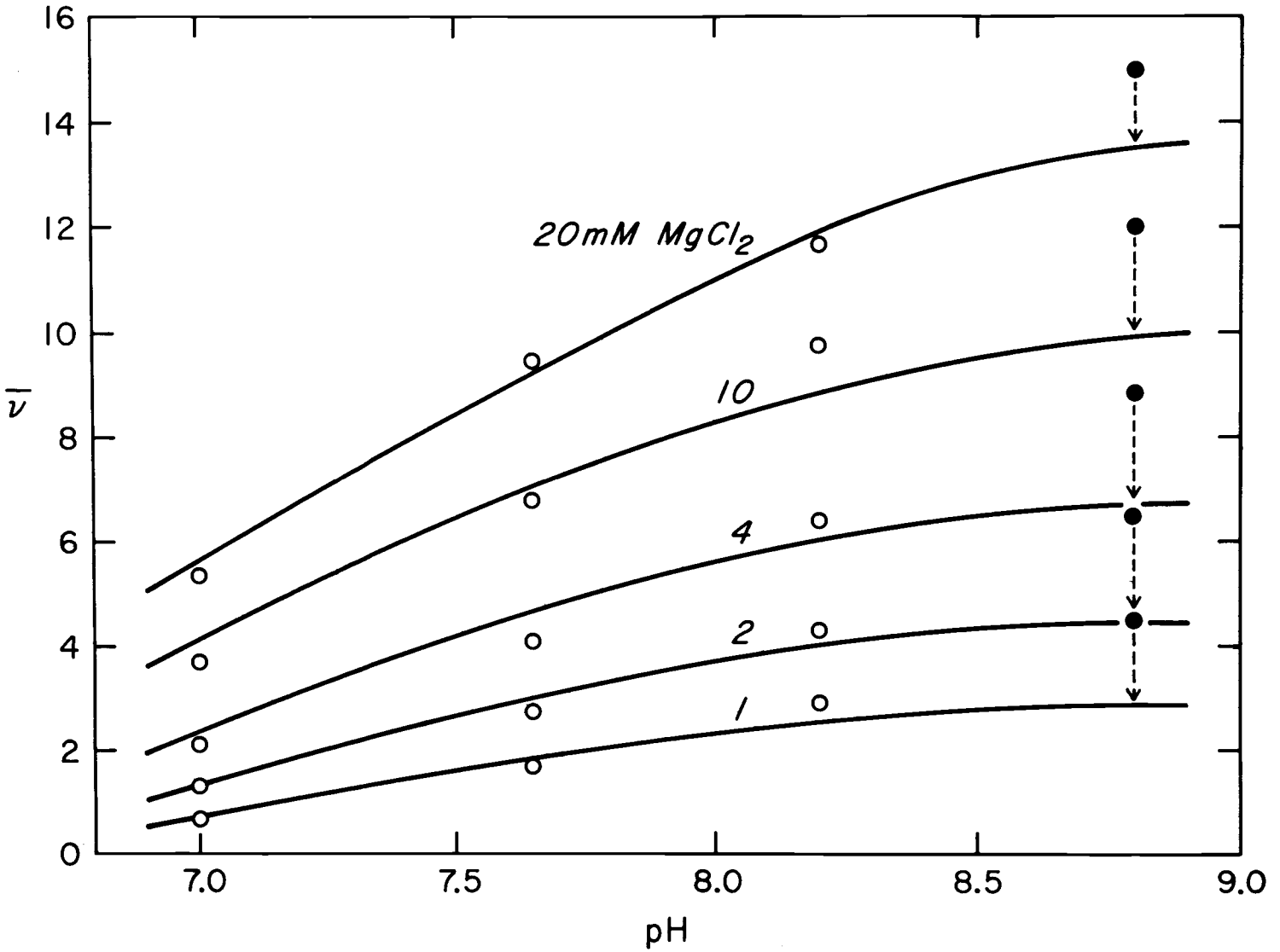

Figure 32. A graph of $\bar{\nu}$ vs. pH. The data were taken from Table II.

Ca^{2+} binding, compared with Mg^{2+} binding, has much less weak nonspecific binding as can be seen in Fig. 4. This is a peculiar, unexplained result, for one would normally expect the weaker binding sites to be less specific.

By using some of the data of Mg^{2+} binding, the effect of the consideration of the excluded volume of the protein is demonstrated in Fig. 33. The activity coefficient of Mg^{2+} changes from 0.42 to 0.30 as the concentration increases from 0 to 50 mM. Although the use of activity instead of concentration does not affect the intercept of the Scatchard plot at the abscissa very much, it naturally affects the position of the intercept at the ordinate, thereby changing the estimation of the binding constant considerably.

Although there has been no report on divalent cation binding study for Arthropod hemocyanin to the author's knowledge, there are two reports on Ca^{2+} binding by Molluscan hemocyanin. Makino has measured the Ca^{2+} binding of hemocyanin from Dolabella auricularia by using the equilibrium dialysis method (Makino, N., 1972). The concentrations of Ca^{2+} inside and outside of the dialysis tube were determined colorimetrically. Combining with the data of released H^+ upon adding Ca^{2+}, he reported that there are 1.7 moles of Ca^{2+} binding sites per 27,900 g protein (3.4 for the functional unit) which has the dissociation constants of 2.5×10^{-4} and 5.6×10^{-7}M for Ca^{2+} and H^+

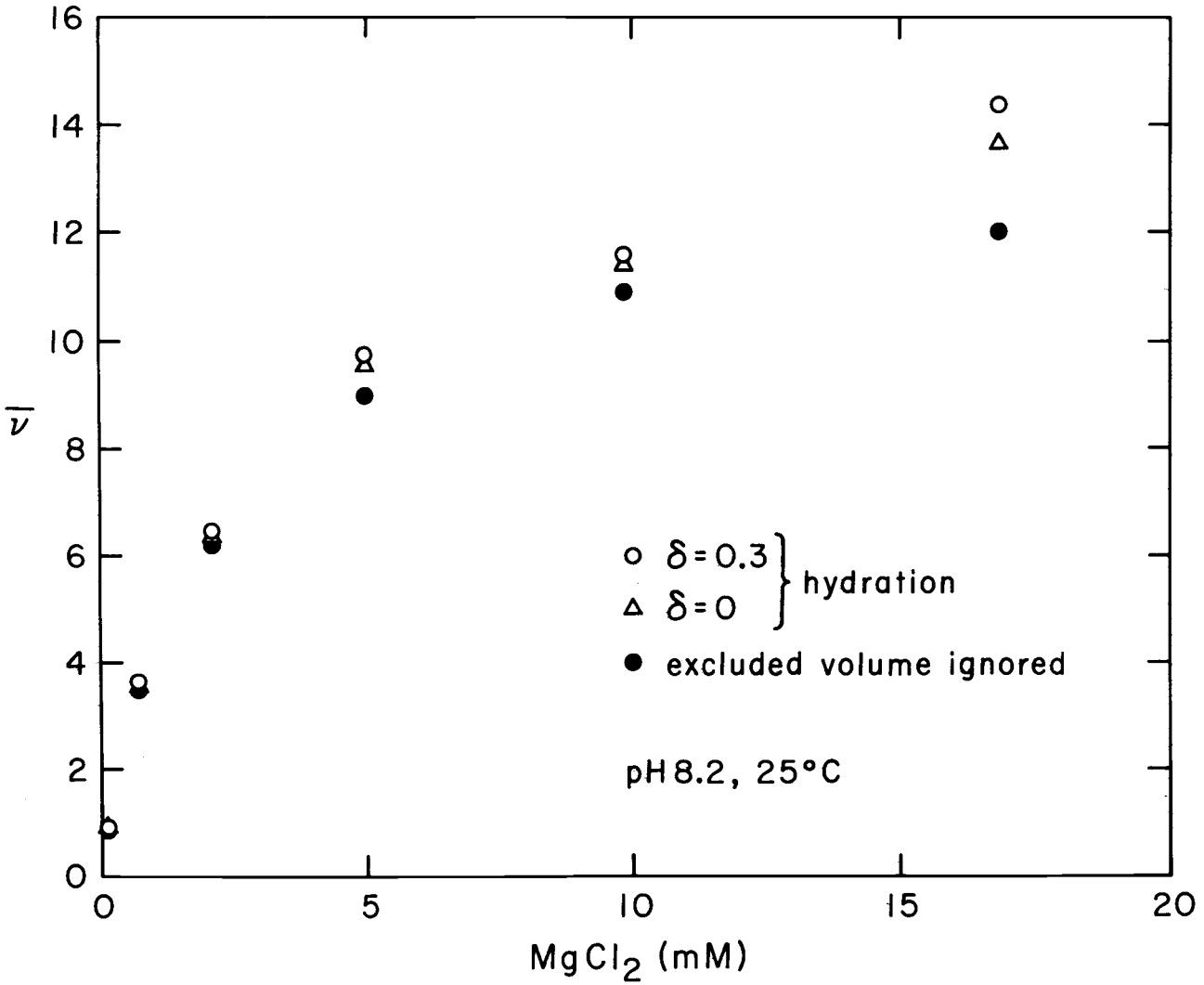

Figure 33. A demonstration of the effect of the consideration of excluded volume on the evaluation of the number of Mg^{2+} bound.

respectively (binding constants 4.0 x $10^3 M^{-1}$ and 1.8 x 10^6 M^{-1}). In this case Ca^{2+} has no effect on the oxygen binding affinity of the hemocyanin, which shows cooperativity (n_H = 1.9) both in the presence and absence of Ca^{2+}. On the other hand, Klarman et al. measured the binding of Ca^{2+} to hemocyanin from Levantina hierosolima at pH 8.2 (physiological pH) by gel filtration (Klarman et al., 1972). Twenty moles of binding sites per unit of 50,000 g protein were found. In this case the hemocyanin does not show cooperativity of oxygen binding in the absence of Ca^{2+}, but shows cooperativity in the presence of Ca^{2+}. The difference of the number of the binding sites between these two hemocyanins is considerably large. It is to be noted that the histidine content of the Dolabella hemocyanin (2.9 mole percent of amino acids) is much lower than that of the usual molluscan hemocyanin (4 to 7 mole percent) (Van Holde and van Bruggen, 1971). We need more information to deduce a general conclusion. Concerning the nature of the binding sites of the divalent cations, Klarman et al. suggested the involvement the formation of the chelate ($-COO^-\text{---}Ca^{2+}\text{---}N\equiv$), where COO^- and $N\equiv$ stand for a carboxylate ion and an unprotonated imidazole group. Since from our results the competition of two H^+ and one Mg^{2+} is more likely, the involvement of two imidazole groups is a possibility. Binding of Zn^{2+} to a pair of imidazole groups has been suggested for insulin by Tanford and Epstein (1954).

Concluding Remarks

It has been the intent of this thesis to characterize the functional properties of the hemocyanin C from Callianassa californiensis and to interpret those properties in terms of a thermodynamic model which is as simple and coherent as possible.

The model which was developed in the Theory section was designed so that it satisfied the constraints from experimental results. The model is based on conformational equilibria coupled with monomer-tetramer association (Fig. 2). Within a monomer or a tetramer the conformational equilibrium is shifted either by oxygen binding (homotropic effect) or by the binding of effectors, $Mg^{2+}(Ca^{2+})$ or H^+ (heterotropic effect). The association equilibrium is regulated by $Mg^{2+}(Ca^{2+})$ and H^+, Mg^{2+} favoring the tetramer state and H^+ favoring the monomer state. Every essential feature of the model is included in eq. (21), where the association constant K is expressed as a function of the concentrations of three ligands, i.e. oxygen, Mg^{2+} and H^+. Although the oxygen molecule is not directly involved in the association process, it still affects the association equilibrium indirectly, because the R state is more abundant in the tetramer state than in the monomer state, which stems from the difference in the allosteric conformational equilibrium constant L'_M and L'_{Te}.

The following are the main conclusions: (1) There are about 42 strong Mg^{2+} binding sites per monomer (17S), each of which binds two H^+ competitively. Among those 42 binding sites, about four are oxygen linked and about three are involved in the association process. The average binding constants of Mg^{2+} and H^+ are $1.6 \times 10^3 M^{-1}$ and $1.6 \times 10^7 M^{-1}$ respectively, from which we obtain $pk_C = 7.2$ for the H^+. (2) From the association equilibrium study, it is revealed that the ratio of the allosteric conformational equilibrium constants L'_m/L'_{Te} was 1.7. In other words this difference can account for the difference of the association profile between oxy and deoxyhemocyanin (Fig. 7). This result implies that the effect of the shift in the association on the oxygen binding curve is small, in spite of the fact that there is an experimentally observable change in the association profile between the oxy and deoxy state of the hemocyanin (Fig. 7). This conclusion justifies the analysis of the oxygen binding data, where the effect of the association equilibria was neglected. Since the shift of the association equilibrium does not affect the oxygen binding behavior significantly, it is unlikely that the association equilibrium itself plays a significant role in vivo. Furthermore the equilibrium is presumably shifted far toward tetramer in vivo, because of the high concentration of the protein (about 100 mg/ml)(Miller et al., 1977). Conceivably, the association has more of a structural

importance than a functional one. In that respect, it is to be noted that the hemocyanin has the maximum value of the association constant at approximately the physiological pH, 8.0 (Fig. 26(a)).

In order to simplify the system only Mg^{2+} was used in most of the experiments. There may be slight functional differences between Mg^{2+} and Ca^{2+}, such as the small difference of the c value (non-exclusive binding coefficient for oxygen) as discussed earlier. However, it appears that every function of Ca^{2+} which has so far been observed can be replaced by higher concentrations of Mg^{2+}.

As mentioned earlier, more detailed thermodynamic or kinetic study will be obstructed by the microheterogeneity of the molecule. The preparative separation of homogeneous Callianassa hemocyanin subunits has not yet been very successful.

Recently a first x-ray diffraction study of an arthropod hemocyanin from the spiny lobster, Panulirus interuptus was published (Kuiper, et al., 1975). The advantage of this arthropod hemocyanin for the x-ray diffraction study is that the monomer molecule (17S) does not polymerize to a larger association state. Schepman has combined the results of the x-ray diffraction with the electron micrograph of the crystals and single molecules and deduced a model which is shown in Fig. 34 (Kuiper, 1976). In this model the six monomers are arranged into two triangles which line

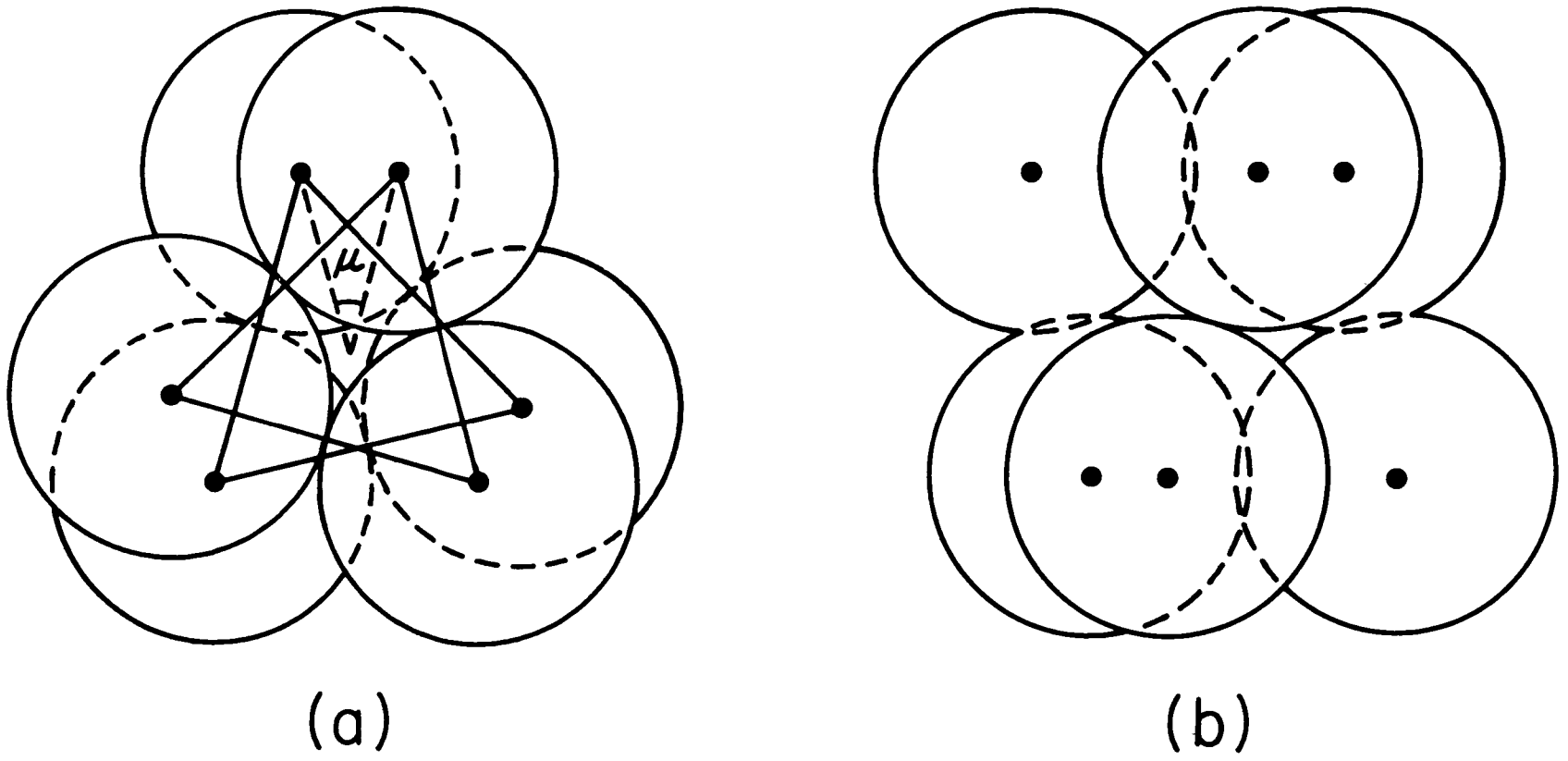

Figure 34. Model structure having point group symmetry 32, and μ = 30°. (a) projection along three fold axis; (b) along two-fold axis.

in parallel planes and have a three-fold symmetry axis in common. One triangle of subunits is rotated with respect to the other through an angle $\mu = 25 \pm 5°$ around this axis.

Although it is not more than a speculation at the present stage, it may be meaningful to discuss possible relationships between the thermodynamic model and the structural model described above. A possible scheme is proposed below. I propose that:

i) In the monomer state, $\mu = 25°$ and the monomer unit has the allosteric conformational equilibrium constant, L'_M.

ii) In the tetramer state, $\mu = 0°$ and the monomer unit in the tetramer has the allosteric conformational equilibrium constant L'_{Te}.

That is to say, in order to associate to tetramer, the two triangles in Fig. 34(a) have to twist with respect to each other so that they superimpose. A possible dimerization process which is the first step for the tetramerization is shown in Fig. 32. Suppose that a and a', b and b', c and c' and d and d' have to contact each other in order to dimerize. This is considered to be a Mg^{2+} dependent process (about three Mg^{2+} are necessary for the twist; see Table V, the value of P).

The dimers thus formed spontaneously associate to tetramer. Because of the high symmetry, D_2, there are a number of possibilities to contact the two monomers, if

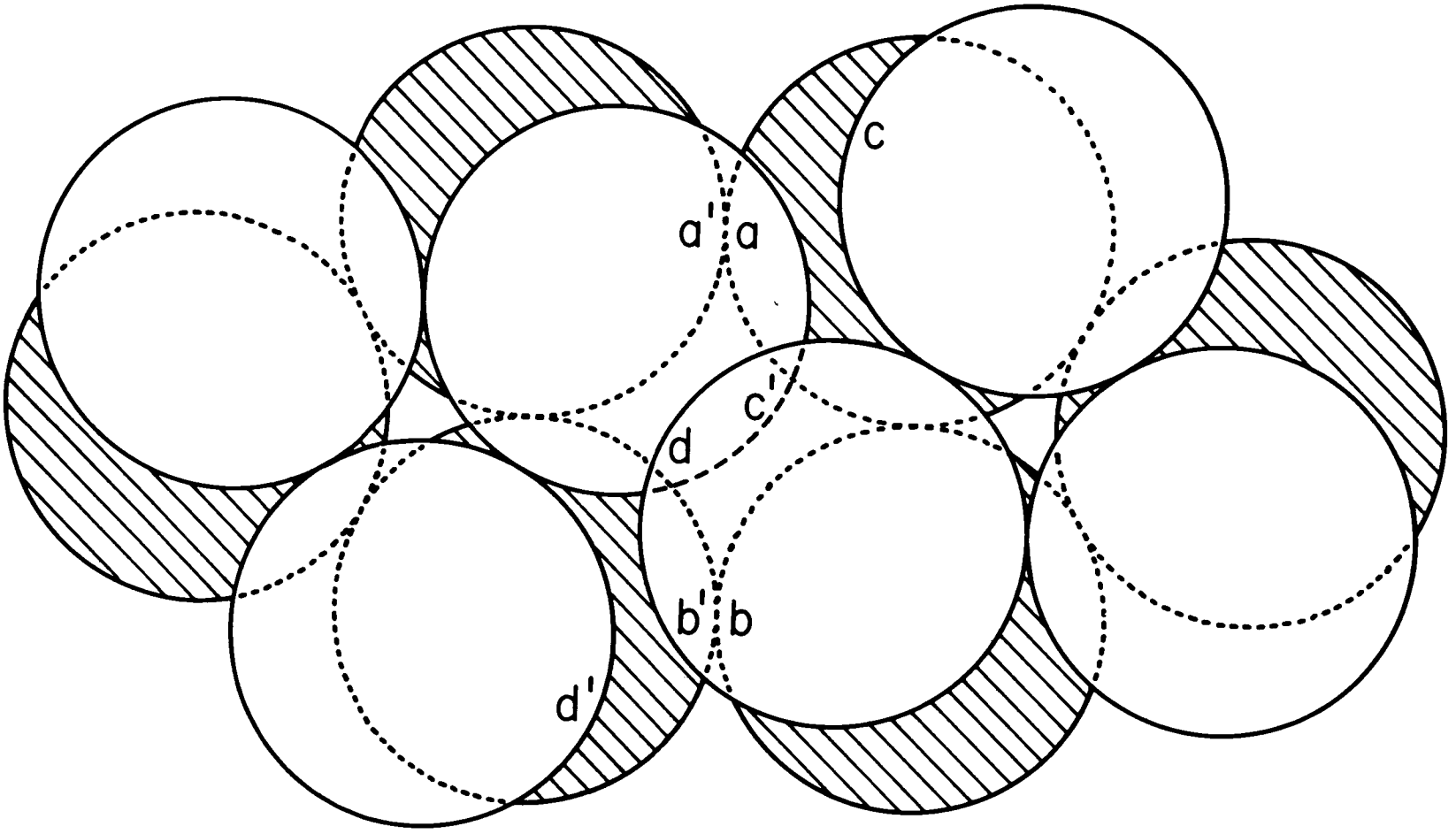

Figure 35. A possible dimerization process. In order to dimerize, the points a and a', b and b', c and d', and d and d' have to contact each other.

they are all identical. It is possible that the microheterogeneity of the subunits makes the contact between monomer units specific.

There are several attractive aspects of the proposal. First of all, it explains the difference between L'_M and L'_{Te} in terms of the difference in the relative positions of triangles in Fig. 34(a). Both monomer and tetramer can show R-T transition with the allosteric conformational equilibrium constants L'_M and L'_{Te} respectively. R-T transition may be independent of association reaction or the twisting of the triangles, although it is naturally related with the free concentrations of ligands. An example of schematic conformational changes which may be possible are drawn in Fig. 36.

We observed that some of the reconstituted monomers from 5S subunits could not associate to a tetramer. It may be possible that only some of the subunits have correct sites for the contact and unless those subunits are located in the right place, the monomers cannot associate to tetramer upon adding $Mg^{2+}(Ca^{2+})$. Hemocyanin I which is present in the hemolymph of the same shrimp as a monomer (15 percent of the total hemocyanin) may possibly have this kind of an incorrect location of the particular subunits in the monomer unit.

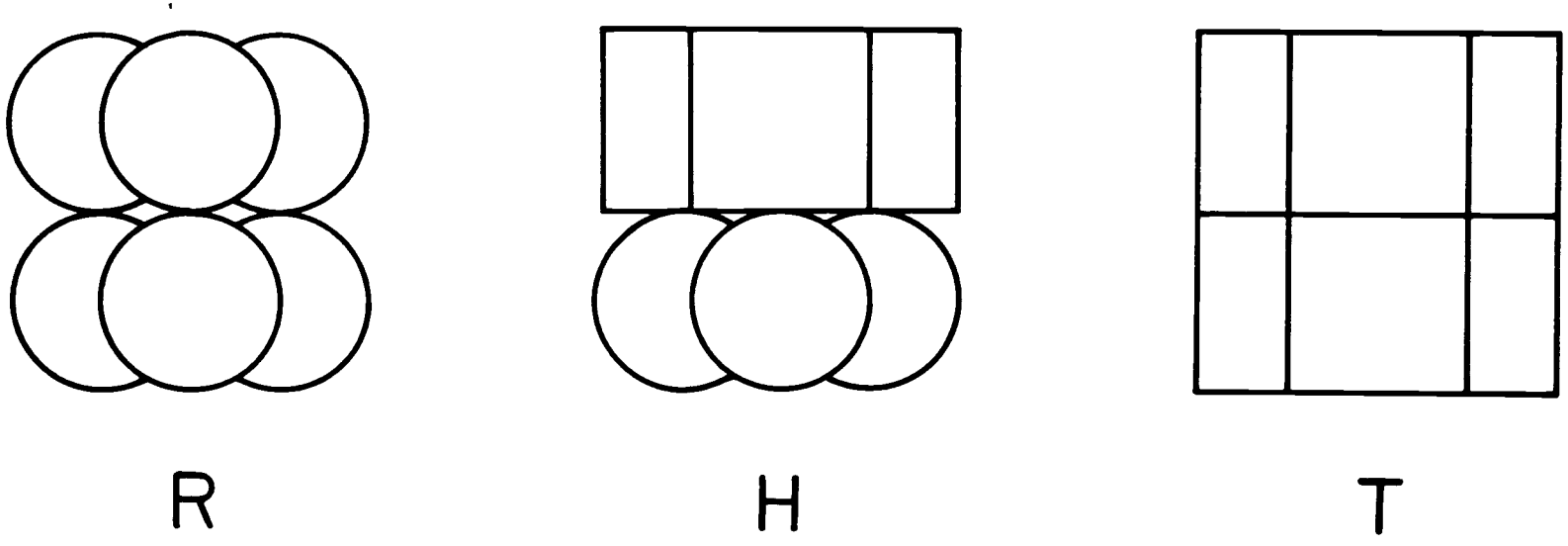

Figure 36. A schematic representation of R-T transitions.

BIBLIOGRAPHY

Ayres, W. A., E. W. Small and I. Isenberg. (1974). A computerized fluorescence spectrometer. Anal. Biochem. 32, 185-190.

Blair, D. and K. E. Van Holde. (1976). Sedimentation Equilibrium Studies of a Complex Association Reaction. Biophysical Chemistry 5, 165-170.

Brouwer, M., M. Walders and E. F. J. van Bruggen. (1975). Proteolytic Fragmentation of Helix pomatia α-Hemocyanin: Structural Domains in the Polypeptide Chain. Biochemistry 15, 2618-2623.

Buc, H., J. K. Johannes, and B. Hess. (1973). (Appendix to paper by Johannes and Hess, 1973). J. Mol. Biol. 76, 199-205.

Cohen, L. B. and K. E. Van Holde. (1964). Physical studies of hemocyanins. II. A comparison of the Hemocyanin and Apohemocyanin of Loligo peali. Biochemistry 3, 1809-1813.

Cohen, E. J. and J. T. Edsall. (1943). Proteins, Amino Acids and Peptides. Reinhold, New York. p. 686.

DePhillips, H. A., K. W. Nickerson, and K. E. Van Holde. (1970). Oxygen binding and subunit equilibria of Busycon Hemocyanin. J. Mol. Biol. 50, 471-479.

Freedman, T. B., J. S. Loehr, and T. M. Loehr. (1976). A resonance raman study of the sopper protein, Hemocyanin. New evidence of the structure of the oxygen binding site. J. Am. Chem. Soc., 98, 2809-2815.

Fujita, H. (1975). Chapter 4 in Foundations of Ultracentrifugal Analysis. Volume 42 in Chemical Analysis: A Series of Monographs on Analytical Chemistry and Its Applications (Elving and Winefordner, eds.), John Wiley and Sons, New York.

Hall, R. L. and E. J. Wood. (1976). The carbohydrate content of gastropod Hemocyanins. Biochem. Soc. Trans. 4, 307-309.

Heck, H. d'A. (1971). Statistical theory of cooperative binding to proteins. The Hill equation and the binding potential. J. Am. Chem. Soc. 93, 23-29.

Hugli, T. E. and S. Moore. (1972). Determination of the tryptophan content of proteins by ion exchange chromatography of alkaline hydrolysates. J. Biol. Chem. 247, 2828-2834.

Imai, K. and T. Yonetani. (1977). The hemoglobin-oxygen equilibrium associated with subunit dissociation. I. An approach with the Hill scheme. Biochim. Biophys. Acta, 490, 164-170.

Johannes, K. J. and B. Hess. (1973). Allosteric kinetics of pyruvate kinase of Saccharomyces carlsbergensis. J.Mol. Biol. 76, 181-205.

Klarman, A., N. Shaklai, and E. Daniel. (1972). The binding of calcium ions to hemocyanin from Levantina hierosolima at physiological pH. Biochim. Biophys. Acta, 257, 150-157.

Kovacic, R. T. (1976). Ph.D. Thesis, Oregon State University.

Kuiper, H. A., W. Gaastra, J. J. Beintema, E. F. J. van Bruggen, A. M. H. Schepman, and J. Dreuth. (1975). Subunit composition, x-ray diffraction, amino acid analysis and oxygen binding behaviour of Panulirus interruptus Hemocyanin. J. Mol. Biol. 99, 619-629.

Kuiper, H. A. (1976). Ph.D. Thesis, Groningen.

Kuntz, I. D. Jr. and W. Kauzmann. (1974). Hydration of proteins and polypeptides. Advan. Protein Chem. 28, 239-345.

Long, C., Ed. (1961). in Biochemists Handbook, Princeton, N. J., van Nostrand, p. 28.

Makino, N. (1972). Hemocyanin from Dolabella auricularia III. Recombination of Ca^{2+} ion to EDTA-treated hemocyanin. J. Biochem. 71, 987-991.

Mellema, J. E. and A. Klug. (1972). Quaternary structure of gastropod haemocyanin. Nature (London), 239, 146-150.

Miller, K. and K. E. Van Holde. (1974). Oxygen binding by Callianassa californiensis hemocyanin. Biochemistry 13, 1668-1674.

Miller, K., H. Eldred, F. Arisaka, and K. E. Van Holde. (1977). Structure and function of hemocyanin from Thalassinid shrimp. J. Comp. Physiol. (in press).

Morimoto, K. and G. Kegeles. (1971). Subunit interaction of lobster hemocyanin. Arch. Biochem. Biophys. 142, 247-257.

Roxby, R., K. Miller, D. P. Blair and K. E. Van Holde. (1974). Subunits and association equilibria of Callianassa californiensis Hemocyanin. Biochemistry 13, 1662-1668.

Rubin, M. M. and J. P. Changeux. (1966). On the nature of allosteric transitions: Implications of non-exclusive ligand binding. J. Mol. Biol. 21, 265-274.

Schellman, J. A. (1975). Macromolecular binding. Biopolymers 14, 999-1018.

Shaklai, N. and E. Daniel. (1970). Fluorescence properties of Hemocyanin from Levantina hierosolima. Biochemistry 9, 564-568.

Siezen, R. J. and van Driel, R. (1974). Structure and properties of hemocyanins. XIII. Dissociation of Helix pomatia α-hemocyanin at alkaline pH. J. Mol. Biol. 90, 41-102.

Spackman, D. H., W. H. Stein, and S. Moore. (1958). Automatic recording apparatus for use in the chromatography of amino acids. Anal. Chem. 30, 1190-1206.

Spencer, R. L. and F. Wold. (1969). A new convenient estimation of total cystine-cysteine in proteins. Anal. Biochem. 32, 185-190.

Stumm, W. and J. J. Morgan. (1970). in Aquatic Chemistry. Chap. 3, Wiley-Interscience, New York.

Sullivan, B., J. Bonanentura, and C. Bonaventura. (1974). Functional differences in the multiple hemocyanins of the horseshoe crab, Limulus polyphemus L. Proc. Nat. Acad. Sci. U.S.A. 71, 2558-2562.

Tai, M. and G. Kegeles. (1975). Mechanism of the Hexamer-dodecamer reaction of lobster hemocyanin. Biophys. Chem. 3. 307-315.

Tanford, C. and J. Epstein. (1954). The physical chemistry of insulin. II. Hydrogen ion titration curve of crystalline zinc insulin. The nature of its combination with zinc. J. Am. Chem. Soc. 76, 2170-2176.

Tanford, C. (1961). In Physical Chemistry of Macromolecules. Chapter 8, John Wiley and Sons, New York.

Tanford, C. (1969). Extension of the theory of linked functions to incorporate the effects of protein hydration. J. Mol. Biol. 39, 539-544.

van Driel, R. and E. F. J. van Bruggen. (1974). Oxygen-linked association-dissocation of Helix pomatia hemocyanin. Biochemistry, 13, 4079-4083.

Van Holde, K.E., D. Blair, N. Eldred, and F. Arisaka. (1977). Association Equilibrium of Callianassa Hemocyanin. In "Structure and Function of Hemocyanins," R. Bannister and J. Bannister, Eds., Springer-Verlag (in press).

Van Holde, K. E. and E. F. J. van Bruggen. (1971). The Hemocyanins. in Biological Macromolecules Series (Timasheff, S. N. and Fasman, G. D., eds.), vol. 5, part A, pp. 1-55, Marcell Dekker, New York.

Wood, E. J. and D. G. Dalgleish. (1973). Murex trunculus Hemocyanin. 2. The oxygenation reaction and circular dichroism. Eur. J. Biochem. 35, 421-427.

Wyman, J. (1948). Heme proteins. Adv. Protein Chem. 4, 407-531.

Wyman, J. (1965). The binding potential, a neglected linkage concept. J. Mol. Biol. 11, 631-644.

Wyman, J. (1967). Allosteric linkage. J. Am. Chem. Soc. 89, 2202-2218.

APPENDICES

APPENDIX 1

Binding Polynomial and Semigrand Partition Function

Schellman (1975) has shown that the binding polynomial is related to the semigrand partition function:

$$\psi_M = \frac{H_O^M V^M \psi_O}{M!} \sum^M , \qquad \text{(I-1)}$$

where ψ_M is the semigrand partition function, M is the number of macromolecules in a volume V, which bind ligands; H_O is an effective partition function for the solute macromolecule apart from translational degrees of freedom; ψ_O is the grand partition function for components 1 (solvent) and 3 (ligands); $\sum$ is the binding polynomial.

ψ_M is related to the grand partition function:

$$= \sum_M \psi_M \lambda_2^M , \qquad \text{(I-2)}$$

where λ_2 denotes the absolute activity of the macromolecule. ψ_M satisfies the following relationships:

$$PV - n_2\mu_2 = RT \ln \psi_M \qquad \text{(I-3)}$$

$$\mu_2 = - \frac{\partial\, RT \ln \psi_M}{\partial M}$$

$$= -RT \ln H_O + RT \ln P_2 - RT \ln \sum \qquad \text{(I-4)}$$

$$(= \mu_0^0 + RT \ln c_P - RT \ln \sum \quad (1))$$

where $\rho_2 (\equiv c_q)$ is the concentration of the macromolecule.

From eq. (I-1),

$$kT \frac{\partial \ln \psi_M}{\partial \mu_3} = \frac{\partial \ln \psi_M}{\partial \ln \lambda_3}$$

$$= M \frac{\partial \ln \Sigma}{\partial \ln \lambda_3}$$

$$= M \bar{\nu}_3 \text{ (total number of bound ligands in volume V)}$$

(See eq. (8a) in the text).

APPENDIX 2

Table of the Activity Coefficients of Divalent Cations at 20°C

From eq. (27),

$$\log \gamma_{+} = -1.82 \times 10^{6} (\varepsilon T)^{-\frac{3}{2}} Z_{+}^{2} \left(\frac{\sqrt{I}}{1 + \sqrt{I}} - 0.3\ I\right) \qquad (27)$$

substituting $\varepsilon = 80.37$ and $T = 293°C$ and $Z_{+} = 2$, we obtain γ_{+} at each value of the ionic strength.

I	$\log \gamma_{+}$	γ_{+}
0.01	-0.177	0.665
2	-0.238	0.579
3	-0.279	0.526
4	-0.312	0.488
5	-0.338	0.459
6	-0.360	0.436
7	-0.379	0.418
8	-0.395	0.402
9	-0.411	0.389
0.10	-0.424	0.377
1	-0.435	0.367
2	-0.446	0.358
3	-0.455	0.350
4	-0.464	0.344
5	-0.472	0.337
6	-0.479	0.332
7	-0.485	0.327
8	-0.491	0.323
0.19	-0.497	0.319
0.20	-0.502	0.315
1	-0.506	0.312
2	-0.510	0.309
3	-0.514	0.306
4	-0.517	0.309
5	-0.521	0.302
6	-0.523	0.300
7	-0.526	0.298
8	-0.528	0.296
9	-0.530	0.295

I	$\log \gamma_+$	γ_+
0.30	-0.532	0.294
0.35	-0.537	0.290
0.40	-0.539	0.292

Within 0.5 percent error, the values of γ_+ at 25°C (ε = 78.54) are almost the same as the above values.